Stimulation of Fibroblast Growth Factor Receptor-1 Occupancy and Signaling by Cell Surface–associated Syndecans and Glypican

Robert Steinfeld, Herman Van Den Berghe, and Guido David

Center for Human Genetics, University of Leuven and Flanders Institute for Biotechnology, B-3000 Leuven, Belgium

EXHIBIT
D

Abstract. The formation of distinctive basic FGF–heparan sulfate complexes is essential for the binding of bFGF to its cognate receptor. In previous experiments, cell-surface heparan sulfate proteoglycans extracted from human lung fibroblasts could not be shown to promote high affinity binding of bFGF when added to heparan sulfate–deficient cells that express FGF receptor-1 (FGFR1) (Aviezer, D., D. Hecht, M. Safran, M. Eisinger, G. David, and A. Yayon. 1994. *Cell.* 79:1005–1013). In alternative tests to establish whether cell-surface proteoglycans can support the formation of the required complexes, K562 cells were first transfected with the IIIc splice variant of FGFR1 and then transfected with constructs coding for either syndecan-1, syndecan-2, syndecan-4 or glypican, or with an antisense syndecan-4 construct. Cells cotransfected with receptor and proteoglycan showed a two- to threefold increase in neutral salt-resistant specific ^{125}I-bFGF binding in comparison to cells transfected with only receptor or cells cotransfected with receptor and antisyndecan-4. Exogenous heparin enhanced the specific binding and affinity cross-linking of ^{125}I-bFGF to FGFR1 in receptor transfectants that were not cotransfected with proteoglycan, but had no effect on this binding and decreased the yield of bFGFR cross-links in cells that were cotransfected with proteoglycan. Receptor-transfectant cells showed a decrease in glycophorin A expression when exposed to bFGF. This suppression was dose-dependent and obtained at significantly lower concentrations of bFGF in proteoglycan-cotransfected cells. Finally, complementary cell-free binding assays indicated that the affinity of ^{125}I-bFGF for an immobilized FGFR1 ectodomain was increased threefold when the syndecan-4 ectodomain was coimmobilized with receptor. Equimolar amounts of soluble syndecan-4 ectodomain, in contrast, had no effect on this binding. We conclude that, at least in K562 cells, syndecans and glypican can support bFGF–FGFR1 interactions and signaling, and that cell-surface association may augment their effectiveness.

BEST AVAILABLE COPY

THE signaling pathways that are activated by the binding of various FGFs, Vascular Endothelial Growth Factor (VEGF) and Heparin-Binding EGF-like growth factor to their cognate receptors have been qualified as "heparin dependent." This contention is based on the failure of these signaling systems in cells that are defective in the synthesis of heparan sulfate (HS)[1] and on the ability to restore the activity of these pathways in these cells by providing an exogenous source of heparin-like polysaccharide. In the case of basic FGF (bFGF or FGF-2), heparin restores the high affinity binding of the growth factor to the tyrosine kinase receptor proteins, and restores the biological effects of this growth factor on cell differentiation and proliferation (Yayon et al., 1991; Rapraeger et al., 1991). The primary defect in the HS-deficient cells appears to be situated at the level of the initiating event, with the growth factor failing to occupy a binding site on the receptor and to induce a receptor configuration that leads to signaling. Different models that have been proposed as explanations for this HS requirement and the pharmacological effects of heparin (reviewed by Mason, 1994) include: a heparin-induced fit, whereby the glycosaminoglycan allows the growth factor to adopt a conformation that is appropriate for receptor engagement (Yayon et al., 1991), the need for HS to participate in the formation of a multimolecular signaling complex, whereby it binds simultaneously to both ligand and receptor (Nugent and Edelman, 1992; Kan et al., 1993; Guimond et al., 1993; Pantoliano et al., 1994), and indirect effects of heparin on the receptor dimerization that is required for signaling, by promoting the formation of ligand dimers (Ornitz et al., 1992; Spivak-Kroizman et al., 1994). On the other hand, these concepts have also been challenged or

Please address all correspondence to Guido David, Center for Human Genetics, Campus Gasthuisberg, O&N6, Herestraat 49, B-3000 Leuven, Belgium. Tel.: 32 16 345863; Fax: 32 16 345997. e-mail Guido.David@med.kuleuven.ac.be

1. *Abbreviations used in this paper*: bFGF, basic fibroblast growth factor; FGFR, fibroblast growth factor receptor; GpA, glycophorin A; GPI, glycosyl phosphatidylinositol; HS, heparan sulfate; HSPG, heparan sulfate proteoglycan.

© The Rockefeller University Press, 0021-9525/96/04/1405/12 $2.00

amended, whereby heparin was shown to only moderately increase the affinity of the growth factor for its receptor (two- to threefold increase) and heparin or HS were proposed only to be needed at low concentrations of ligand (Roghani et al., 1994). In all models, the direct binding interactions between the growth factor and heparin-like glycosaminoglycan are proposed as essential for the activation of the signaling pathway.

bFGF binds preferentially to exon IIIc-containing forms of the FGF receptors (FGFRs) 1–3, which are predominantly mesenchymally expressed (Dionne et al., 1990; Johnson et al., 1991; Keegan et al., 1991; Miki et al., 1992; Yayon et al., 1992; Werner et al., 1992; Chellaiah et al., 1994). In vitro the affinity of bFGF for the IIIc splice variant of FGFR1 is increased by about one order of magnitude when heparin is added (Pantoliano et al., 1994), and in HS-expressing cells, the affinity of bFGF for the receptors (10^{-10}–10^{-11} M) is about two orders of magnitude higher than the affinity of the growth factor for cell-surface HS (10^{-8}– 10^{-9} M) (Moscatelli, 1987; Wennström et al., 1991). Clusters of IdoA(2-OSO_3)α1,4GlcNSO_3 units have been identified as bFGF-binding sequences in HS chains derived from human skin fibroblasts (Turnbull et al., 1992) and bovine aortic muscle cells (Habuchi et al., 1992). Heparin-derived penta- or hexasaccharides of similar structure effectively bind to bFGF and inhibit bFGF binding to cell surface HS proteoglycans (HSPGs), but fail to promote FGFR binding (Tyrrell et al., 1993; Maccarana et al., 1993). The minimal structural requirements to enhance bFGF binding to its receptor and to support bFGF-induced mitogenesis appear to be realized in a dodecasaccharide containing the bFGF-binding site and additional 6-O sulfated groups (Ishihara et al., 1993; Guimond et al., 1993; Walker et al., 1994).

The ability of cells to generate HS of a defined sequence complexity varies during ontogenesis (David et al., 1992*a*; Kato et al., 1994), and some observations directly imply that part of the cellular controls on signaling by FGF-like growth factors may occur at the level of the expression of the required HS cofactor/receptor sequences (Nurcombe et al., 1993). The possibility of PG specificity in this respect is supported by the observation that, in vitro, some heparins and whole PG extracts from human lung fibroblasts were able to induce the binding of bFGF to an immobilized recombinant FGFR–alkaline phosphatase fusion protein, whereas some specific PG forms, such as syndecans 1 and 2, that were purified from these cell extracts were inactive and even inhibited the effect of the active heparin fraction (Aviezer et al., 1994*a*). In subsequent studies, the major activating component of these PG extracts was identified as perlecan, the large extracellular matrix (basement membrane) PG (Aviezer et al., 1994*b*). These observations, together with indications that overexpression of syndecan-1 inhibits the bFGF-induced growth promotion of 3T3 cells (Mali et al., 1993), have lead to the suggestion that the local expression of active perlecan and the synergies and balances between activating and nonactivating classes of PGs will determine the degree and extent of bFGF-induced cellular responses (Aviezer et al., 1994*b*).

Our investigations were aimed at identifying cell surface–associated HSPGs that might promote bFGF binding and receptor activation. Using a cell system in which we were able to express independently the IIIc variant of FGFR1 and four types of PG (i.e., syndecans 1, 2, 4, and glypican), as well as a cell-free system in which we used 6xHis-tailed recombinant forms of receptor and PG to mimic their colocalization at the cell surface, we demonstrate that all these cell-surface HSPGs can support the bFGF–receptor interaction.

Materials and Methods

Plasmid Isolation and Construction

Clones for bFGF and FGFR1 were isolated from a human embryonic lung fibroblast λZAPII phage library using oligolabeled PCR-derived probes for bFGF and FGFR1 and standard screening procedures (Sambrook et al., 1989).

The bFGF clones were used as PCR templates. The primer set 5′-GGTGTCGACATCGAAGGTAGACCCGCCTTGCCCGAGGATGGC-3′ and 5′-GGCCTGCAGTCAGCTCTTAGCAGACAT-3′ used for the amplification reaction (Saiki et al., 1988) was designed to introduce unique restriction sites flanking the coding sequence and a Factor Xa cleavage site at the amino-terminal end. The PCR products were sequenced using an automated fluorescent sequencer (Pharmacia Biotechnology Benelux, Roosendaal, The Netherlands) and cloned into the prokaryotic expression vector pQE-9 (Qiagen, Chatsworth, CA), which introduces a 6xHis tag at the amino-terminal end of the encoded protein.

One FGFR1 clone, identified as the two Ig-like domain isoform (Ig II/IIIc) (Eisemann et al., 1991), was restricted with PstI to remove 370 bp of the 5′ untranslated sequence and cloned into the eukaryotic expression vector pcDNA/Neo (Invitrogen, Leek, The Netherlands), using the HindIII and NotI sites from the multiple cloning sites of the vectors.

The cDNAs for human syndecan-4 (David et al., 1992*b*), syndecan-2 (Marynen et al., 1989), and syndecan-1 (Mali et al., 1990) were cloned into the KpnI and NheI sites of the episomal expression vector pREP4 (Invitrogen). The cDNA for glypican (David et al., 1990) was released with HindIII and NotI, and cloned into the corresponding sites of pREP4. A 630-bp fragment containing the complete coding sequence of syndecan-4 was antisense cloned into the HindIII and BamHI sites of the same vector.

Plasmids coding for 6xHis-tagged ectodomains of FGFR1 and syndecan-4 were constructed by PCR. A 300-bp fragment of FGFR1 was amplified using the primer set 5′-GACCCGCAGCCGCACATCCAGTGG-3′ and 5′-CCGCTCGAGTCAGTGATGGTGATGGTGATGCTCCAGGTACAGGGGCGAGGTCATCACTGCC-3′, digested with BfrI and XhoI, and cloned into the corresponding restriction sites of the FGFR1 plasmid, replacing the sequences that code for the transmembrane and cytoplasmatic domains. The resulting insert, FGFR1e, was cloned into pMEP4 via HindIII and XhoI. A sequence coding for a 6xHis-tagged ectodomain of syndecan-4 was constructed using the primers 5′-GCAATTAACCCTCACTAAAGGG-3′ and 5′-CGCGTCGACTCAGTGATGGTGATGGTGATGCTCCGTTCTCTCAAAGATGTTGCTGCCCTGC-3′. The PCR fragment was restricted with BglII and SalI, and cloned in the corresponding sites of the syndecan-4 plasmid. The resulting insert, syn4e, was released with SpeI and XhoI, and cloned into the NheI and XhoI sites of the vector pMEP4. All constructs were sequenced to exclude mismatches.

Purification and Characterization of Recombinant bFGF

Nondenaturing purification of the recombinant 6xHis-bFGF was carried out according to standard protocols (Seno et al., 1990). In short, *Escherichia coli* M15 containing the appropriate pQE-9 construct plus the repressor plasmid pREP4 were induced with 1 mM IPTG at an OD of 0.9. Before sonication for 3 min on ice in the presence of 10 mM β-mercaptoethanol, the harvested cells were incubated for 1 h at 4°C in 50 mM NaH_2PO_4, 10 mM Tris, 300 mM NaCl, 15% sucrose, 0.1 mg/ml lysozyme, and 1 mM PMSF. After centrifugation, the bacterial lysate was applied to an Ni-NTA resin column (Qiagen), equilibrated at pH 8.0 (50 mM NaH_2PO_4, 300 mM NaCl), and eluted at pH 4.5 (50 mM NaH_2PO_4, 500 mM NaCl) (Hochuli et al., 1987). After readjustment to pH 8.0, this eluate was applied to Heparin-Ultrogel (IBF Pharmindustrie, Villeneuve-la-Garenne, France), washed with 1 M NaCl, and eluted with 2 M NaCl. Total yield was ~4 mg purified bFGF per liter of culture (20 g of cells), as determined

by colorimetric assay. The purified protein migrated as a 18-kD peptide in Tricine–SDS-PAGE (Schägger and von Jagow, 1987), and was detectable with an anti–bovine bFGF mAb on Western blot. Stimulation of thymidine incorporation in serum-starved Swiss 3T3 fibroblasts, induced with 2 ng/ml 6xHis-bFGF for 18 h, confirmed the biological activity of this recombinant product.

Extraction and Purification of Cell-surface PGs

Cell surface PGs were extracted with a Triton X-100 buffer in the presence of proteinase inhibitors, concentrated on a DEAE–Trisacryl M column (IBF Pharmindustry, Villeneuve-la-Garenne, France), and further purified by ion exchange chromatography on MonoQ in Triton-urea-Tris buffer (Lories et al., 1987). Immunopurification was carried out with core protein–specific mAbs immobilized on CNBr-activated Sepharose 4B (Lories et al., 1989).

Purification of Recombinant FGFR1 and Syndecan-4 Ectodomains

Recombinant 6xHis-tagged ectodomains of FGFR1 (FGFR1e) and syndecan-4 (Syn4e) were isolated from the conditioned culture media of K562 cells that were transfected with the corresponding episomal plasmid constructs. Serum-free media from pMEP4-transfected cells were harvested 12–16 h after induction with 5 μM $CdCl_2$. FGFR1e was purified by two consecutive absorptions on Ni-NTA resin (see above). Syn4e was first absorbed on DEAE–Trisacryl M and then purified by metal chelate chromatography. The final eluates were concentrated by ultrafiltration (Centricon 30; Amicon, Inc., Beverly, MA), and the quantity (~400) μg/liter medium) and purity (>90%) of the product were estimated by SDS-PAGE.

Western Blotting

Heparitinase and chondroitinase ABC–digested PG were fractionated by SDS-PAGE and blotted on Z probe membranes. The blots were first incubated with the designated mAbs, and then with alkaline phosphatase–conjugated second antibodies, and finally developed with AMPPD (Tropix, Bedford, MA) for chemiluminescence and autoradiography.

Analysis of the GAG Compositions

Free glycosaminoglycan side chains were obtained by proteinase K digestion of purified $^{35}SO_3$-labeled PGs. The GAG chains were either subjected to the low pH nitrous acid procedure (Shively and Conrad, 1976) or digested with chondroitinase ABC. Both preparations and an untreated control were precipitated with cetyl pyridinium chloride and then collected on glass filter papers. The HS content was calculated as $(cpm_{untreated} - cpm_{HNO_2})/cpm_{untreated})$, the chrondroitin sulfate (CS) content was calculated as $(cpm_{untreated} - cpm_{ABCase})/cpm_{untreated})$. All analyses were performed in duplicates.

Affinity Chromatography of HSPG on Chelate Complex-bound bFGF

Purified 6xHis-bFGF was reapplied to an Ni-NTA column at a concentration of 50–100 μg/ml gel (~1/100 of the maximal binding capacity), washed with assay buffer (50 mM Na_2HPO_4, pH 7.5, 0.1% Triton X-100, 20 μg/ml BSA) and increasing NaCl concentrations (0–2 M), and reequilibrated with assay buffer. No bFGF leakage could be detected during the wash. Immunopurified HSPGs were dialyzed against the assay buffer and applied to aliquots of bFGF–Ni-NTA resin. Bound HSPGs were eluted with a NaCl step gradient (0–2 M). Every chromatographic experiment was repeated at least once, with similar results.

Cell Transfections

K562 cells (ATCC CCL 243) were routinely grown in DME F12 medium supplemented with 10% FCS and L-glutamine. For transfection, K562 cells were prewashed with Ca^{++}- and Mg^{++}-free PBS and incubated for 10 min at 4°C (10^7 cells/ml Ca/Mg-free PBS) with 30 μg linearized FGFR1-pcDNA/Neo, or pcDNA/Neo, before electroporation at 240 V and 960 μF with a gene pulser (Bio Rad Laboratories, Richmond, CA). Selection was started 48 h later with 500 μg/ml G418. Stable transfection was achieved after 12 d, and subclones were established by two consecutive limited dilution procedures. Individual clones were characterized for specific ^{125}I-bFGF binding. The transfections with the episomal replicons pREP4[−], pREP4[Syn1], pREP4[Syn2], pREP4[Glyp], pREP4[Syn4], and pREP4 [antiSyn4] were performed in similar ways. Selection with 200 μg/ml of hygromycin over 2 wk resulted in stable cell populations that were not further subcloned.

^{125}I-bFGF-binding Assays

Iodinated bFGF (specific activity = 800–1,200 Ci/mmol) was purchased from New England Nuclear (Boston, MA), aliquoted directly upon arrival, and stored at −70°C. For the cellular binding assays the K562 transfectants were grown for 72 h in a serum-free medium (DME F12) containing 1 g/liter BSA, 8 mg/l transferrin, and 4 mg/l of insulin, or in Ham's F12 medium supplemented with 30 mM $NaClO_3$ (to suppress the sulfation of the GAG chains) and the same additives. Samples of 200,000 cells were incubated for 90 min at 4°C in 200 μl DME F12 supplemented with 1 mg/ml BSA, 25 mM Hepes, pH 7.5, and 10 ng/ml ^{125}I-bFGF, in the absence or presence of 1 μg/ml unlabeled bFGF and with or without 100 ng/ml heparin. The cells were then washed two times with cold PBS and once with 2 M NaCl, 50 mM NaH_2PO_4, pH 7.5. The radioactivities of the salt washes and the cell pellets were counted separately. The values obtained in the presence of 100-fold excess of unlabeled bFGF were considered unspecific binding and were substracted from the total counts. The data are displayed as the means and SDs of three independent experiments.

In the cell-free binding assay, increasing amounts of ^{125}I-bFGF were combined with FGFR1e (6 ng) in the presence or absence of Syn4e (0.8 ng), trypsinized Syn4e (0.8 ng), or heparin (100 ng/ml), in 500 μl of assay buffer (50 mM NaH_2PO_4, pH 7.5, 150 mM NaCl, 2 mg/ml gelatin, and 0.5% Tween 20). Control mixtures consisted of increasing ^{125}I-bFGF or ^{125}I-bFGF and heparin concentrations in assay buffer. All mixtures were supplemented with 20 μl of Ni-NTA resin and incubated on a roller shaker at room temperature for 2 h. Bound label was recovered by centrifugation, washing of the beads in PBS, and discarding of the supernatant. Specific ^{125}I-bFGF binding was measured by substracting the amounts of label bound in control mixtures from the counts associated with the beads in test mixtures. This experiment was carried out three times with two different batches of ^{125}I-bFGF. The data were transformed into concentration equivalents and analyzed as Scatchard plots (Scatchard, 1949) using a computer program for linear curve fitting.

Covalent Cross-linking of ^{125}I-bFGF to FGFR1

Wild-type K562 cells and FGFR1-transfected K562 cells were prepared and incubated with ^{125}I-bFGF, as in the other bFGF-binding studies. After washing with 2 × 1 ml of cold PBS, the cells were incubated with 100 μg/ml (0.27 mM) disuccinimidyl suberate (Pierce, Rockford, IL) in PBS at 15°C for 45 min. The reaction was quenched with 20 mM Tris, pH 7.4, in PBS. The cell samples were boiled for 5 min in 2% SDS, 10% glycerol, 20 mM Tris pH 6.8, 1 mM EDTA, and 0.005% bromophenol blue, and were applied on 6–20% polyacrylamide gradient gels. After running, the gels were stained with Coomassie brilliant blue and dried for autoradiography. Quantitative analysis of the intensity of the bFGF–FGFR1 band was performed with an ImageQuant personal densitometer (Molecular Dynamics, Sunnyvale, CA). Reference bands in the Coomassie-stained gels were also measured to exclude differences in loading.

Immunofluorescence Cytometry

Immunocytofluorometry was performed with a FACSort® (Becton Dickinson & Co., Mountain View, CA), and data were analyzed with the program Lysis II. For indirect immunofluorescence staining, K562 cells were incubated with the designated mouse mAbs at a concentration of 10 μg/ml for 30 min, washed 2×, and then incubated with FITC-labeled goat anti–mouse Ab (Nordic Immunology, El toro, CA). Nonreactive, isotyped-matched mouse mAbs were used to measure background fluorescence. FITC-labeled anti–glycophorin A (GpA) mAb (clone JC159; Dako Glostrup, Denmark) and R-phycoerythrin-labeled anti-CD14 mAb (clone TÜK4; Dako) were incubated together and used at the concentration proposed by the manufacturer. Background was determined with correspondingly labeled isotyped-matched mAbs (Dual Colour Reagent; Dako). The relative mean fluorescence intensity (rMFI) for GpA was calculated as:

$$\text{GpA rMFI} = \frac{MFI_{\text{GpA-treated cells}} - MFI_{\text{background treated cells}}}{MFI_{\text{GpA-untreated cells}} - MFI_{\text{background untreated cells}}}$$

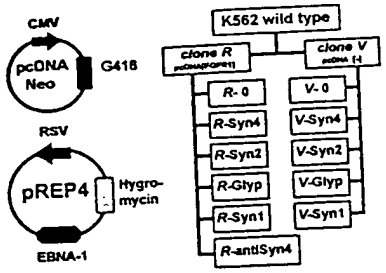

Figure 1. Transfection strategy. K562 cells were first transfected with the integratable vector pcDNA/Neo containing an FGFR1 cDNA or no insert. Two stable subclones, referred to as clone *R* for the FGFR1 transfection and clone *V* for the vector transfection, were then transfected with the episomal vector pREP4, either as such or provided with cDNAs coding for syndecans 4, 2, 1, or glypican (*R*-0, *R*-Syn4, *R*-Syn2, *R*-Glyp, *R*-Syn1, and corresponding *V* cells). In addition, clone *R* was transfected with an antisense syndecan-4 construct (*R*-antiSyn4 cells). The cotransfection was realized using the two different selection markers, G418 for pcDNA/Neo and hygromycin for pREP4.

All experiments were performed at least twice; SEM for all MFI values was <4%.

Results

Cell-surface PG Expression in K562 Cells

The transfection strategy that was adopted to study the FGFR system is illustrated in Fig. 1. Wild-type K562 cells, which do not bind bFGF in specific ways (Partanen et al., 1991), lack any transcriptional message for FGFR1 (Armstrong et al., 1992; our own unpublished data), and express only low levels of cell-surface HS (see below), were first transfected with an integratable pcDNA/Neo vector provided with cDNA for FGFR1(IIIc) or without insert. One stable subclone from the receptor transfection that showed specific binding of ^{125}I-bFGF (further referred to as clone *R*) and one subclone from the control transfection (further referred to as clone *V*) were then further transfected with the episomal vector pREP4, either as such or provided with cDNA inserts coding for syndecans 4, 2, 1, or glypican to enhance the levels of HS in these cells. Clone *R* was also transfected with a syndecan-4 antisense construct, since this syndecan seems to account (at least in part) for the small amounts of endogenous HS expressed by K562 cells. Several approaches were then used to evaluate the effect of these transfections on the expression of HS by K562 cells.

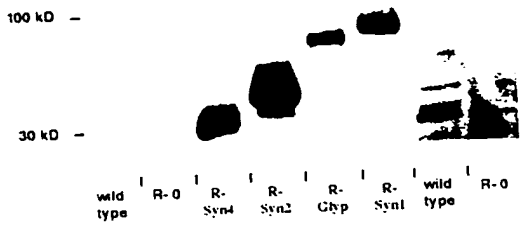

Figure 2. HSPG expression in K562 cells. Triton X-100 extracts of transfected K562, normalized for cell number, were purified by ion exchange chromatography and fractionated by SDS-PAGE after digestion with heparitinase. The Western blot was developed with mAb 3G10, which recognizes the terminal desaturated glucuronate that caps the HS stubs after heparitinase digestion, to detect all proteins substituted with HS, and as an assessment of the number of HS chains that were expressed. Detection was performed by chemiluminescence. Film exposure was given 1 min (*first six lanes*) or 5 min (*last two lanes*). PG-transfected K562 populations expressed high numbers of HS chains, which were readily detected after 1 min of exposure, on a single core protein. HS expression was barely detectable in wild-type and *R*-0 cells after 1 min, but bands of 120 kD, 50 kD, and mostly 35 kD were visible after the longer exposure. The stronger 35-kD band in these cells reacted with the syndecan-4–specific mAb 8G3 (not shown).

After heparitinase digestion, any protein that is substituted with HS can be traced by mAb 3G10, since this antibody recognizes the Δ-glucuronate that caps the HS stubs (David et al., 1992*a*). In Western blots of PG extracts, this antibody detected several weak bands in wild-type and in *R*-0 cells (mainly ~35-kD bands visible after more prolonged exposures), and strong ~35-, 48-, 64-, and 85-kD bands in the *R*-Syn4, *R*-Syn2, *R*-Glyp, and *R*-Syn1 transfectants, respectively (Fig. 2). These proteins were positively identified as the expected transfectant proteins with the core protein–specific mAbs 8G3 (syndecan-4), 10H4/6G12 (syndecan-2), S1 (glypican), and 2E9 (syndecan-1) (not shown).

Analysis of the amount of HS expressed at the surface of the transfectants, by quantitative immunofluorescence flow cytometry using the HS-specific mAb 10E4 (David et al., 1992*a*), revealed marked (5–10-fold) increases in cell-surface HS in all *R*-PG transfected cell populations (Fig. 3, *a* and *b*). The expression of the 10E4 epitope at the surface of *R* antisense transfectants, in contrast, was reduced by ~50% in comparison with *R*-0 cells (Fig. 3 *c*). Similar analyses with protein-specific antibodies confirmed the cell-surface expression of the transfectant PGs in transfectant cells, the cell-surface expression of endogenous syndecan-4 in wild-type cells, a >10-fold increase of the cell-surface expression of the syndecan-4 core protein in *R*-Syn4 cells, and the decrease (by 80%) of the cell-surface expression of this syndecan in the syndecan-4 antisense transfectants (not shown). Very similar PG expressions were also achieved in *V*-PG cotransfection experiments (data not shown).

All *R* transfectants were also metabolically labeled with [^{35}S]sulfate for 24 h. PG was extracted from the cells with Triton X-100, and then further purified by ion exchange chromatography on DEAE and MonoQ, as shown for the *R*-0 and the *R*-Syn4 transfectants in Fig. 4 *a*. Extracts from *R*-PG cells yielded two to fourfold more label per cell than the *R*-0 cell extract. The amount of [^{35}S]syndecan-4 recovered by immunoprecipitation from *R*-Syn1, *R*-Syn2, or *R*-Glyp extracts, in contrast, was identical or slightly lower than the amount of [^{35}S]syndecan-4 recovered from *R*-0 cells (not shown). Both the *R*-PG and *R*-0 materials eluted as a broad early peak (0.45–0.65 M; peak A) and a more distinct later peak (0.70–0.85 M, peak B). All PG transfections lead to increases in both peak A and B materials, but the A/B peak ratio was always higher in *R*-PG extracts than in the *R*-0 extract. Qualitatively similar elution profiles were obtained for immunopurified PG (not shown). Endogenous syndecan-4 immunopurified from *R*-0 cells mimicked the profile obtained for the total PG extract

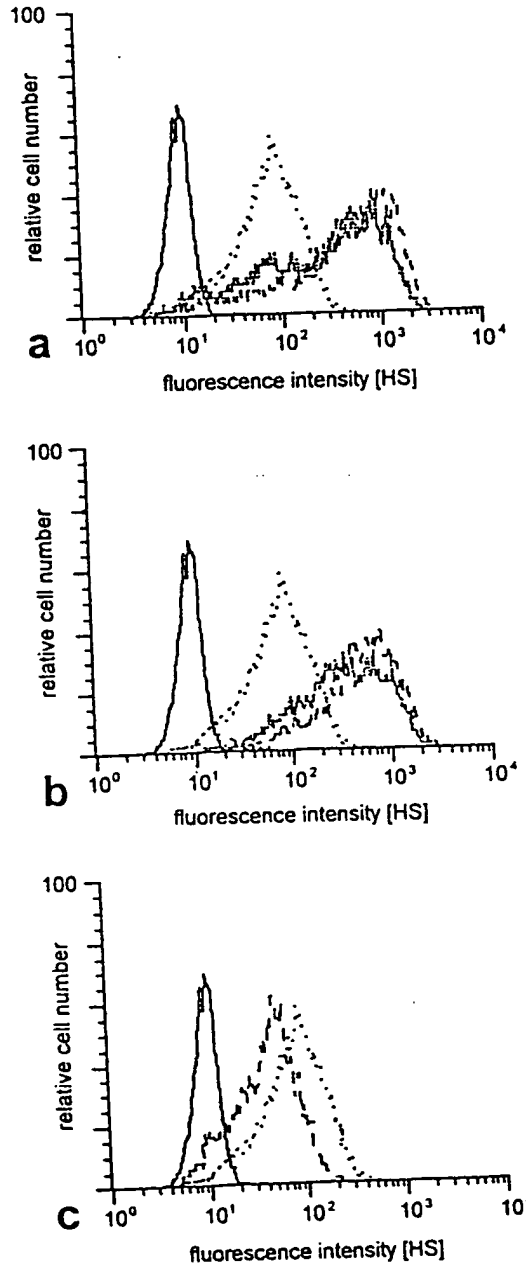

Figure 3. Cell-surface expression of HS in K562 cells. Cell-surface HS was measured by quantitative immunofluorescence cytometry using the HS-specific mAb 10E4. The background fluorescent signal (*solid line*) and the cell-surface HS expression in *R*-0 cells (*dotted line*), *R*-Syn1 cells (*narrow dotted line*), and *R*-Syn2 cells (*dashed line*). (*b*) The background fluorescence and the cell-surface HS expression in *R*-0 cells, *R*-Glyp (*narrow dotted line*), and *R*-Syn4 (*dashed line*) cells. (*c*) The background fluorescence and cell-surface HS expression in *R*-0 cells (*dotted line*) and *R*-antiSyn4 cells (*dashed line*).

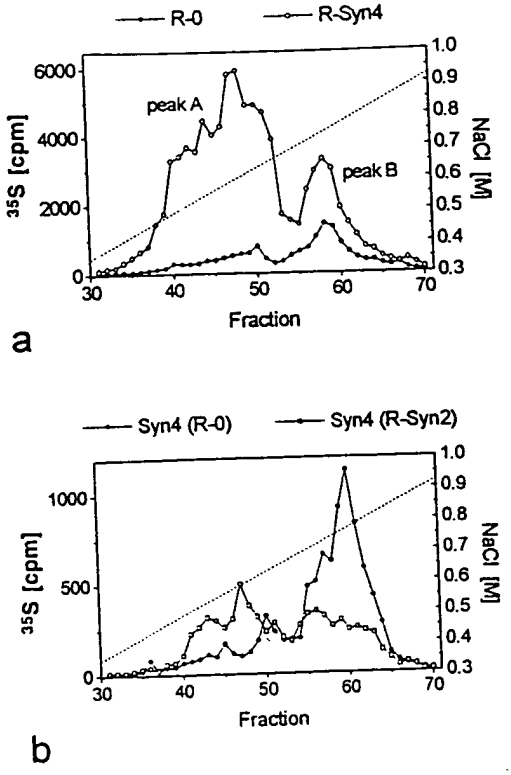

Figure 4. Ion exchange chromatography of the K562 PGs. ^{35}S-labeled PGs produced by the various transfectants were extracted with detergent and subjected to ion exchange chromatography. (*a*) The MonoQ elution profiles obtained for the total extracts from the *R*-0 and the *R*-Syn4 transfectant. The elution profiles obtained for the other PG transfectants were qualitatively similar to the one obtained for *R*-Syn4. The profile obtained for the *R*-anti-Syn4 transfectant was similar to that obtained for *R*-0 cells. (*b*) The elution profiles obtained for the endogenous syndecan-4 immunopurified from *R*-0 and *R*-Syn2 cells after digestion with chondroitinase ABC to remove the CS-substituted forms.

from these cells (prominent B peak), whereas the recombinant PGs and also the endogenous syndecan-4 immunopurified from *R*-PG cells eluted like total *R*-PG extracts (more prominent A peak).

Early (A peak) and late (B peak) eluting materials from total extracts were collected as separate pools and used for the further immunopurification of endogenous and/or transfectant PG on the corresponding antibody. Similar pools were also made for the eluted immunopurified PGs. Analysis of the GAG chain compositions of these immunopurified PGs revealed that the syndecans 1, 2, and 4 isolated from the corresponding transfections contained [^{35}S]HS as well as [^{35}S]CS. This was observed for both A and B peak–derived PGs (with a tendency for a higher HS content in B peak than in A peak materials, 40–60% versus 20–50%). This was also the case for the endogenous syndecan-4 expressed by *R*-0 cells. Glypican isolated from either the A or the B peak of the *R*-Glyp extract, on the other hand, carried almost exclusively HS (>90%). The fractionation of intact, heparitinase-, chondroitinase-, and doubly digested immunopurified PG samples by SDS-PAGE analysis and Western blotting indicated that in all instances (except for syndecan-1), the HS and CS chains were present on separate coreprotein populations, with little evidence for hybrid PG (shown for syndecan-4 from *R*-Syn4 extracts in Fig. 5).

Gel filtration chromatography indicated that the sizes of the protein-free HS chains were nearly invariant (~14 kD), whether isolated from different immunopurified PGs or from peak A or B materials (not shown). Ion exchange chromatography indicated that protein-free HS chains derived from A peaks were less anionic than chains derived

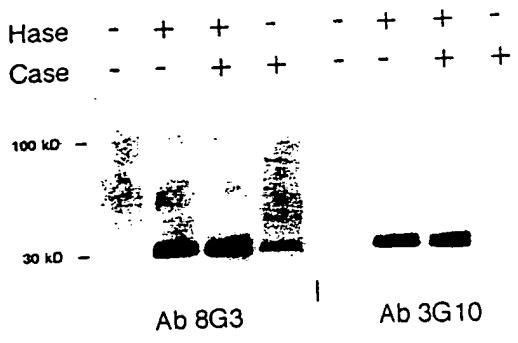

Figure 5. GAG chain composition of the K562 PGs. Immunopurified syndecan-4 derived from the corresponding transfectant (*R*-Syn4) was left untreated (−) or subjected (+) to heparitinase (*Hase*), chondroitinase ABC (*Case*), or both enzymes. The digests were fractionated by SDS-PAGE, blotted, and incubated with the syndecan-4 core protein–specific mAb 8G3 or the anti-Δ-HS mAb 3G10. Comparison of the banding patterns after combined and single enzyme digestions indicated that the majority of syndecan-4 molecules were substituted with HS and a smaller proportion were substituted with CS, with little or no evidence for hybrid molecules. Similar results were obtained for the syndecan-2. Syndecan-1 materials contained higher amounts of CS, in part as true hybrids. Glypican carried almost exclusively HS chains.

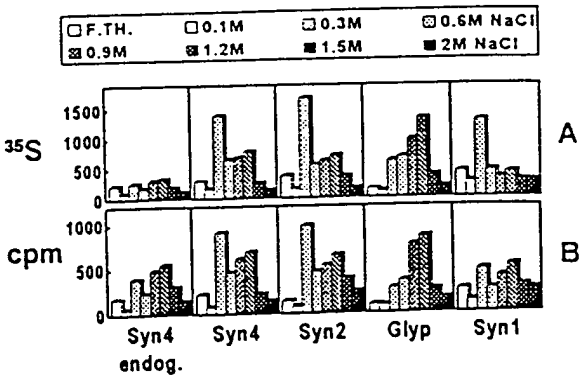

Figure 6. K562 PG binding to immobilized bFGF. Immunopurified, ^{35}S-labeled PGs isolated from peak A and peak B fractions (see Fig. 4) were applied to a bFGF column and eluted with a salt step gradient (up to 2 M NaCl). Glypican eluted as nearly one peak (at 1.2 M), the syndecans eluted as two major peaks, one at 0.3 M and a second at 1.2 M NaCl. The low salt eluates (fall through, 0.1, 0.3, and 0.6 M) contained ~70% CS, and the high salt eluates (0.9, 1.2, 1.5, and 2 M) contained ~90% HS.

from B peaks, but no differences in charge density were observed between HS chains from corresponding peaks derived from different PGs (not shown). Finally, sizing of the different immunopurified cell-surface PGs by SDS-PAGE (after a treatment with chondroitinase ABC to remove the CS-substituted forms) indicated that the more anionic forms of each HSPG species (B peak) were significantly more retarded than the less anionic forms (A peak). Yet, after heparitinase, A and B peak PGs yielded core proteins of similar sizes, indicating increasing numbers of HS-side chains per core protein in the more anionic PGs (not shown).

In another series of experiments, the ^{35}S-labeled *R*-0 and *R*-PG transfected cells were surface biotinylated immediately before the detergent extraction, subjected to ion exchange chromatography, and PG was immunopurified as described above. Early (A peak) and late (B peak) eluting fractions of each PG were then incubated with streptavidin beads to isolate the surface-exposed forms of these PGs. The percentage of streptavidin-bound label did not differ among A and B fractions, indicating that the various forms of a particular PG were equally well represented on the cell surface. This percentage ranged from 60 to 80% for syndecans or glypican isolated from the corresponding PG-transfected cells, but was only ~30% for syndecan-4 isolated from *R*-0 cells (data not shown). From the total label, the HS content, and the size of the biotinylated fraction, it was calculated that the PG transfections resulted in five- to sevenfold increases in cell surface [^{35}S]HSPG.

Altogether, these data demonstrated that overexpression of various cell-surface PGs in K562 cells lead to marked enhancements in cell-surface HS expression. This enhancement was most pronounced for the lesser sulfated forms of this glycosaminoglycan that were present on PGs of low chain valency, and it occurred at the detriment of the glycanation of the endogenous cell-surface PG (lower average HS sulfation and chain valency). The latter was confirmed by the immunopurification of endogenous syndecan-4 from *R*-0 and *R*-PG cells, digestion of the PG with chondroitinase ABC, and analysis of the HS-substituted syndecan-4 by ion exchange chromatography over MonoQ (Fig. 4 *b*). These findings indicated that the effects of the transfections on HS and HSPG synthesis were not simply additive, but also competitive, somewhat analogous to the effect of β-xylosides on the synthesis of CS (stimulation) and CSPG (inhibition) by cells. They also underscored the conclusion that the gain in cell-surface HS in the transfectants is driven by the transfectant PG.

Cell-surface PGs from K562 Cells Bind bFGF

To evaluate the bFGF-binding properties of the cell surface PGs, the various forms were immunopurified from the corresponding *R*-PG transfectants and allowed to bind to biologically active recombinant bFGF that was immobilized on Ni-NTA agarose via an aminoterminal 6xHis-tag. After equilibration, the column was eluted with an NaCl step gradient (Fig. 6). Syndecans (isolated from A or B peaks) eluted as two major peaks, one at 0.3 M and a second at 1.2 M NaCl. Analysis of the GAG compositions of the eluted syndecan fractions indicated that the pool of the first four fractions (nonbound, and eluting ≤0.6 M NaCl) contained mainly CS (~70%), whereas the pool of the four last fractions (eluting ≥0.9 M) contained almost exclusively HS chains (~90%). Glypican, which contained only HS, eluted as nearly one peak at 1.2 M NaCl. These data indicate that only HS-carrying forms of the PGs bind significantly to bFGF, and they confirm that most syndecan cores expressed in K562 cells display either HS or CS chains rather than a combination of both.

Heparin Sensitivity of the Binding of bFGF to FGFR1 in K562 Cells

We then measured the binding of ^{125}I-bFGF to PG- and

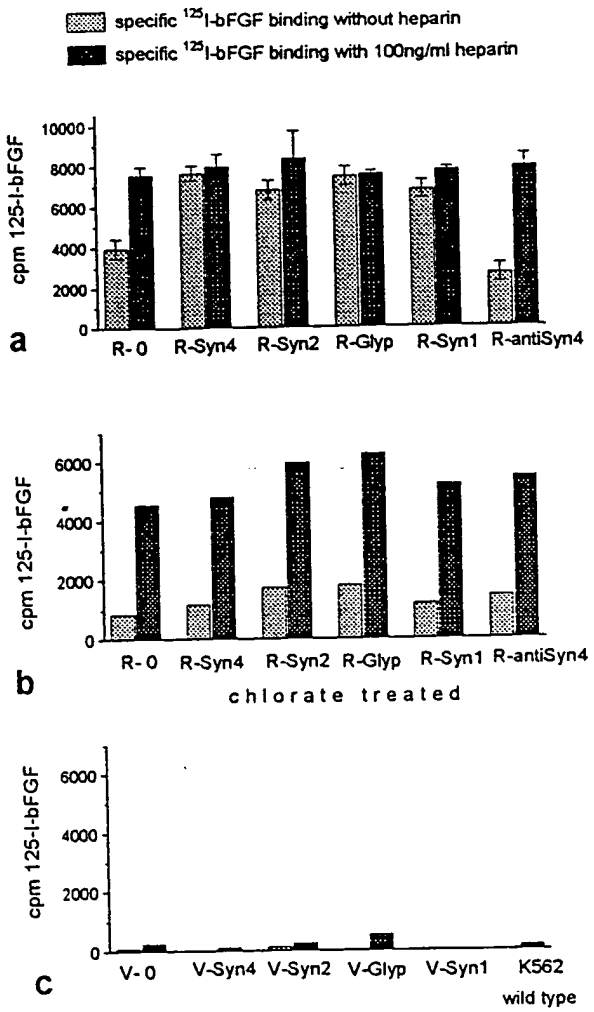

Figure 7. Binding of bFGF to FGFR1 in K562 cells. Aliquots, of 200,000 cells each, were incubated with 10 ng/ml of ^{125}I-bFGF for 90 min at 4°C in the absence or presence of 1 μg/ml of unlabeled bFGF and with or without 100 ng/ml of heparin. The bars indicate the amounts of iodinated bFGF that remained specifically bound after a neutral 2-M NaCl wash of the cells. Results are shown for receptor-transfected cells (*a*), chlorate-treated, receptor-transfectant cells (*b*), and for non-receptor-transfected cells (*c*). The values for receptor-transfectant cells are given as the means and SDs of three independent experiments.

non–PG–transfected *V* and *R* cells, as well as the effect of exogenous heparin on this binding (see Materials and Methods). Compared to non–PG transfectants, the *V*-PG and the *R*-PG transfectants showed similar (near 10-fold) increases in label in the neutral salt washes of the cells, and this label could barely be displaced by a 100-fold excess of unlabeled bFGF (not shown). All *R*-PG transfectants showed an increase in specific salt-resistant binding of ^{125}I-bFGF when compared with the *R*-0 and the *R*-antiSyn4 transfectants (Fig. 7 *a*). Adding soluble heparin at a concentration of 100 ng/ml doubled specific bFGF binding to RO cells and tripled specific bFGF binding to R-antiSyn4 cells, but had no effect on specific bFGF binding by the *R*-PG transfectant cells (Fig. 7 *a*). The specific bFGF binding in the presence of heparin was roughly constant for all *R* cell populations (excluding differences in the number of FGFR1 receptors per cell among the various transfectants), and was calculated to correspond to ~30,000 binding sites per cell. Chlorate treatment of all *R* transfectant cell populations resulted in a decrease of the specific binding to 15–25% of the value obtained in the presence of 100 ng/ml of heparin (Fig. 7 *b*). Neither wild-type K562 cells nor any of the PG transfectants of the *V* clone revealed significant levels of specific ^{125}I-bFGF binding, demonstrating that the assay was measuring FGFR1-related bFGF binding only (Fig. 7 *c*).

Heparin Sensitivity of the Affinity Cross-linking of bFGF to FGFR1 in K562 Cells

The participation of the cell-surface HS in the bFGF–receptor interaction was also investigated by affinity cross-linking experiments. Covalent cross-linking of ^{125}I-bFGF to the various *R*-transfectants demonstrated a putative bFGF–FGFR1 complex with an apparent molecular mass of ~140 kD. The formation of this labeled complex was inhibited by adding an excess of cold bFGF, and it did not occur in wild-type K562 cells. Quantitative densitometric analysis of the bFGF–FGFR1 complexes in the various transfectants, formed in the presence and in the absence of exogenous heparin, gave the following results: 100 ng/ml of heparin *increased* the yield of labeled bFGFR cross-links by 26% for *R*-0, by 40% for *R*-antiSyn4, and eightfold for chlorate-treated *R*-0 cells; the same heparin concentration *decreased* ligand cross-linking by 33% for *R*-Syn4, 46% for *R*-Syn2, 58% for *R*-Glyp, and 23% for *R*-Syn1 (Fig. 8). Increased yields of specific growth factor–receptor complexes in non–PG transfectants and sulfate-starved cells when heparin was added, were consistent with the results from the binding experiments that had revealed an enhancement of the bFGF–FGFR1 interaction by heparin in these cells (Fig. 7). Negative effects of heparin on the yield of growth factor–receptor cross-links in PG transfectants, where heparin did not affect the extent of the specific binding of the growth factor (Fig. 7), suggested modal differences between heparin- and PG-mediated specific bFGF–FGFR1 interactions.

FGFR1 and HS Dependency of the bFGF-induced Block in Erythroid Differentiation of K562 Cells

K562 cells are multipotential malignant hematopoietic cells that spontaneously differentiate into recognizable progenitors of the erythrocytic, granulocytic, and monocytic series. A treatment with hemin or the tyrosine kinase inhibitor herbimycin A reduces the intracellular tyrosine phosphorylation in K562 cells and stimulates their erythroid differentiation (Richardson et al., 1987; Honma et al., 1989). Exposure of K562 cells to 10^{-9} M PMA, in contrast, results in a reduced expression of erythroid-specific proteins, along with a weak myelomonocytic induction (Papayannopoulou et al., 1983). Erythroid differentiation of the K562 transfectants in the presence of growth factor was therefore measured as a test for the functionality of the FGFR1 and to evaluate the possible contributions of cell-surface PG in receptor-mediated growth factor effects.

For these experiments, PG- and receptor-transfected K562 cells were grown in a defined serum-free medium (see Materials and Methods). After 72 h of growth under these conditions, bFGF was added in concentrations of

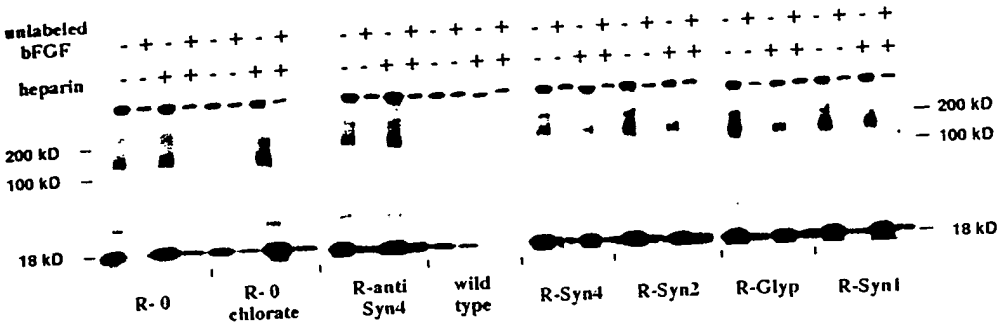

Figure 8. Cross-linking of bFGF to FGFR1 in K562 cells. For affinity cross-linking, the various cell populations were incubated with ^{125}I-bFGF, following the same procedures as described in the legend to Fig. 7. After washing off free label, cell-bound bFGF was cross-linked with 0.27 mM freshly dissolved DSS. The cells were then boiled in SDS buffer and fractionated by SDS-PAGE. After autoradiography, the intensities of the ~140-kD bFGF–FGFR1 bands were measured with a densitometer. 100-fold excess of unlabeled bFGF eliminated the formation of a labeled bFGF–FGFR1 complex in all receptor-transfected cells. Heparin potentiated receptor cross-linking in non–PG-transfected populations (by 26% in *R*-0 cells, by 40% for *R*-antiSyn4 cells) and most strikingly in chlorate-treated *R*-0 cells (eightfold increase). Wild-type K562 cells lacked any specific receptor cross-linked band. Heparin, on the other hand, decreased the cross-linking of ligand to the receptor in the PG-transfected cell populations (by 33% for *R*-Syn4, 46% for *R*-Syn2, 58% for *R*-Glyp, and 23% for *R*-Syn1).

0.5–10 ng/ml, and 72 h later, the GpA and CD14 expressions were measured by immunofluorescence flow cytometry. A dose-dependent suppression of GpA was obtained in all these cells (Fig. 9 *a*). At the high concentration of 10 ng/ml of bFGF, the mean GpA level in all *R* transfectants was suppressed to approximately one third of the control value (without bFGF), but at lower bFGF concentrations, the PG-transfected *R* cells were more responsive than the *R*-0 and the *R*-antiSyn4 cells. At a bFGF concentration of 10 ng/ml, the CD14 expression was increased by ~50% for all six *R* transfectants (data not shown). When treated with chlorate, the same cell populations were nearly unresponsive to bFGF, but the effect of bFGF on the GpA expression could largely be restored by the addition of heparin (Fig. 9 *b*). Neither wild-type K562 cells nor any *V* transfectant showed a change in GpA or CD14 expression when exposed to bFGF, with or without heparin (Fig. 9 *c*). Yet, these cells and the *R* cell populations showed similar decreases in GpA expression in response to 10^{-9} M PMA after 72 h (shown only for wild-type cells in Fig. 9 *c*). The interpretation that stimulation of FGFR1 increased intracellular tyrosine phosphorylation and consequently blocked erythroid differentiation was supported by the reverting effect of tyrosine kinase inhibitors. In *R* cells that were preincubated with 30 μM of genistein for 2 h before the addition of 10 ng/ml of bFGF, the GpA and CD14 expressions remained largely unchanged (data not shown).

Binding of bFGF to Surface-bound FGFR1 and HSPG Ectodomains

Finally, to exclude possible contributions by non transfectant PGs or other membrane-anchored molecules, we also measured the effect of HSPG on the binding of bFGF to its receptor under cell-free conditions. In this assay, we used recombinant FGFR1e and Syn4e provided with COOH-terminal 6xHis tags that bind with high affinity (K_d = 10^{-13}) (Hochuli et al., 1987) to Ni-loaded beads (Fig. 10 *a*). The affinity of bFGF for the ectodomains was calculated from the label coprecipitated with the Ni-NTA beads versus the free label at various bFGF concentrations (Fig. 10 *b*). The dissociation constant for the interaction of bFGF with Syn4e in the absence of FGFR1e was 2.7 nM (not shown). The calculated dissociation constant for the direct bFGF–FGFR1e interaction in the absence of any source of HS in this assay was 1.8 nM, threefold higher than the dissociation constant for the interaction of bFGF with the combination of FGFR1e and Syn4e (0.6 nM) or the combination of FGFR1e and chondroitinase ABC–treated Syn4e (not shown). In contrast, the affinity of bFGF for the combination of FGFR1e and heparitinase-treated Syn4e was identical to its affinity for FGFR1e. The addition of soluble heparin (100 ng/ml) to bFGF slightly increased the affinity of the growth factor for FGFR1e (K_d = 1.1 nM), whereas trypsin-treated Syn4e added at similar concentrations as Syn4e had no effect on the binding (K_d = 1.7 nM). For the combination of FGFR1e and Syn4e, the concentrations of the ectodomains were chosen such that the maximal number of bFGF-binding sites contributed by each component were individually similar. Yet the maximal number of binding sites obtained for the combination of FGFR1e and Syn4e did not differ from the maximal number of binding sites obtained for these ectodomains tested individually. This suggested a simultaneous binding of bFGF to both ectodomains, as a ternary complex that has greater stability than that mediated by soluble heparin.

Discussion

Our results demonstrate that three different syndecans and glypican can promote the binding and activation of a specific kinase receptor form, i.e., the IIIc splice variant of the FGFR1, by a specific member of the FGF family, i.e., bFGF (FGF2), when expressed with the FGFR1 as coreceptor pairs in transfectant K562 cells. All the forms that were tested boost the expression of cell-surface HS in these hematopoietic cells, facilitating the saturation of the receptor with growth factor and increasing the sensitivity of the cells to low doses of the growth factor that inhibit their erythroid differentiation. We conclude that cell-surface PGs can function as partners for the tyrosine kinases in a dual FGFR system, and that several different forms of this category of cell-surface components can provide the source of HS that is required for effective FGF–FGFR bind-

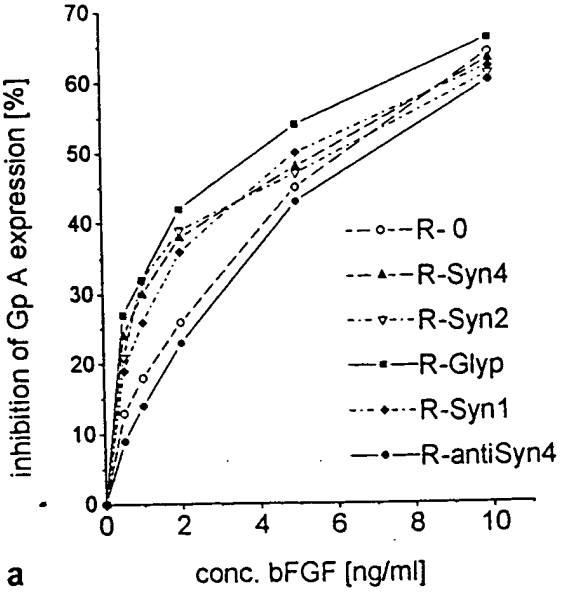

a

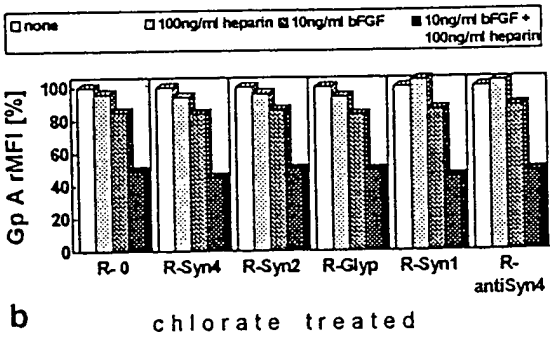

b

chlorate treated

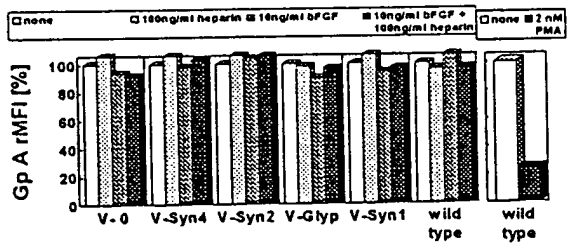

c

Figure 9. Effect of bFGF on GpA expression in K562 cells. The various K562 cell populations were cultured for 72 h in serum-free medium supplemented with BSA, transferrin, and insulin. After exposure to the indicated concentrations of bFGF for an other 72 h in this medium, the cell-surface GpA expression was measured by quantitative immunofluorocytometry. The displayed relative mean fluorescence intensity values were calculated as indicated in Materials and Methods. Receptor-transfected cell populations (*a*) responded with a dose-dependent decrease in GpA expression. At the maximal concentration of 10 ng/ml of bFGF, the GpA was reduced by 60–70% in all transfectants. PG-transfected clones, however, responded at significantly lower bFGF concentrations than *R*-0 and *R*-anti-Syn4 cells, e.g., at bFGF concentrations as low as 0.5 ng/ml *R*-Glyp still showed a 27% suppression, and *R*-anti-Syn4 cells showed only a 9% suppression. Chlorate-treated *R* cells (*b*) were nearly unresponsive to bFGF, but the effect of bFGF could be restored with exogenous heparin (added at 100 ng/ml). Exposure of the wild-type or the non–receptor-transfected cell populations (*c*) to bFGF in combination with or without heparin did not result in significant changes in GpA mean fluorescence intensity. Treatment of K562 cells with the phorbol ester PMA (2 nM, over 72 h) induced an 80% loss of GpA expression (shown only for wild-type cells in *c*).

ing interactions. A low incidence of active HS sequences in these PGs may be compensated by their membrane anchorage and concentration at the cell surface.

K562 Cells as a Model for Studying Cell-surface HS

K562 cells were selected for these studies because a survey of a large panel of cells with the HS-specific mAbs 10E4 and 3G10 had indicated that these cells were able to synthesize authentic HS, a minimal requirement to potentially support bFGF–receptor interactions, but in low and possibly insufficient amounts to support these interactions efficiently. The aim was to test whether transfections with cDNAs coding for cell-surface PGs could compensate for this relative HS deficiency. The results show that after these transfections, K562 cells are capable of expressing ~5–10-fold higher levels of cell-surface HS, and that the endogenous and transfectant cell-surface PGs that account for this HS can be fractionated in distinctive charge and size classes that result from the intrinsic variability of the posttranslational modifications of these proteins. Comparative quantitative immunocytofluorometry indicated that the HS expression in the K562 transfectants reached similar levels as in human lung fibroblasts (not shown), suggesting that these transfectants provide relevant models for the display of cell-surface HS in constitutive high expressors. It may be significant, however, that the gain of HS in these cells is more pronounced for the PG fractions that elute early from MonoQ (substituted with fewer and less sulfated chains) than for those that elute later in the salt gradient (substituted with more and more highly sulfated chains) (Fig. 4). Together with the reduced levels of HS glycanation of the endogenous syndecan-4 in the transfectants, these results suggest that in K562 cells, individual core proteins compete with each other for a limiting HS glycanation machinery, and that in high expressors, a smaller proportion of the PGs therefore reaches the most extensive levels of substitution and modification. These findings are reminiscent of results obtained for the synthesis of antithrombin III–binding HS sequences in transfectant endothelial and fibroblastic cells, where several consecutive transductions of a syndecan-4 expression vector progressively enhanced the production of core protein and total HS in these cells, but reduced the levels of antithrombin III–binding HS present on transfectant and endogenous PG (Shworak et al., 1994). This suggests that the production of defined HS sequences can be saturated and that the specific activities of the PGs in terms of these sequences depend at least in part on the core protein expression levels. In the K562 PG transfectants, the transfectant cores drive the synthesis of ~90% of the cell-surface HS, but these expression levels still appear compatible with the production of fully modified forms of PG and the produc-

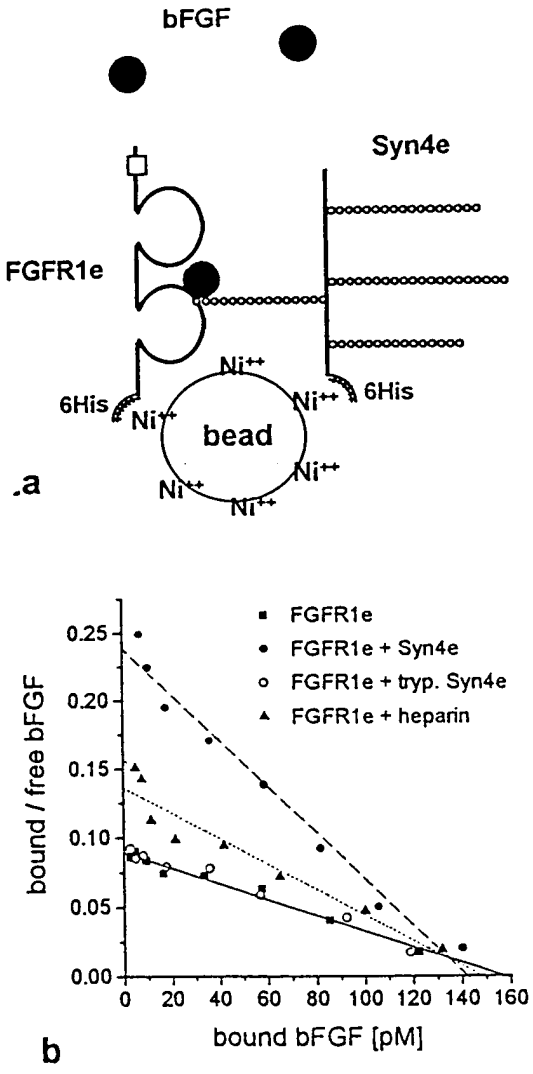

Figure 10. Coimmobilized HSPG increases the affinity of bFGF for the ectodomain of FGFR1. Plasmids coding for COOH-terminal 6xHis-tailed forms of the ectodomain of FGFR1 (*FGFR1e*) and syndecan-4 (*Syn4e*) were expressed in K562 cells. These 6xHis tags bind with high affinity ($K_d = 10^{-13}$) to Ni-loaded beads (*a*). Binding of radiolabeled bFGF to Ni-NTA–immobilized FGFR1e in the presence or absence of Syn4e, trypsinized Syn4e (which lacks the 6xHis tag and therefore can not bind to the Ni-NTA resin), or heparin was measured at varying concentrations of growth factor (*b*). The affinity of the binding was calculated from the specifically bound versus free radiolabel at various bFGF concentrations. The data are depicted as Scatchard plots. The concentrations of FGFR1e and Syn4e used were such that the maximal number of bFGF-binding sites provided by each component individually (as determined from separate binding experiments) were identical.

tion of the sequences required for bFGF binding and activation. It is conceivable, however, that similar transfections in cells that express large near-saturating amounts of endogenous HSPG could have adverse effects on the synthesis or colinearity of the sequences that are required for bFGF activation, and that this competition might explain how the expression of syndecan-1 in 3T3 cells suppresses the growth response of these cells to bFGF (Mali et al., 1993).

Facilitation of bFGF–Receptor Binding by Cell-surface HS

The effects of chlorate on the binding of bFGF to *R* transfectants and of heparin on chlorate-treated *R* transfectants were consistent with the observations of several other investigators, suggesting a clear HS-dependency of the specific binding of bFGF to FGFR1(IIIc) and indicating that K562 cells were able to produce the HS sequences that are required for the stimulation of this binding. Heparin, however, also enhanced the levels of specific bFGF binding in *R*-0 cells that were not treated with chlorate, indicating lack of receptor saturation in these cells despite normally saturating concentrations of added growth factor, possibly caused by PG receptor imbalances in these receptor-overexpressing cells. The saturation of the receptor in the *R*-PG transfectants confirms this interpretation and indicates that all the different cell-surface PGs tested can complement for the relative HS deficiency of these cells. Reduced levels of receptor saturation in *R*–anti–syndecan-4 transfectants in comparison to *R*-0 cells support the contention that cell-surface PGs contribute to receptor binding in K562 cells, in apparent discrepancy with previous suggestions that these forms are inactive or even inhibitory in this respect (Aviezer et al., 1994*a*). Distinctive PG requirements for activation of the receptor in *cis*- and *trans*-modes, or unique activities of the PGs in these cells, could account for this discrepancy.

Our cell-free assay demonstrates that bFGF binds to the ectodomain of the two-Ig domain form of human FGFR1 in the absence of heparin, and that heparin moderately enhances the affinity of this binding interaction, which agrees with the results reported by several other investigators with similar constructs (Kiefer et al., 1991; Bergonzoni et al., 1992; Roghani et al., 1994). In this assay, a syndecan ectodomain made by K562 cells that could be coimmobilized with receptor proved to be an effective strengthener of the binding interaction, whereas the same ectodomain provided in equimolar amounts, but in soluble form, had no detectable activity. The failure of these soluble ectodomains is in agreement with previous binding results obtained for receptor–reporter fusion proteins and soluble cell-surface PG in cell-free assays (Aviezer et al., 1994*a*) and for the activation of receptor in HS-deficient cells by exogenously added PG (Aviezer et al., 1994*b*), whereby several of the cell-surface PGs that were studied here were proven to be ineffective. All together, these findings suggest that cell-surface PGs are not intrinsically ineffective, but that membrane-imbedded and solubilized forms of the PGs from a particular cell differ in their activities on bFGF–receptor binding in that the former lead to higher effective concentrations of reactants with higher apparent binding affinities as a result.

The results from the affinity cross-linking experiments are also consistent with a role for cell-surface HS in the receptor–ligand interaction. They show specific receptor binding in *R* cells and an increase in receptor–cross-linked ^{125}I-bFGF for the *R*-0 and chlorate-treated *R*-PG cell populations upon the addition of heparin, consistent with the stimulatory effect of heparin on receptor occupancy in these cells. Somewhat surprisingly, since heparin did not promote or decrease receptor occupancy in *R*-PG trans-

fectants, heparin very consistently decreased the cross-linking efficiency in all *R*-PG cells. This difference in receptor–ligand cross-linking efficiency between PG-mediated and (in the presence of a large excess of heparin) probably heparin-mediated receptor–ligand complexes suggests the formation of distinctive receptor–ligand complexes in the two situations. Cross-linking likely involves sites within the bFGF–receptor complex other than those directly involved in the binding interaction, and depends on the configuration of the complex, the realized approximations, and the stability of the complex. Conformational changes induced by exogenous heparin, but not by HS, that may be irrelevant for binding might disturb bFGF cross-linking. The finding that ternary complexes mediated by surface-immobilized ectodomains are more stable than heparin-mediated complexes might also be relevant and relate to the reduction in FGFR–FGF cross-links in the presence of heparin. The observation at least suggests that exogenously added heparin does not exactly reproduce the process of PG-mediated binding and cannot be used as the sole model to define the molecular requirements for receptor occupancy by growth factor and activation.

Receptor Activation by Cell-surface HS

The fact that K562 cells that expressed high levels of cell-surface HS, (*R*-PG cells) responded more clearly to low bFGF concentrations than low expressors, (*R*-0 and *R*-anti-Syn4 cells) further supports the contention that, at low doses of growth factor, ligand-induced FGFR stimulation and signaling depend on the availability of sufficient and appropriate sources of HS at the cell surface (Roghani et al., 1994). Our data show that several different cell-surface PGs originating from separate molecular families are able to provide this source, at least for the bFGF–FGFR1 interaction, in cells with the appropriate HS-synthesizing machinery, and when expressed at the cell surface of the receptor-expressing cells. Relatively low specific activities of the cell surface PGs with respect to the fostering of receptor–growth factor interactions may be compensated by this membrane association, essentially limiting the activity of these PGs to the *cis* mode. Considering the relative ineffectiveness of the soluble PG ectodomains as promoters of the bFGF–receptor interaction, it may be significant that all syndecans have conserved a putative protease cleavage site in their ectodomain, and that glypicans are linked to the cell surface by phospholipase-susceptible bonds. Syndecan shedding is known to occur, at least under in vitro conditions, and phospholipase D activities that release soluble bFGF–HSPG complexes have recently been identified in HeLa cell and bone marrow stromal cell cultures (Metz et al., 1994). From our results, we would predict that at low concentrations of growth factor, protease- and lipase-induced sheddings of the cell-surface PGs will lead to a dilution of the reactants, dissociation of the receptor complexes, and downregulation of the signaling pathway, unless other PGs with possibly unique *trans*-activation potentials, such as the perlecan synthesized by cultured fetal lung fibroblasts (Aviezer et al., 1994*b*), can compensate for this loss. This leads to the speculation that PG shedding may provide means for acute regulation of *cis*-activated heparin-dependent pathways, next to possibly slower regulations via controls on the synthesis of the core proteins and the required HS sequences.

The authors are particularly grateful to Helga Ceulemans, Christien Coomans, and An Rayé for their expert technical assistance, and to Bart de Strooper, Mathijs Baens, Luc van Rompaey, and Peter Marynen for many helpful suggestions. We also thank the staff of the Laboratories for Experimental Immunology and Experimental Hematology for advice on the use of the FACSort and the Lysis II program.

This work was supported by grants 3.0073.91 and 1.5.418.93 from the Nationaal Fonds voor Wetenschappelijk Onderzoek of Belgium, by grant 7.0033.92 from the action Levenslijn-Multiple Sclerose, by a grant from the Belgian Cancer Association, and by the Interuniversitary Network for Fundamental Research sponsored by the Belgian government (1991–1995). G. David is a research director of the Nationaal Fonds voor Wetenschappelijk Onderzoek of Belgium.

Received for publication 10 February 1995 and in revised form 22 November 1995.

References

Armstrong, E., S. Vainikka, J. Partanen, J. Korhonen, and R. Alitalo. 1992. Expression of fibroblast growth factor receptors in human leukemia cells. *Cancer Res.* 52:2004–2007.

Aviezer, D., E. Levy, M. Safran, C. Svahn, E. Buddecke, A. Schmidt, G. David, I. Vlodavsky, and A. Yayon. 1994*a*. Differential structural requirements of heparin and heparan sulfate proteoglycans that promote binding of basic fibroblast growth factor to its receptor. *J. Biol. Chem.* 269:114–121.

Aviezer, D., D. Hecht, M. Safran, M. Eisinger, G. David, and A. Yayon. 1994*b*. Perlecan, basal lamina proteoglycan, promotes basic fibroblast growth factor-receptor binding, mitogenesis, and angiogenesis. *Cell.* 79:1005–1013.

Bergonzoni, L., P. Caccia, O. Cletini, P. Sarmientos, and A. Isacchi. 1992. Characterization of a biologically active extracellular domain of fibroblast growth factor receptor 1 expressed in *Escherichia coli*. *Eur. J. Biochem.* 210:823–829.

Chellaiah, A.T., D.G. McEwen, S. Werner, J. Xu, and D.M. Ornitz. 1994. Fibroblast growth factor receptor (FGFR) 3. Alternative splicing in immunoglobulin-like domain III creates a receptor highly specific for acidic FGF/FGF-1. *J. Biol. Chem.* 269:11620–11627.

David, G., V. Lories, B. Decock, P. Marynen, J.-J. Cassiman, and H. van den Berghe. 1990. Molecular cloning of a phosphatidylinositol-anchored membrane heparan sulfate proteoglycan from human lung fibroblasts. *J. Cell Biol.* 111:3165–3176.

David, G., X.M. Bai, B. van der Schueren, J.-J. Cassiman, and H. van den Berghe. 1992*a*. Developmental changes in heparan sulfate expression: in situ detection with monoclonal antibodies. *J. Cell Biol.* 119:961–975.

David, G., B. van der Schueren, P. Marynen, J.-J. Cassiman, and H. van den Berghe. 1992*b*. Molecular cloning of amphiglycan, a novel integral membrane heparan sulfate proteoglycan expressed by epithelial and fibroblastic cells. *J. Cell Biol.* 118:961–969.

Dionne, C.A., G. Crumley, F. Bellot, J.M. Kaplow, G. Searfoss, M. Ruta, W.H. Burgess, M. Jaye, and J. Schlessinger. 1990. Cloning and expression of two distinct high-affinity receptors cross reacting with acidic and basic fibroblast growth factors. *EMBO (Eur. Mol. Biol. Organ.) J.* 9:2685–2692.

Eisemann, A., J.A. Ahn, G. Graziani, S.R. Tronick, and D. Ron. 1991. Alternative splicing generates at least five different isoforms of the human basic-FGF receptor. *Oncogene.* 6:1195–1202.

Guimond, S., M. Maccarana, B.B. Olwin, U. Lindahl, and A.C. Rapraeger. 1993. Activating and inhibitory heparin sequences for FGF-2 (basic FGF). Distinct requirements for FGF-1, FGF-2, and FGF-4. *J. Biol. Chem.* 268: 23906–23914.

Habuchi, H., S. Suzuki, T. Saito, T. Tamura, T. Harada, K. Yoshida, and K. Kimata. 1992. Structure of a heparan sulphate oligosaccharide that binds to basic fibroblast growth factor. *Biochem. J.* 285:805–813.

Hochuli, E., H. Döbeli, and A. Schacher. 1987. New metal chelate adsorbant selective for proteins and peptide containing neighboring histidine residues. *J. Chromatogr.* 411:177–184.

Honma, Y., J. Okabe-Kado, M. Hozumi, Y. Uehara, and S. Mizumi. 1989. Induction of erythroid differentiation of K562 human leukemic cells by herbimycin A, an inhibitor of tyrosine kinase activity. *Cancer Res.* 49:331–334.

Ishihara, M., D.J. Tyrrell, G.B. Stauber, S. Brown, L.S. Cousens, and R.J. Stack. 1993. Preparation of affinity-fractionated, heparin-derived oligosaccharides and their effects on selected biological activities mediated by basic fibroblast growth factor. *J. Biol. Chem.* 268:4675–4683.

Johnson, D.E., J. Lu, H. Chen, S. Werner, and L.T. Williams. 1991. The human fibroblast growth factor receptor genes: a common structural arrangement underlies the mechanism for generating receptor forms that differ in their third immunoglobulin domain. *Mol. Cell. Biol.* 11:4627–4634.

Kan, M., F. Wang, J. Xu, J.W. Crabb, J. Hou, and W.L. McKeehan. 1993. An es-

sential heparin-binding domain in the fibroblast growth factor receptor kinase. *Science (Wash. DC).* 259:1918–1921.

Kato, M., H. Wang, M. Bernfield, J.T. Gallagher, and J.E. Turnbull. 1994. Cell surface syndecan-1 on distinct cell types differs in fine structure and ligand binding of its heparan sulfate chains. *J. Biol. Chem.* 269:18881–18890.

Keegan, K., D.E. Johnson, L.T. Williams, and M.J. Hayman. 1991. Isolation of an additional member of the fibroblast growth factor receptor family, FGFR-3. *Proc. Natl. Acad. Sci. USA.* 88:1095–1099.

Kiefer, M.C., A. Baird, T. Nguyen, C. George-Nascimento, O.B. Mason, L.J. Boley, P. Valenzuela, and P.J. Barr. 1991. Molecular cloning of a human basic fibroblast growth factor receptor cDNA and expression of a biologically active extracellular domain in a baculovirus system. *Growth Factors.* 5:115–127.

Lories, V., J.-J. Cassiman, H. van den Berghe, and G. David. 1989. Multiple distinct membrane heparan sulfate proteoglycans in human lung fibroblasts. *J. Biol. Chem.* 264:7009–7016.

Lories, V., H. De Boeck, G. David, J.-J. Cassiman, and H. van den Berghe. 1987. Heparan sulfate proteoglycans of human lung fibroblasts. *J. Biol. Chem.* 262:854–859.

Maccarana, M., B. Casu, and U. Lindahl. 1993. Minimal sequence in heparin/heparan sulfate required for binding of basic fibroblast growth factor. *J. Biol. Chem.* 268:23898–23905.

Mali, M., K. Elenius, H.M. Miettinen, and M. Jalkanen. 1993. Inhibition of basic fibroblast growth factor-induced growth promotion by overexpression of syndecan-1. *J. Biol. Chem.* 268:24215–24222.

Mali, M., P. Jaakkola, A.-M. Arvilommi, and M. Jalkanen. 1990. Sequence of human syndecan indicates a novel gene family of integral membrane proteoglycans. *J. Biol. Chem.* 265:6884–6889.

Marynen, P., J. Zhang, J.-J. Cassiman, H. van den Berghe, and G. David. 1989. Partial primary structure of the 48- and 90-kilodalton core proteins of cell surface-associated heparan sulfate proteoglycans of lung fibroblasts. *J. Biol. Chem.* 264:7017–7024.

Mason, I.J. 1994. The ins and outs of fibroblast growth factors. *Cell.* 78:547–552.

Metz, C.N., G. Brunner, N.H. Choi-Muira, H. Nguyen, J. Gabrilove, I.W. Caras, N. Altszuler, D.B. Rifkin, E.L. Wilson, and M.A. Davitz. 1994. Release of GPI-anchored membrane proteins by a cell-associated GPI-specific phospholipase D. *EMBO (Eur. Mol. Biol. Organ.) J.* 13:1741–1751.

Miki, T., D.P. Bottaro, T.P. Fleming, C.L. Smith, W.H. Burgess, A.M. Chan, and S.A. Aaronson. 1992. Determination of ligand-binding specificity by alternative splicing: two distinct growth factor receptors encoded by a single gene. *Proc. Natl. Acad. Sci. USA.* 89:246–250.

Moscatelli, D. 1987. High and low affinity binding sites for basic fibroblast growth factor on cultured cells: absence of a role for low affinity binding in the stimulation of plasminogen activator production by bovine capillary endothelial cells. *J. Cell. Physiol.* 131:123–130.

Nugent, M.A., and E.R. Edelman. 1992. Kinetics of basic fibroblast growth factor to its receptor and heparan sulfate proteoglycan: a mechanism for cooperativity. *Biochemistry.* 31:8876–8883.

Nurcombe, V., M.D. Ford, J.A. Wildschut, and P.F. Bartlett. 1993. Developmental regulation of neural response to FGF-1 and FGF-2 by heparan sulfate proteoglycan. *Science (Wash. DC).* 260:103–106.

Ornitz, D.M., A. Yayon, J.G. Flanagan, C.M. Svahn, E. Levi, and P. Leder. 1992. Heparin is required for cell-free binding of basic fibroblast growth factor to a soluble receptor and for mitogenesis in whole cells. *Mol. Cell. Biol.* 12:240–247.

Pantoliano, M.W., R.A. Horlick, B.A. Springer, D.E. Van Dyk, T. Tobery, D.R. Wetmore, J.D. Lear, A.T. Nahapetian, J.D. Bradley, and W.P. Sisk. 1994. Multivalent ligand-receptor binding interactions in the fibroblast growth factor system produce a cooperative growth factor and heparin mechanism for receptor dimerization. *Biochemistry.* 33:10229–10248.

Papayannopoulou, T., B. Nakamoto, T. Yokochi, A. Chait, and R. Kannagi. 1983. Human erythroleukemia cell line (HEL) undergoes a macrophage-like shift with TPA. *Blood.* 62:832–845.

Partanen, J., T.P. Mäkelä, E. Eerola, J. Korhonen, H. Hirvonen, L. Claesson-Welsh, and K. Alitalo. 1991. FGFR-4, a novel acidic fibroblast growth factor receptor with a distinct expression pattern. *EMBO (Eur. Mol. Biol. Organ.) J.* 10:1347–1354.

Rapraeger, A.C., A. Krufka, and B.B. Olwin. 1991. Requirement of heparan sulfate for bFGF-mediated fibroblast growth and myoblast differentiation. *Science (Wash. DC).* 252:1705–1708.

Richardson, J.M., A.O. Morla, and J.Y.J. Wang. 1987. Reduction in protein tyrosine phosphorylation during differentiation of human leukemia cell line K562. *Cancer Res.* 47:4066–4070.

Roghani, M., A. Mansukhani, P. Dell'Era, P. Bellosta, C. Basilico, D.B. Rifkin, and D. Moscatelli. 1994. Heparin increases the affinity of basic fibroblast growth factor for its receptor but is not required for binding. *J. Biol. Chem.* 269:3976–3984.

Saiki, R.K., D.H. Gelfand, S. Stoffel, S.J. Scharf, R. Higuchi, G. T. Horn, K.B. Mullis, and H.A. Ehrlich. 1988. Primer-directed enzymatic amplification of DNA with a thermostable DNA polymerase. *Science (Wash. DC).* 239:487–491.

Sambrook, J., E.F. Fritsch, and T. Maniatis. 1989. Molecular Cloning: A Laboratory Manual. Cold Spring Harbor Laboratory Press. Cold Spring Harbor, NY.

Scatchard, G. 1949. The attractions of proteins for small molecules and ions. *Ann. NY Acad. Sci.* 51:660–672.

Schägger, H., and G. von Jagow. 1987. Tricine-sodium dodecyl sulfate-polyacrylamide gel electrophoresis for the separation of proteins in the range from 1 to 100 kDa. *Anal. Biochem.* 166:368–379.

Seno, M., R. Sasada, T. Kurokawa, and K. Igarashi. 1990. Carboxyl-terminal structure of basic fibroblast growth factor significantly contributes to its affinity for heparin. *Eur. J. Biochem.* 188:239–245.

Shively, J.E., and H.E. Conrad. 1976. Formation of anhydrosugars in the chemical depolymerization of heparin. *Biochemistry.* 15:3932–3942.

Shworak, N.W., M. Shirakawa, S. Colliec-Jouault, J. Liu, R.C. Mulligan, L.K. Birinyi, and R.D. Rosenberg. 1994. Pathway-specific regulation of the synthesis of anticoagulantly active heparan sulfate. *J. Biol. Chem.* 269:24941–24952.

Spivak-Kroizman, T., M.A. Lemmon, I. Dikić, J.E. Ladbury, D. Pinchasi, J. Huang, M. Jaye, G. Crumley, J. Schlessinger, and I. Lax. 1994. Heparin-induced oligomerization of FGF molecules is responsible for FGF receptor dimerization, activation, and cell proliferation. *Cell.* 79:1015–1024.

Turnbull, J.E., D.G. Fernig, Y. Ke, M.C. Wilkinson, and J.T. Gallagher. 1992. Identification of the basic fibroblast growth factor binding sequence in fibroblast heparan sulfate. *J. Biol. Chem.* 267:10337–10341.

Tyrrell, D.J., M. Ishihara, N. Rao, A. Horne, M. C. Kiefer, G. B. Stauber, L.H. Lam, and R.J. Stack. 1993. Structure and biological activities of a heparin-derived hexasaccharide with high affinity for basic fibroblast growth factor. *J. Biol. Chem.* 268:4684–4689.

Walker, A., J.E. Turnbull, and J.T. Gallagher. 1994. Specific heparan sulfate saccharides mediate the activity of basic fibroblast growth factor. *J. Biol. Chem.* 269:931–935.

Wennström, S., C. Sandström, and L. Claesson-Welsh. 1991. cDNA cloning and expression of a human FGF receptor which binds acidic and basic FGF. *Growth Factors.* 4:197–208.

Werner, S., D.S. Duan, C. de Vries, K.G. Peters, D.E. Johnson, and L. T. Williams. 1992. Differential splicing in the extracellular region of fibroblast growth factor receptor 1 generates receptor variants with different ligand-binding specificities. *Mol. Cell. Biol.* 12:82–88.

Yayon, A., M. Klagsbrun, J.D. Esko, P. Leder, and D.M. Ornitz. 1991. Cell surface, heparin-like molecules are required for binding of basic fibroblast growth factor to its high affinity receptor. *Cell.* 64:841–848.

Yayon, A., Y. Zimmer, G.H. Shen, A. Avivi, Y. Yarden, and D. Givol. 1992. A confined variable region confers ligand specificity on fibroblast growth factor receptors: implications for the origin of the immunoglobulin fold. *EMB (Eur. Mol. Biol. Organ.) J.* 11:1885–1890.

The Melanocortin Receptors: Agonists, Antagonists, and the Hormonal Control of Pigmentation

ROGER D. CONE,* DONGSI LU,* SANDHYA KOPPULA,* DAG INGE VAGE,† HELGE KLUNGLAND,† BRUCE BOSTON,* WENBIAO CHEN,* DAVID N. ORTH,‡ COLIN POUTON,§ AND ROBERT A. KESTERSON*

**Vollum Institute for Advanced Biomedical Research, Oregon Health Sciences University, Portland, Oregon 97201; †Department of Animal Science, Agricultural University of Norway, Ås, Norway N-1432; ‡Department of Medicine, Vanderbilt University Medical Center, Nashville, Tennessee 37232–6306; §School of Pharmacy and Pharmacology, University of Bath, Bath, BA2 7AY United Kingdom*

ABSTRACT

Molecular cloning experiments have led to the identification and characterization of a family of five receptors for the melanocortin (melanotropic and adrenocorticotropic) peptides. The first two members of the family cloned were the well-characterized melanocyte-stimulating hormone receptor (MSH-R) and adrenocorticotropin receptor (ACTH-R). The three new melanocortin receptors have been termed the MC3-R, MC4-R, and MC5-R, according to the order of their discovery, and little is known at this point concerning their function.

Agouti and *extension* are two genetic loci known to control the amounts of eumelanin (brown-black) and phaeomelanin (yellow-red) pigments. Chromosomal mapping demonstrated that the MSH-R, now termed MC1-R, mapped to *extension*. *Extension* was shown to encode the MC1-R, and mutations in the MC1-R are responsible for the different pigmentation phenotypes caused by this locus. Functional variants of the MC1-R, originally characterized in the mouse, have now also been identified in the guinea pig and cow. Dominant constitutive mutants of the MC1-R are responsible for causing dark black coat colors while recessive alleles result in yellow or red coat colors.

Agouti, a secreted 108 amino acid peptide produced within the hair follicle, acts on follicular melanocytes to inhibit α-MSH-induced eumelanin production. Experiments demonstrate that *agouti* is a high-affinity antagonist, acting at the MC1-R to block α-MSH stimulation of adenylyl cyclase, the effector through which α-MSH induces eumelanin synthesis. The MC1-R is thus a unique bifunctionally controlled receptor, activated by α-MSH and antagonized by *agouti*, both contributing to the variability seen in mammalian coat colors. The variable tan and black coat color patterns seen in the German Shepherd, for example, can now be understood on the molecular level as the interaction of a number of *extension* and *agouti* alleles encoding variably functioning receptors and a differentially expressed antagonist of the receptor, respectively.

I. Introduction

Pigmentation is not ordinarily classified as an endocrinological phenomenon. Nevertheless there are many fascinating and striking examples of hormonal control of hair and skin color, such as the seasonal control of pelage in the snowshoe

Copyright © 1996 by The Endocrine Society
All rights of reproduction in any form reserved.

hare, *Leptus americanus* (Searle, 1968), or the arctic fox, *Alopex lagopus* (Nes *et al.*, 1988); adaptation to background color in reptiles; and the hyperpigmentation in humans from endocrine disorders such as Addison's disease that result in elevation of circulating adrenocorticotropin (ACTH) levels. One pathway for hormonal control of pigmentation has been elucidated recently with the molecular characterization of the melanocyte-stimulating hormone (MSH) receptor (Mountjoy *et al.*, 1992) and the antagonist of this receptor, known as the *agouti* signaling peptide (Bultman *et al.*, 1992; Lu *et al.*, 1994; Miller *et al.*, 1993). It has been known for many years that two genetic loci, *extension*, which encodes the MSH receptor, and *agouti* are commonly involved in controlling the regional distribution of brown-black (eumelanin) and yellow-red (phaeomelanin) pigments in the coat of an animal, as well as the distribution of these two pigments along each individual hair shaft (Searle, 1968). For example, the varying distribution of tan and black pigments in the German Shepherd dog results from the interaction of a number of alleles at *extension* and *agouti* (Little, 1957).

The principal pigment cells, melanocytes, elaborate a number of enzymes that act in concert to synthesize from tyrosine both eumelanin and phaeomelanin, the two major classses of melanin pigments. The rate-limiting enzyme in this process, tyrosinase (Hearing and Jimenez, 1987; Pawelek, 1976), is regulated both transcriptionally and post translationally by intracellular cAMP (Fuller *et al.*, 1987; Halaban *et al.*, 1984; Hoganson *et al.*, 1989; Wong and Pawelek, 1975). Phaeomelanin is the major default product of this biosynthetic pathway, with eumelanin synthesis resulting from increased tyrosinase activity. MSH, produced by the melanotroph cells of the intermediate lobe of the pituitary and also possibly by the melanocytes and hair follicle cells, is the primary hormonal regulator of pigmentation and acts by binding to its receptor and elevating intracellular cAMP, thus inducing tyrosinase activity. Similarly, *agouti* has been known for some time to be produced by the hair follicle and act in trans on the follicular melanocytes to inhibit eumelanin synthesis, thereby resulting in phaeomelanin production (Silvers, 1958; Silvers and Russel, 1955).

The molecular nature of different MSH receptor alleles and their interaction with the agonist MSH and the antagonist *agouti* to produce variation in mammalian coat color is the main subject of this review. The ability of the *agouti* peptide, when expressed outside of the hair follicle, to cause obesity will also be examined. To discuss either of these subjects it is necessary to first review the melanocortin peptides and their receptors.

II. The Melanocortin Peptides

The term "melanocortin" refers to peptides derived from the larger proopiomelanocortin (POMC) polypeptide precursor that possess melanotropic or adrenocorticotropic activity (Fig. 1A). These peptides are produced primarily in the anterior and intermediate lobes of the pituitary and in lower levels in the arcuate nucleus and nucleus of the solitary tract in the brain. POMC has also been

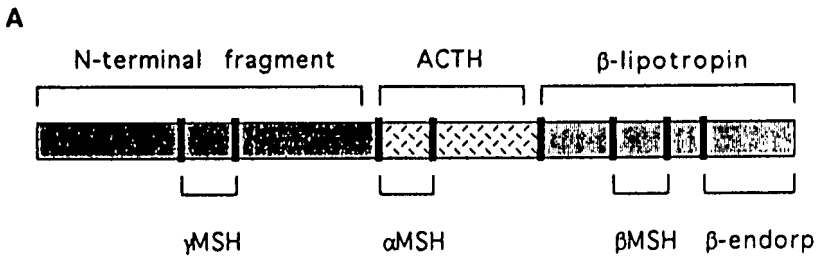

B

ACTH	H2N-SYSMEHFRWGKPVGKKRRPVKVYPNGAEDESAEAFPLEF-
α-MSH	AC-SYSMEHFRWGKPV-NH2
β-MSH	H2N-AEKKDEGPYRMEHFRWGSPPKD-OH
γ-MSH	H2N-YVMGHFRWDRFG-OH
NDP-MSH	AC-SYSXEHZRWGKPV-NH2

FIG. 1. The melanocortin peptides. (A) Structure of the proopiomelanocortin (POMC cursor. Major melanocortin peptides are indicated by brackets and basic dipeptide proteolytic cle. sites are indicated by the heavy bars. (B) Amino acid sequence of the major melanocortin pep All peptides are derived from human POMC with the exception of Nle⁴, D-Phe⁷-α-MSH (NDP-M a potent synthetic analogue. The conserved H-F-R-W pharmacophore is underlined. In the seq of NDP-MSH, X represents norleucine and Z represents D-phenylalanine. [Reprinted with perm from *Ann. N.Y. Acad. Sci.* **680**, 343. 1995.]

reported to be expressed in several other tissues, including keratinocytes and follicle cells, which may be particularly relevant to pigmentation as discu below. These peptides are processed from three different regions of POMC, of which contains a conserved sequence, -His-Phe-Arg-Trp-, that serves a pharmacophore for melanocortin receptor recognition and activation (Fig. (Eberle, 1988; Eberle *et al.*, 1984). Peptides from the amino terminus or N minal POMC are called γ-MSH peptides and are found in a variety of fo ACTH and α-MSH are overlapping peptides cleaved from the middle portion consist of amino acids 1–39 and 1–13, respectively. β-MSH, β-LPH, and γ- all derive from the carboxy-terminal portion of the POMC precursor. A det account of the tissue-specific cleavage and processing of these peptides has reviewed elsewhere (Smith and Funder, 1988).

III. The Melanocortin Receptors

Prior to cloning, two melanocortin receptors, the MSH receptor (MSI and the ACTH receptor (ACTH-R) were known from classical physiological pharmacological studies. The MSH receptor was specifically found on mel

cytes and melanoma cells from a variety of vertebrate organisms, and was reported to respond to nanomolar concentrations of α-MSH by stimulating tyrosinase activity and melanogenesis subsequent to activation of adenylyl cyclase and elevation of intracellular cAMP (Pawelek, 1976). Cross-linking studies had demonstrated this receptor to be present as a molecular species of approximately 45 kd (Gerst *et al.*, 1988; Solca *et al.*, 1989). A high-affinity ACTH receptor had been demonstrated to be expressed in both adrenocortical cells as well as adipocytes, and like the MSH receptor, was found to couple to activation of adenylyl cyclase (Buckley and Ramachandran, 1981; Oelofsen and Ramachandran, 1983).

Two lines of evidence also suggested the presence of high-affinity melanocortin receptors outside of the melanocyte and adrenal cortex, particularly in the central nervous system. First, a large body of literature demonstrated a variety of activities for the melanocortin peptides in the brain (for review, see DeWied and Jolles, 1982). These included, for example, central effects on learning and memory (Garrud *et al.*, 1974; Sandman *et al.*, 1969), temperature regulation (Feng *et al.*, 1987), hypothalamic-pituitary-adrenal (H-P-A) axis control (Calogero *et al.*, 1988; Motta *et al.*, 1965; Suda *et al.*, 1986), and cardiovascular homeostasis (Calogero *et al.*, 1988; Gruber and Callahan, 1989; Motta *et al.*, 1965; Suda *et al.*, 1986). Peripheral effects on inflammation (Catania and Lipton, 1993), nerve regeneration (Bijlsma *et al.*, 1981; Strand and Kung, 1980; Strand *et al.*, 1991), and myoblast proliferation (De Angelis *et al.*, 1992) had also been reported.

Second, high-affinity MSH and ACTH binding sites were reported in the lacrimal gland, brain, and a variety of peripheral sites (Hnatowich *et al.*, 1989; Salomon *et al.*, 1993; Tatro, 1990; Tatro and Reichlin, 1987). Little pharmacological data accompanied these reports, so it was not possible to ascertain whether these were MSH-R, ACTH-R, or novel melanocortin receptor sites.

Our first cloning of melanocortin receptors resulted from attempts to isolate the MSH-R from a human melanoma sample known to express a high number of MSH binding sites (Mountjoy *et al.*, 1992). Degenerate oligonucleotides were designed to recognize all G protein-coupled receptor sequences known as of approximately 1991, and these were used in polymerase chain reaction (PCR) with first-strand cDNA from the melanoma tissue. A large number of resulting fragments were subcloned and sequenced, and one fragment was identified as a putative MSH receptor based on its ability to recognize a mRNA specifically expressed in melanocytes. This fragment was then used as a hybridization probe to clone a mouse MSH-R cDNA and a human genomic MSH-R sequence. The human MSH-R was independently cloned by Chhajlani and Wikberg (1992) using a similar method.

The amplification from human melanoma tissue also produced a sequence fragment that was clearly a unique G protein-coupled receptor highly related to the MSH-R. Northern hybridization analysis clearly demonstrated that this fragment recognized a mRNA specific to adrenal tissue and was thus a candidate ACTH-R. This probe was used to isolate a human genomic ACTH-R sequence

(Mountjoy *et al.*, 1992) as well as a bovine ACTH-R cDNA (Cone and Mount 1993).

PCR using degenerate oligonucleotide primers and low-stringency hyb ization with existing MSH-R and ACTH-R sequences rapidly led to the disco of three additional members of the melanocortin receptor gene family (Barr *al.*, 1994; Chhajlani *et al.*, 1993; Desarnaud *et al.*, 1994; Fathi *et al.*, 1995; G *et al.*, 1993a,b, 1994a; Griffon *et al.*, 1994; Labbe *et al.*, 1994; Mountjoy *et* 1994; Roselli-Rehfuss *et al.*, 1993). Since these receptors had not been cha terized previously using classical pharmacological or physiological methods, have been called the melanocortin-3 , melanocortin-4, and melanocortin-5 re tors (MC3-R, MC4-R, and MC5-R), according to the order of their discovery avoid confusion, many in the field now refer to the MSH-R and ACTH-F MC1-R and MC2-R, respectively, and the corresponding loci in the mouse human genome use this nomenclature as well.

As mentioned above, the MSH-R and ACTH-R appear to be restricte their expression primarily to melanocytes and adrenocortical cells. Northern bridization analysis has demonstrated MC3-R expression in brain and place although reverse transcription-polymerase chain reaction (RT-PCR) has b used to detect the mRNA in stomach, duodenum, and pancreas (Gantz *et* 1993a). *In situ* hybridization has been used to map MC3-R mRNA to 30 diffe rat brain nuclei primarily in hypothalamus and other limbic system struct (Roselli-Rehfuss *et al.*, 1993).

The MC4 receptor mRNA has been found by northern hybridization t expressed only in the brain (Gantz *et al.*, 1993b). Detailed neuroanatomical n ping by *in situ* hybridization demonstrated that this receptor mRNA is much n widely expressed in the rat brain than the MC3-R, being found in 148 diffe brain nuclei in virtually every brain region including cortex, thalamus, hypot amus and limbic system, brain stem, and spinal cord (Mountjoy *et al.*, 1994)

More recently, the MC5-R was cloned from human (Chhajlani *et al.*, 19 mouse (Fathi *et al.*, 1995; Gantz *et al.*, 1994a; Labbe *et al.*, 1994), rat (Gril *et al.*, 1994), and sheep (Barret *et al.*, 1994). This receptor mRNA has a rem ably wide distribution of expression, being found in skin, muscle, thymus, spl ovary, testis, adrenal cortex, lung, brain, and pars tuberalis. The distributio all five receptors is summarized in Table I.

TABLE I
The Melanocortin Receptors

Receptor	Sites of expression	Functions
MC1 (MSH-R)	Melanocytes	Pigmentation
MC2 (ACTH-R)	Adrenal cortex, adipocytes	Steroidogenesi
MC3	Hypothalamus, limbic system, placenta, gut	Unknown
MC4	Hypothalamus, limbic system, cortex, brain stem	Unknown
MC5	Muscle, liver, spleen, lung, brain, adipocytes ...	Unknown

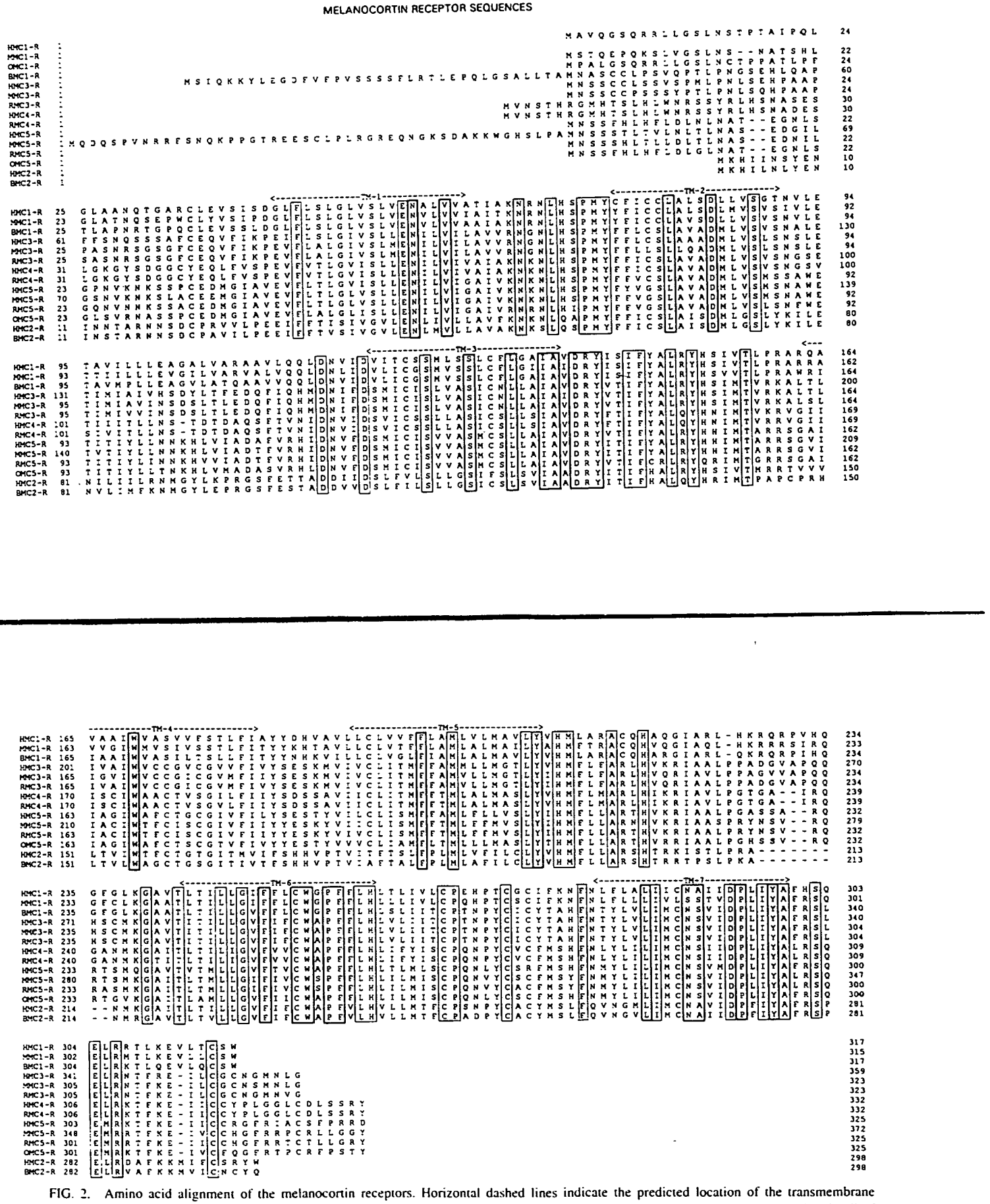

FIG. 2. Amino acid alignment of the melanocortin receptors. Horizontal dashed lines indicate the predicted location of the transmembrane domains. Amino acid residues conserved in many of the G protein-coupled receptors are indicated by heavy boxes, while residues identical in all of the known melanocortin receptors are indicated by the light boxes. Prefixes to each receptor indicate the species (H, human; M, mouse; R, rat; B, bovine; O, ovine).

The five melanocortin receptors are 39–61% identical to one another on the amino acid level, and all belong to the large superfamily of G protein-coupled receptors (Fig. 2). Interestingly, the MC3, MC4, and MC5 receptors appear more related to one another (55–61%) than to the MC1 and MC2 receptors (43–46%), and the MC1 and MC2 receptors are the most distantly related (39%).

Each of the melanocortin receptors couples to activation of adenylyl cyclase but displays a unique pharmacological profile for activation by the different melanocortin peptides (Fig. 3). One report suggests that the MC3-R may also couple to Gq, resulting in a modest activation of inositol 1,3,4-trisphosphate turnover as well (Konda *et al.*, 1994). In a sense, the MC1 and MC2 receptors are the most specialized in terms of ligand recognition. The MC2 receptor exhibits an absolute specificity for ACTH, requiring two peptide domains for recognition and activation, the core H-F-R-W sequence present in all the melanocortin peptides and a highly basic motif found only in the midportion of ACTH. This makes the ACTH receptor unique; the core H-F-R-W pharmacophore is a full agonist, albeit at low affinity, of the other four melanocortin receptors. Most mammalian MC1-Rs demonstrate a preference for α-MSH over ACTH. α-MSH is five-fold more

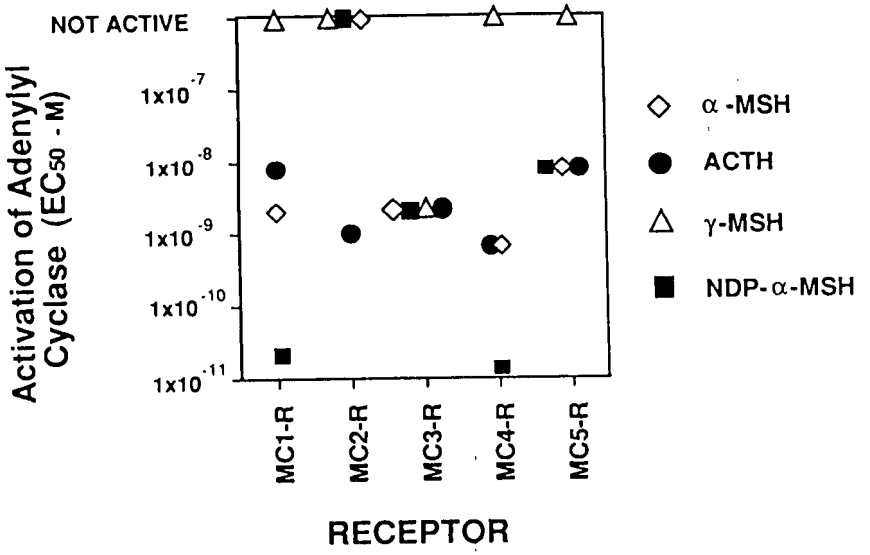

FIG. 3. Pharmacology of the melanocortin receptors. Data represent published EC_{50} values for activation of adenylyl cyclase for each receptor by the peptides indicated. Not active means an EC_{50} >> 10 $^{-7}$M. In the case of the MC2-R, except for ACTH, no activity at all is seen at peptide concentrations up to μM. Data from Mountjoy *et al.*, 1992 (MC1-R), Buckley *et al.*, 1981 (MC2-R), Roselli-Rehfuss *et al.*, 1993 (MC3-R), Mountjoy *et al.*, 1994 (MC4-R), and W. Chen, unpublished data (MC5-R).

potent than ACTH at the murine receptor but may be as high as 1000-fold the MC1-R in *Rana pipiens* or *Anolis carolinenesis* (Eberle, 1988; Eberle *et* 1984). The human MC1-R is apparently unique in responding to ACTH at simi or even lower EC_{50} values than those for α-MSH (Abdel-Malek *et al.*, 1995; H *et al.*, 1994; Mountjoy, 1994).

In contrast, the MC3-R, MC4-R, and MC5-R are less selective, being ec potently activated by α-MSH or ACTH. Furthermore, the MC3-R and MC4 are activated equally well by the predominant form of α-MSH found in the riphery (monoacetyl-α-MSH) as well as the brain (desacetyl-α-MSH) (Mount *et al.*, 1994). The peripheral MC1-R tends to be less potently activated by desacetyl form (Eberle, 1988; Mountjoy, 1994). Interestingly, only one of the f receptors, MC3-R, binds γ-MSH with high affinity (Gantz *et al.*, 1993a; Rosc Rehfuss *et al.*, 1993).

The chromosomal location of all five melanocortin receptors has been de mined in humans by fluorescent *in situ* hybridization (Chowdhary *et al.*, 19 Gantz *et al.*, 1993b, 1994b; Magenis *et al.*, 1994; Malas *et al.*, 1994; Vamva poulos *et al.*, 1993) (Table II). The chromosomal locations in the mouse of MC1-R, MC2-R, MC3-R, and MC5-R have been determined using an inters specific mapping panel (Magenis *et al.*, 1994; R. Cone, unpublished data). surprisingly, the MC1-R was found to map to the distal end of chromosome 8 the mouse, near a pigmentation locus known as *extension*. None of the ot receptors mapped to previously identified gene loci in humans or in the mou However, a rare endocrine disorder, inherited ACTH resistance or familial g cocorticoid deficiency, does map to the ACTH receptor locus in about half of individuals with this disease . In these cases the disease appears to result fi mutations in the coding sequence of the ACTH-R (Clark *et al.*, 1993; Tsigo *al.*, 1993). Difficulty in expression of the ACTH-R in heterologous cells, repo by a number of laboratories, has hampered the study of these ACTH-R alle The recent report of a subclone of the mouse adrenocortical Y1 cell line that l endogenous receptor expression may lead the way for further studies of clo

TABLE II

Human and Murine Map Locations of the Melanocortin Receptors

Receptor	Mouse chromosome	Human chromos
MSH-R	Distal end of Chr 8 identical with the *extension* locus	16q2
ACTH-R	Distal end of Chr18 near *Pdea*	18p11.2
MC3-R	Distal half of Chr 2 near *El-2*	20q13.2
MC4-R	RFLP not yet found	18q22
MC5-R	Distal end of Chr 18, near D18Mit9 and *sy*	18p11.

ACTH receptors (Schimmer *et al.*, 1995). Additionally, it has recently been reported that, in contrast to the human ACTH-R, the mouse ACTH-R is readily expressed in HeLa cells (Cammas *et al.*, 1995).

IV. Allelic Variants of the MC1 Receptor

The *extension* locus, characterized in a wide variety of mammalian species, was named for the extension of black pigmentation that results from the expression of dominant *extension* alleles (Fig. 4; Table III). Cloning of the MC1-R from mice containing different *extension* locus alleles (*e*, E^{So}, and E^{tob}) confirmed that the *extension* locus encoded the MC1 receptor, since 18 of 18 clones isolated from the homozygous recessive yellow *e/e* mouse had a frameshift mutation at amino acid position 183 of the receptor (Robbins *et al.*, 1993). At the time this

FIG. 4. Coat pigmentation in mice containing dominant, wild-type, and recessive alleles at the *extension* locus. The genotypes of the mice, from left to right, are $E^{sw}E^{+}$, $E^{+}E^{+}$, and *ee*.

TABLE III
Examples of Mammalian Extension *Alleles*

Mice	Foxes	Cattle
E^{sw}. . . . . dominant black	E^{A}. . . . dominant black	E^{I}. . . . dominant black
E^{tob}. . . . . dominant black		
E. . . . . normal extension of black	E. . . . . normal extension of black	E. . . . . normal extension of black
		e^{br}. . . . . brindled
e. . . . . non-extension of black		e. . . . . non-extension of black

was determined, no other naturally occuring functional variants in the G prote coupled receptors had been reported. Consequently, the existence of a large nu ber of dominant alleles of this receptor across a wide number of species wa very exciting prospect. A summary of all the mutations in the MC1-R identifi to date is shown in Figure 5.

A. MOUSE

Initially we characterized two of the three dominant alleles found in t mouse, E^{So-J} and E^{tob}. The tobacco allele, E^{tob}, is found in the darkly pigment wild tobacco mouse (*M. poschiavinus*) and results from a serine-to-leucine chan at position 69 in the first intracellular loop of the receptor. Pharmacological when expressed in the heterologous 293 cell line, this receptor has a sligh elevated basal activity but is also able to more significantly stimulate adeny cyclase when compared directly to the wild-type receptor (Robbins *et al.*, 199. In contrast, the sombre allele E^{So-J}, which occurred spontaneously in the CB J strain to produce a dark black mouse (Fig. 4), creates a receptor that is poten constitutively activated and not significantly stimulated even by treatment w

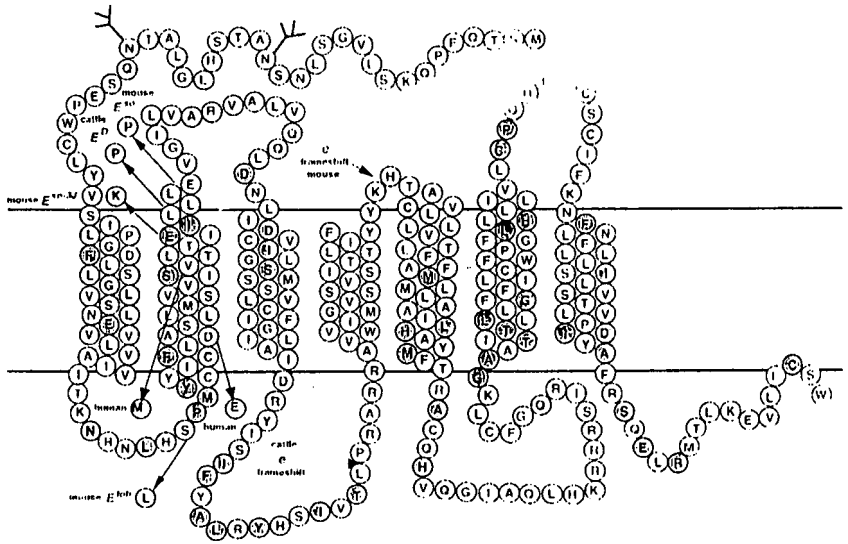

FIG. 5. Summary of mutations identified in the MC1-R. Graphic is a pseudostructural plot the MC1-R indicating putative transmembrane topology. Residues shaded gray are identical in m melanocortin receptors. Mutations are described in more detail in Robbins *et al.*, 1993 (mouse), a Klungland *et al.*, 1995 (cattle). [Reprinted with permission from *Cell* 72, 827–834. Copyright 19 Cell Press.]

high concentrations of α-MSH (Fig. 6A). Preliminarily, we only examined the ability of α-MSH to stimulate this receptor. In subsequent experiments (Fig. 6B), we have discovered that the superpotent α-MSH analogue Nle^4, D-Phe^7-α-MSH (NDP-MSH) is capable of further activating the sombre receptor to maximal levels.

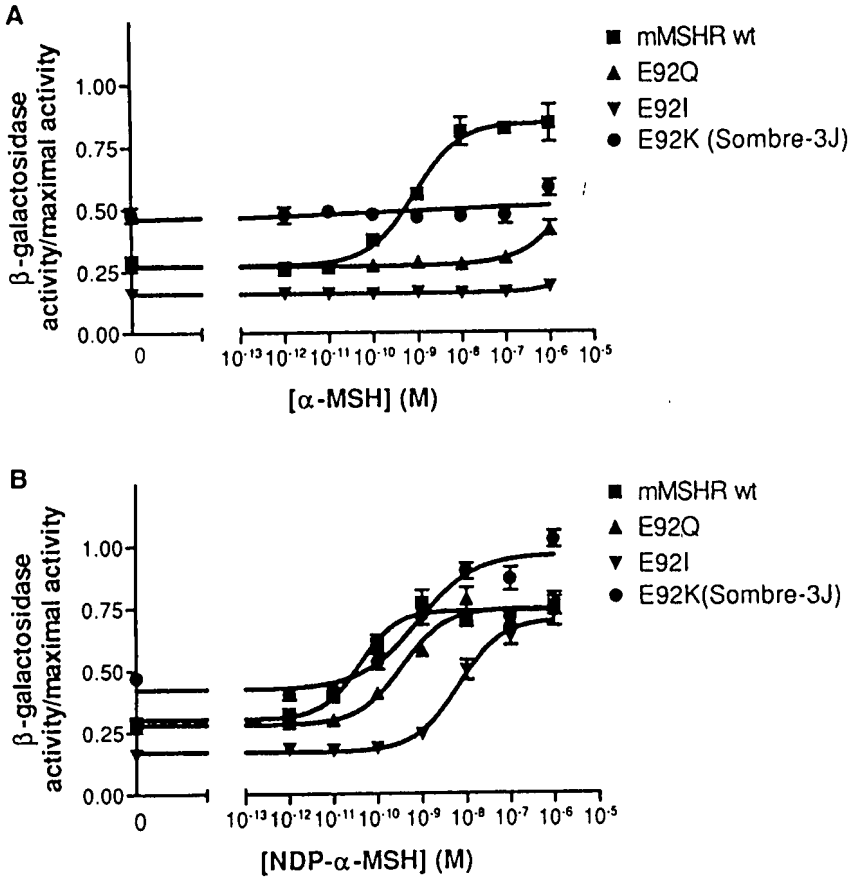

FIG. 6. Pharmacological properties of the mouse $E^{Sm\text{-}J}$ allele of the MC1-R. The wild-type MC1-R, $E^{Sm\text{-}J}$ allele containing the E92K mutation, and *in vitro*-generated E92Q and E92I mutants, cloned into the pcDNA Neo expression vector (Invitrogen), were transfected stably into the HEK 293 cell line. G418^r cell populations were selected and assayed for intracellular cAMP levels following hormone stimulation using a cAMP-dependent β-galactosidase reporter construct as described previously (Chen *et al.*, 1995). Data points are the average of triplicate determination with error bars indicating the standard deviation. Data is normalized to cell number and presented as % maximal activity (10 μM forskolin-stimulated) for each individual cell population. The forskolin-stimulated activities did not vary significantly among cell populations. Panels show data from stimulations with α-MSH (A) and NDP-MSH (B).

Pharmacological data from an independent occurence of the sombre al the mouse (E^{Sm}) has also been obtained recently. This allele results from a le to-proline change at position 98, and is pharmacologically very similar E92K allele ($E^{Sm\text{-}J}$) (Fig. 7).

B. CATTLE

Recent data show that black coat color in Norwegian cattle is due to a inant extension allele, E^D, resulting from a L99P mutation (Fig. 5) (Klungl *al.*, 1995). This mutation is one amino acid carboxy-terminal to the mou mutation, and suggests that any disruption of the α-helix in this region migl be expected to constitutively activate the receptor, although this mutation h yet been characterized pharmacologically. This group also demonstrated th coat color in Norwegian cattle breeds is due to a frameshift in the MSH re (Fig. 5). Since the frameshift in the mouse results in a yellow coat colo clear that modifier genes must exist that can control the range of phaeom pigment.

C. HUMANS

Tremendous polymorphism of skin, hair, and eye color is seen in hu and it would be interesting to determine if any of this results from func variants of the MC1 receptor. To approach this problem we have obtained sa resulting from dermatologic procedures derived from patients characterize

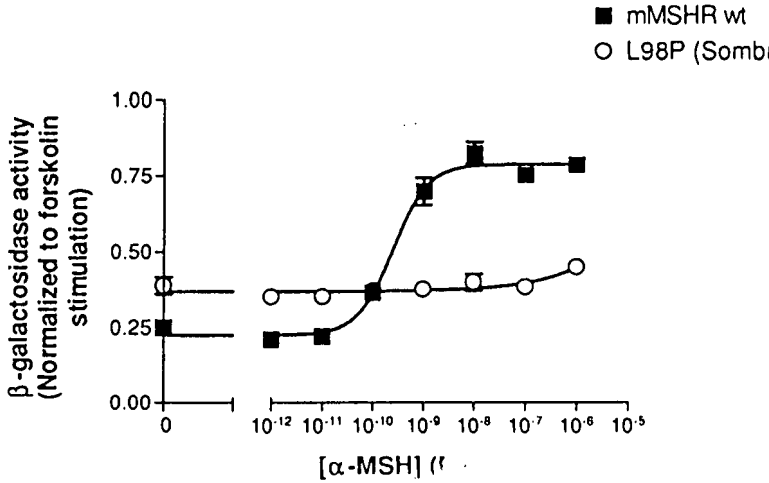

FIG. 7. Pharmacological properties of the mouse E^{Sm} allele of the MC1-R. The E^{Sm} al the MC1-R, containing the L98P mutation, was characterized as described in Figure 6.

regard to hair and eye color and skin type. This latter characteristic was determined according to the method of Fitzpatrick (Pathak *et al.*, 1987) and is a general indicator of the degree of melanization of the skin. MC1 receptor coding fragments were isolated from these samples by PCR and sequenced following subcloning. After completing the sequence of the receptors from only a small number of individuals, two coding polymorphisms of the MC1-R were identified, V92M and D84E. Individuals were found that were both heterozygous and homozygous for V92M, and the one D84E allele was found in an individual that was a compound heterozygote, also containing the V92M allele (Table IV). Interestingly, the V92M allele does appear nonrandomly distributed across individuals categorized according to skin type, being present in type I individuals with an allele frequency of 0.11 and individuals with type II skin at a frequency of 0.02. In preliminary experiments we do not see any pharmacological consequences of these polymorphisms. Nevertheless, it is intriguing that these alterations cluster in TM2 along with other naturally occuring variants of the receptor found in other species (Fig. 5).

D. GUINEA PIG

Variegated pigment patterns (i.e. coats containing an irregular patchwork of two or more colors) have often been associated with heterozygosity of X-linked pigment genes in the female animal. A classic example is the orange locus (*O*) in the cat, resulting from X chromosome inactivation in the female as proposed by Lyon (1961). Males and homozygous females containing this allele are yellow-orange while heterozygous females (+/*O*) have the tortoise-shell or calico coat consisting of irregularly distributed patches of yellow and brown pigment. Yet variegated brindle and tortoise-shell coat color patterns map to the autosomal *extension* locus in a variety of mammals, including the rabbit, dog, cattle, pig, and guinea pig (Searle, 1968).

We were fascinated by this example of variegated gene function at the *extension* locus, and chose to begin a study of the problem in the guinea pig, in which an allele, e^{p}, produces the tortoise-shell coat pattern in homozygous male or female animals. Our initial hypothesis was that such a phenotype might result from variable MC1-R gene expression that could be easily detectable as a gene

TABLE IV
Characteristics of Individuals with MC1R Polymorphisms

Individuals	Skin type	Eye color	Hair color	Genotype
1	I	Blue	Blond	D84E/V92M
2	I	Blue	Blond	+/V92M
3	I	Green	Blond	V92M/V92M
4	II	Brown	Black	+/V92M

re-arrangement. Analysis of the MC1-R gene locus by Southern hybridizatio not confirmed this (Fig. 8). Interestingly, however, after probing DNA fron black, tortoise-shell, and red guinea pig with a small coding sequence frag of the mouse MC1-R, we did observe a large deletion in this gene in the guinea pig. This confirms the observations in the mouse and in cattle that abs of functional MC1 receptor does not affect melanocyte development or migr into the skin and hair follicle, but simply ablates expression of eumelanin i coat of the animal. Further work will be required to understand the mecha of variegated function of the MC1-R in tortoise-shell and brindle animals.

V. Structure/Function Studies of the MSH Receptor

We have taken information from three different lines of experimentati attempt to develop a model of the structure of the MC1-R. First, cloning sequence determination of all five melanocortin receptors has allowed us t certain which residues are identical or conserved in all the receptors (Figs. 2 5). Second, this information was then used by one of us (C.W.P.) to constr three-dimensional computer model of the receptor (Fig. 9) using recent i mation from a low-resolution model of rhodopsin (Schertler *et al.*, 1993) a with the molecular model for rhodopsin proposed by Baldwin (1993). These pieces of information have suggested the presence, in particular, of five conse residues in close proximity (Phe43, Phe278, Glu92, Asp119, and Asp 115) might form the basis of a binding pocket for the His-Phe-Arg-Trp pharmacop of the melanocortins. The Phe and Trp residues might form stacking interac with the two receptor Phe residues, while the Arg and His residues in the p macophore could form electrostatic interactions with the Glu92 and/or Asp 115 residues.

Finally, we have tried to use information from constitutively active rec mutants to understand how the receptor can undergo a transition from a quie state to an active state, albeit in this case in the absence of ligand. Initially proposed a model for the sombre receptor similar to that proposed for muta that constitutively activate rhodopsin (Robinson *et al.*, 1992). In the case of dopsin, a naturally occuring mutation in K296 resulted in a receptor that co tutively activates transducin in the absence of light or 11-cis-retinal. The c mophore 11-cis retinal is covalently attached to the receptor via a Schiff linkage involving the ε amino group of K296. Stabilization of the protor Schiff base is brought about through interaction with the negatively charged tamic acid at position 113. It is thought that light-induced isomerization o chromophore moves the protonated Schiff base away from E113, and disru of the E113-K296 salt bridge results in deprotonation of the Schiff base nitr known to be involved in formation of the active state of rhodopsin. Thus, i been proposed that mutagenesis of either of these residues produces an a

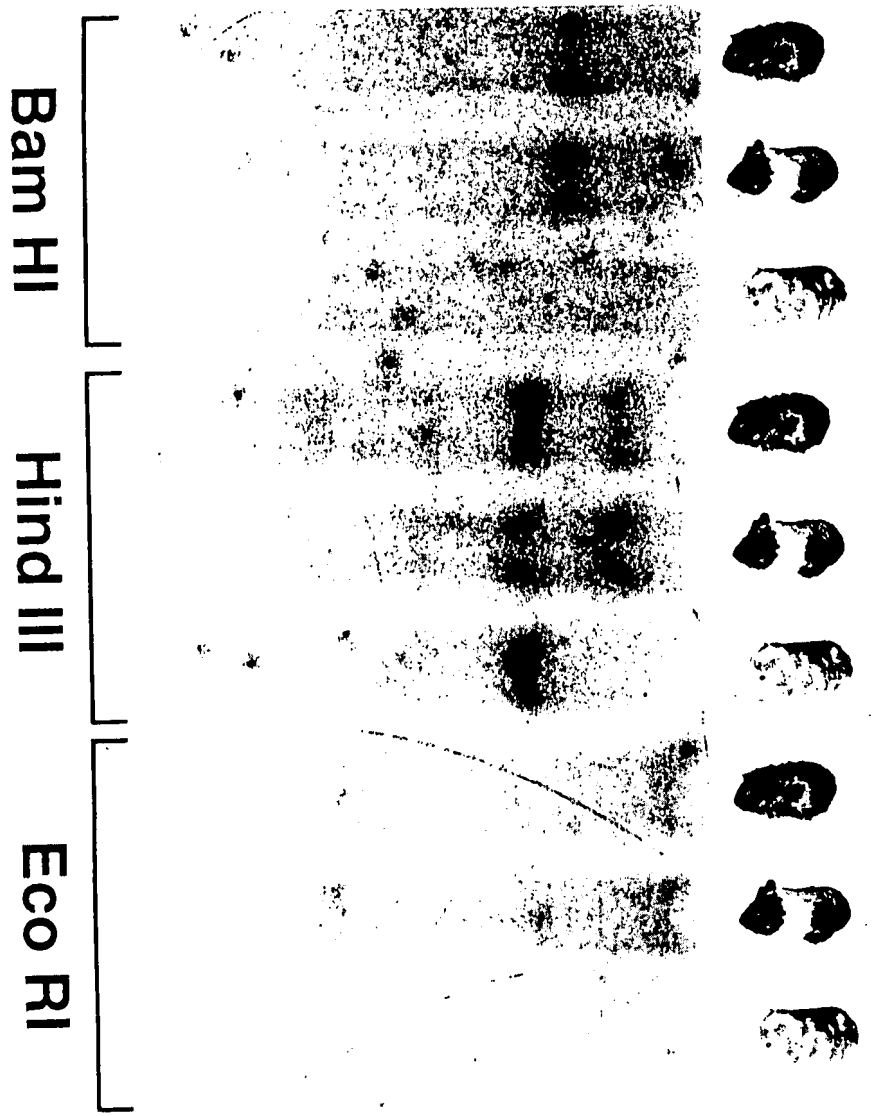

FIG. 8. Southern hybridization analysis of the guinea pig MC1-R locus. Whole blood from the black, tricolor, and red guinea pig was obtained from Pioneer Animal Supply (Mt. Vernon, OH). Genomic DNAs were prepared and treated with the restriction enzymes indicated. The order of samples in each panel are (from left to right) black, tricolor, and red. The radiolabelled probe was a ~ 1 kb fragment of MC1-R coding sequences from the mouse.

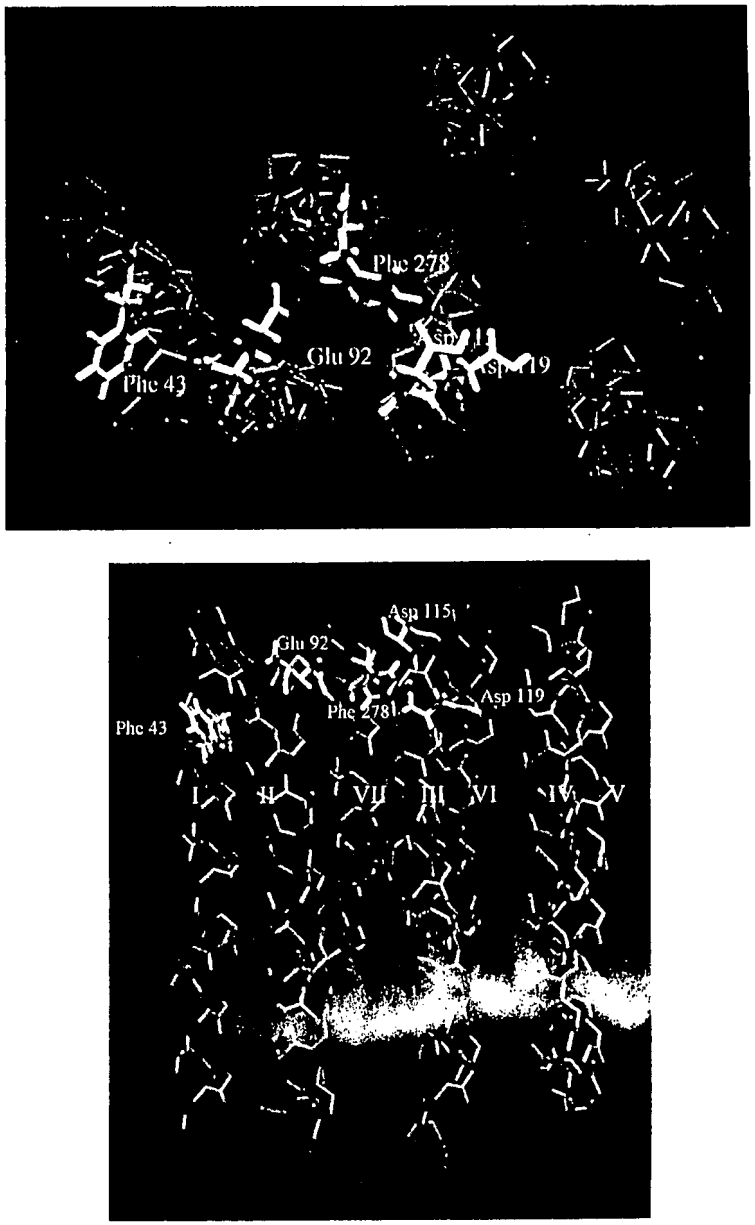

FIG. 9. Three-dimensional computer model of the mouse MC1-R. The peptide backbon each helical transmembrane domain are shown in dark grey. Key residues thought to be involv ligand binding and activation are highlighted and include Phe 78 (TMI), Glu 92 (TMII), Asp 11 Asp 119 (TM III), and Phe 278 (TMVII). Views are looking down at receptor from outside th (A) and in the plane of the membrane (B). Models were derived using the projection structu bovine rhodopsin and the model of Baldwin, and do not utilize molecular dynamic or energy mization corrections.

receptor in a manner that is mechanistically similar to stimulation of the receptor by light (Cohen *et al.*, 1992).

We initially proposed that the E92 in TM2 of the MSH-R was likely to be stabililized via electrostatic interaction with a basic residue somewhere else in the receptor (Robbins *et al.*, 1993). Disruption of this interaction by the E92K mutation would break this internal constraint and produce a partial hormone-independent activation of this receptor. In rhodopsin, this model has been supported by two observations (Robinson *et al.*, 1992). First, a variety of mutations at position 296 constitutively activate the receptor, demonstrating that the absence of the lysine is critical for the activation. Second, disruption of the other member of the salt bridge, E113, produces a similar phenotype.

Subsequent experiments have discounted the salt-bridge model for constitutive activation of the MC1-R. The conserved basic residues in the transmembrane domains of the MC1-R have been altered by *in vitro* mutagenesis without any significant change in the basal functioning of the receptor (Lu and Cone, unpublished data). More importantly, we have been unable to constitutively activate the receptor unless we change E92 to a basic residue; alteration of the glutamic acid to an isoleucine or glutamine disrupts the affinity of the receptor for ligand but produces no constitutive activation (Fig. 6).

We are considering the possibility that E92K introduces a positive charge capable of an electrostatic interaction with one of the aspartic acid residues, and constitutively activates by indirectly disrupting the constraining bond(s) that these residues form. For example, E92K might pair electrostatically with D119, thus disrupting the ability of D119 to hydrogen bond with some other residue. This would be an example of a model by which the E92K change indirectly disrupts an internal constraint to activate the receptor. This model predicts that the residues involved directly in the constraint might also activate the receptor when mutagenized, and we have made a large number of mutations in the mouse MSH receptor to test this hypothesis (Lu and Cone, unpublished data).

To further understand the constitutively active MC1 receptors it would be valuable to also examine the affinity of the receptors for ligand. Unfortunately, it has been difficult to perform the necessary binding experiments with these mutants. Presumably as a consequence of a dramatic decrease in ligand affinity and/or a potent downregulation of the constitutively active receptors, we are unable to detect ligand binding to the E92K receptor at tracer concentrations expected to result in approximately 30% receptor occupancy (Fig. 10). The very high concentrations of NDP-MSH required to further activate these receptors fit the model that these receptors have greatly reduced affinity for ligand.

VI. Pharmacological Mechanisms of Agouti Action

Agouti is a pigmentation locus that, like *extension*, regulates the relative levels of eumelanin versus phaeomelanin, but generally acts in a diametrically

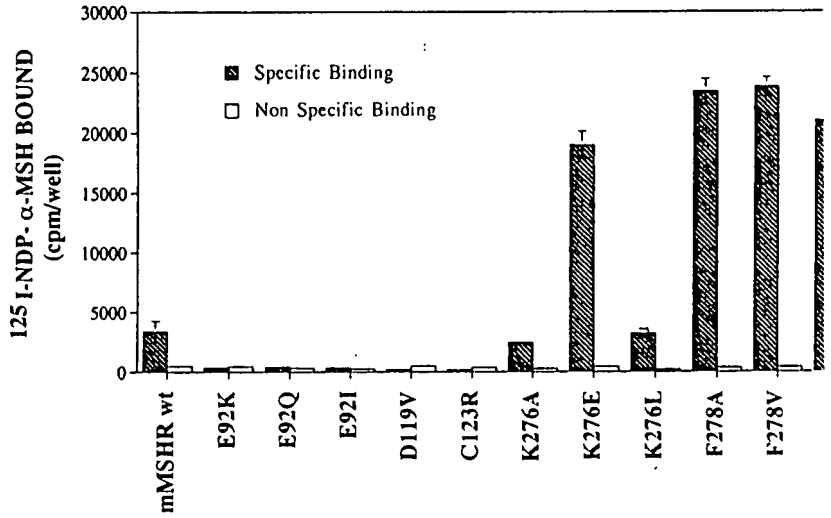

FIG. 10. Binding of ^{125}I-NDP-MSH to wild-type and mutant MC1 receptors. Cells (ap mately 5 × 10^6) expressing the wild-type or mutant MC1 receptors indicated were incubatec ^{125}I-NDP-MSH (100,000 CPM) for 1 hr at 37°C, washed twice, lysed, and counted in a γ-scintil counter. Nonspecific binding was that remaining in the presence of 10 ^{6}M unlabelled NDP- Tracer concentrations used were calculated, in the case of the wild-type receptor, to result in aj imately 30% receptor occupancy.

opposed manner. That is, dominant *agouti* alleles produce animals with ye or red coat colors (e.g. the red fox or yellow A^y mouse), while homozy recessive animals have dark black coat colors (Searle, 1968; Siracusa, 1994) wild-type allele results in the subterminal band of phaeomelanin in the hair seen in the coats of many animals, and named after the prominent pattern i South American rodent, the agouti. Melanocyte transplantation experin clearly demonstrated that an animal's *agouti* phenotype did not transplant the melanocyte, but rather was produced by the hair follicle and acted on to inhibit the MSH-induced synthesis of eumelanin in the transplanted mel cytes (Silvers, 1958; Silvers and Russel, 1955).

Cloning of *agouti* in the mouse demonstrated that this locus encoded a tative secreted protein of 108 amino acid residues (Bultman *et al.*, 1992; M *et al.*, 1993). Naturally, this led to the hypothesis that *agouti* is an antagoni the MC1 receptor, elaborated by follicle cells to act in a paracrine fashion o MC1-R during the phase of the hair growth cycle when the subterminal bar yellow pigment is laid down in the growing hair shaft (Jackson, 1993). examples of endogenous peptide antagonists of a G protein-coupled receptor previously been reported (Taminaga *et al.*, 1990; Zhu and Solomon, 1992); sequently, a counterhypothesis was also proposed that *agouti* might act o own receptor to inhibit the induction of adenylyl cyclase downstream of e

at the MC1 receptor (Conklin and Bourne, 1993). One piece of genetic evidence weighed heavily in favor of the former hypothesis, however. In the mouse, the sombre allele E^{So} is epistatic to even the most dominant *agouti* alleles, A^{y}, A^{w}, and A^{vy}, that is, when a dominant black (E^{So}) animal is crossed to a dominant yellow (Bateman, 1961; Wolff *et al.*, 1978) animal, a black animal results. This suggests that *agouti* can only act upstream of the MC1-R and cannot independently modify adenylyl cyclase levels.

At this point, evidence strongly supports the former hypothesis (Fig. 11). The murine *agouti* peptide has been demonstrated to be a potent antagonist of the MC1 receptor in an heterologous cell expression system, and also blocks the binding of melanotropic peptides to the receptor (Ki = 6×10^{-10}M), an action suggesting competitive antagonism (Lu *et al.*, 1994).

Much remains to be learned about this fascinating peptide, however. For example, there are at least three known gene loci that are required for *agouti* function, *mahogany*, *mahoganoid*, and *umbrous* (Silvers, 1979). When these loci are crossed into a dominant yellow animal, *agouti* action is blocked and an eumelanized animal results (e.g. Lane and Green, 1960).

Second, recent evidence has suggested that *agouti* might also increase intra-

FIG. 11. Murine *agouti* is an antagonist of the MC1-R. (A) *Agouti* inhibits activation of the mMC1-R by α-MSH in stably transfected 293 cells as monitored by stimulation of adenylyl cyclase activity. *Agouti* (0.7nM) increased the EC_{50} for activation of adenylyl cyclase from $1.5 \pm 1.1 \times 10^{-9}$ M to $2.2 \pm 1.2 \times 10^{-8}$ M. Cells were stimulated with varying concentrations of α-MSH in the presence or absence of 0.7nM *agouti* for 40 min. Medium was aspirated and 2.5% perchloric acid containing 0.1 mM cAMP was used to stop the incubation. Adenylyl cyclase activity was calculated by determining the percent conversion of [^{3}H]-adenine to [^{3}H]-cAMP as described (Johnson and Salomon, 1991). Data represent means and standard deviations from triplicate data points. (B) *Agouti* inhibits the binding of $ACTH_{1-39}$ to the mMC1-R. Competition binding studies demonstrated *agouti* protein blocked [^{125}I]-$ACTH_{1-39}$ binding to the mMC1-R with an IC50 value of $6.6 \pm 3.8 \times 10^{-10}$ M. As a control, baculovirus supernatants from SF9 cells infected with a virus containing an unrelated gene insert were purified in parallel with *agouti* protein and used for competition binding studies at the same range of protein concentrations as that used for *agouti*. Values are displayed in protein concentrations in order to directly compare *agouti* with control post-cation column protein. Data represent means and standard errors from triplicate data points. EC_{50} values were calculated using GraphPad InPlot version 4.0. The methods used for competition binding with radiolabelled ACTH were essentially those of Rainey *et al.* (1989). Cells (5×10^5) were incubated in binding medium contained 200,000 cpm of [^{125}I]-$ACTH_{1-39}$ (Amersham). [^{125}I]-$ACTH_{1-39}$ and varying concentrations of *agouti* protein, post-cation control protein, or cold ACTH were added to the cell culture dish and incubated at room temperature for 2 hours. Cells were then washed 3 times with ice-cold binding medium and lysed. Bound radioactivity was then determined using a γ-scintillation counter, and data were analyzed using the Kaleidagraph software package. Nonspecific binding, determined as the amount of radioactivity bound in the presence of 10^{-5} M unlabeled ACTH, was 10% of the total counts bound. [Reprinted with permission from *Nature* 371, 801. Copyright 1994, Macmillan Magazines Limited.]

cellular Ca^{2+} concentrations in cells via a mechanism that may not involve a
tagonism of the melanocortin receptors (Zemel *et al.*, 1995). Interestingly, t
spacing of cysteines in the *agouti* peptide is nearly identical to that found
conotoxins and plectotoxins of snails and spiders, respectively (Manne *et a*
1995). These peptide toxins are agonists and antagonists of a variety of ion cha

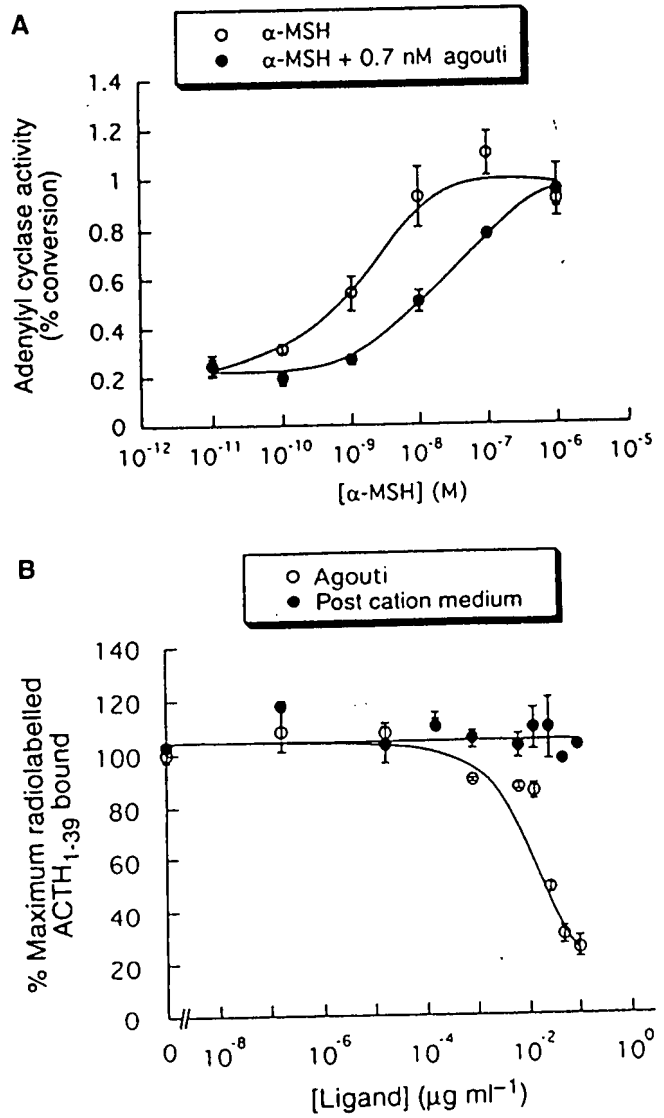

nels including Ca^{2+} channels, thus perhaps *agouti* also binds and stimulates activation of Ca^{2+} channels.

Finally, the most intriguing question concerns how some dominant *agouti* alleles in the mouse cause obesity. It has been known for many years that several dominant *agouti* alleles in the mouse, notably A^{y} and A^{vy}, cause hyperinsulinemia, obesity, and increased somatic growth (for reviews see Siracusa, 1994; Yen *et al.*, 1994). Recent molecular biological experiments have demonstrated that, for each these alleles, promoter re-arrangements have resulted in the expression of high levels of *agouti* mRNA throughout the animal, in contrast to the normally tightly regulated expression of the gene only in the hair follicle during a brief period of the hair cycle (Bultman *et al.*, 1992; Michaud *et al.*, 1994; Miller *et al.*, 1993; Vrieling *et al.*, 1994). Furthermore, ectopic expression of *agouti* in a transgenic animal in which the β-actin promoter drives *agouti* expression also leads to obesity (Klebig *et al.*, 1995; Perry *et al.*, 1995).

How might *agouti* cause obesity? We have observed that mouse *agouti* protein not only is an antagonist of the MC1-R in melanocytes, but is also a potent antagonist of the neural MC4 receptor (Fig. 12) (Lu *et al.*, 1994). This has led us to propose the "melanocortin hypothesis" for the induction of obesity by *agouti*: aberrant ectopic expression of *agouti* leads to obesity as a consequence of pathogenic antagonism of one or more of the melanocortin receptors. This hypothesis has led us to carefully examine the expression of melanocortin receptors in tissues involved in weight homeostasis. Since adrenalectomized A^{y} animals still become obese, the adrenocortical MC2-R can be ruled out as the critical site of *agouti* action (Jackson *et al.*, 1976). Two potential sites of *agouti* action are adipocytes and brain regions involved in feeding behavior and weight homeostasis (Fig. 13). It has been known for some time that adipocytes express a high-affinity ACTH binding site, and that ACTH induces lipolysis (Oelofsen and Ramachandran, 1983). We have recently characterized these sites as resulting from the expression of the MC2-R in all adipose tissues tested and MC5-R in a subset of those (Fig. 13A). Perhaps more intriguing is the expression of both the MC3 and MC4 receptors in different regions of the hypothalamus (Fig. 13B) (Mountjoy *et al.*, 1994; Roselli-Rehfuss *et al.*, 1993). This brain region has long been known, from lesioning studies, to be important in the regulation of feeding behavior. Furthermore, both of the neural melanocortin receptors are expressed throughout regions of the brain regulating autonomic outflow, and thus may impact weight homeostasis by other mechanisms in addition to alteration of feeding.

VII. Development of Melanocortin Receptor Antagonists

While many significant advances have been made in the peptide chemistry of the melanocortins (for review, see Eberle, 1988), surprisingly no high-affinity antagonists of the melanocortin receptors have ever been identified. To better understand the structure and function of these receptors, we set out to remedy

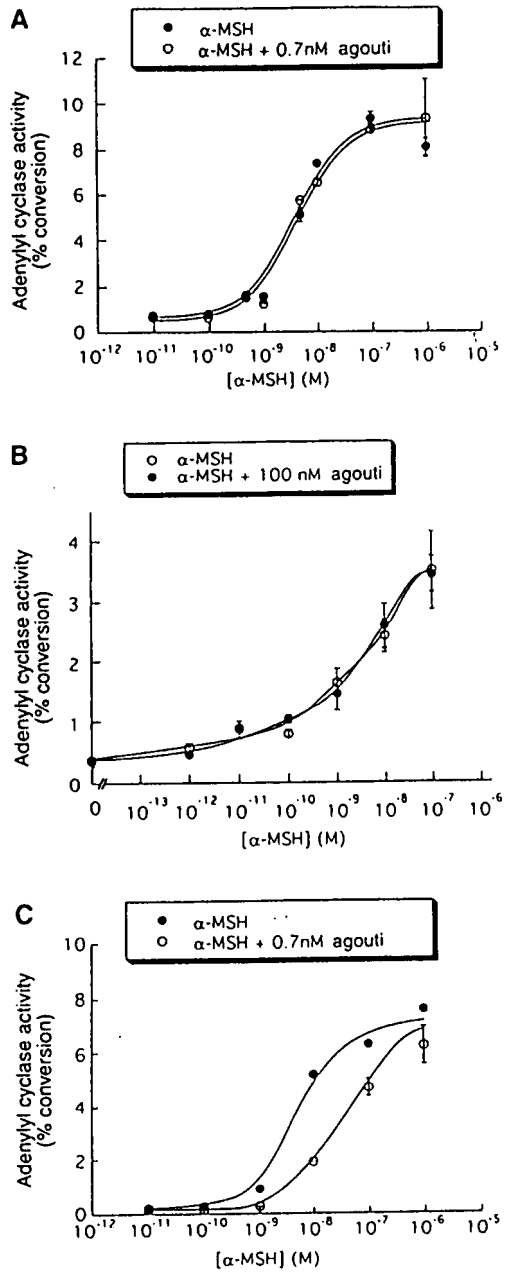

FIG. 12. Murine *agouti* is an antagonist of the MC4-R. The ability of murine *agouti* to a onize the rMC3-R (A), hMC5-R (B), and mMC4-R (C) was examined as described in Figur [Reprinted with permission from *Nature* **371**, 801. Copyright 1994, Macmillan Magazines Lim

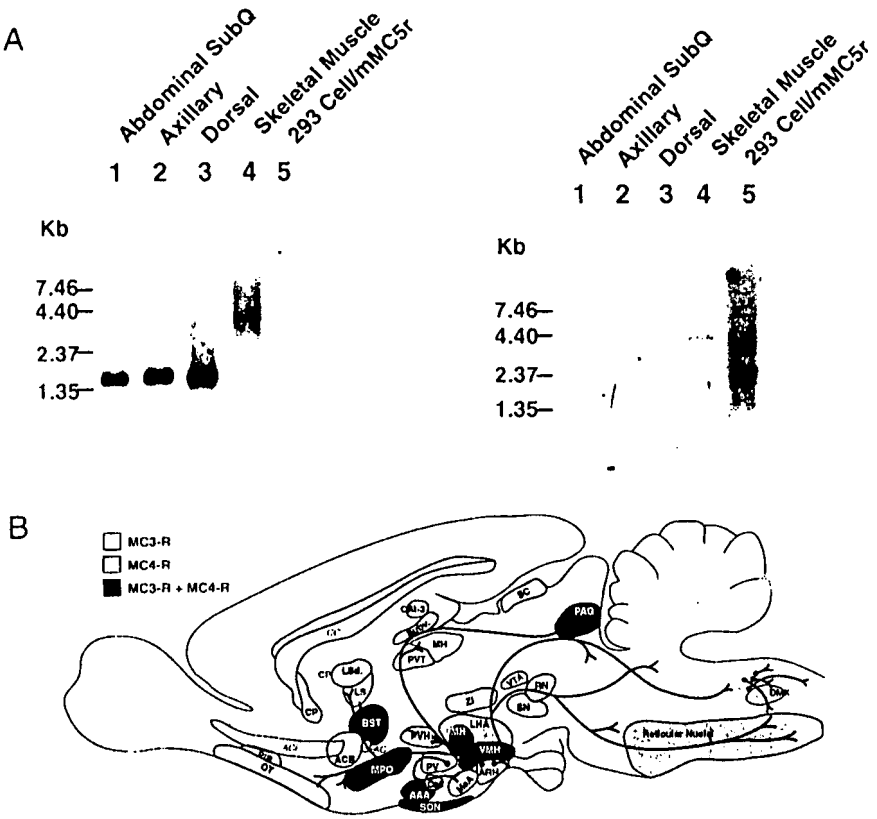

FIG. 13. Expression of melanocortin receptors in putative target tissues of *agouti* action. (A) Melanocortin receptor mRNA expression in adipocytes. Murine adipocytes from the fat pads indicated were used for the preparation of RNA. Poly A+ mRNA (2 μg) was electrophoresed on a formaldehyde agarose gel and transferred to a nylon membrane. The membrane was then hybridized to a mouse MC2-R probe (left panel) or mouse MC5-R probe (right panel). [Reprinted with permission from Boston, B., and Cone, R.D., Characterization of melanocortin receptor subtype expression in murine adipose tissues and in the 3T3-L1 cell line. *Endocrinology*, in press, 1996. © The Endocrine Society]. (B) Melanocortin receptor mRNA expression in the rat brain. The distribution of MC3-R and MC4-R mRNA in the rat brain was examined by *in situ* hybridization. Detailed accounts of the distributions are published elsewhere (Mountjoy *et al.*, 1994; Roselli-Rehfuss *et al.*, 1993). A schematic representation of brain regions containing the MC3 receptor mRNA (light gray), MC4 receptor mRNA (medium gray), or both (dark grey) is shown here.

this situation. We began by first developing a high-throughput screening method for measuring agonism and antagonism of these receptors (Chen *et al.*, 1995). The melanocortin receptors couple to adenylyl cyclase, but conventional cyclase or cAMP assays are expensive and time consuming, requiring large numbers of cells and the use of radionuclides. First, all five melanocortin receptors were

transfected into the human 293 cell line, and clonal lines expressing each r were isolated. Next, a β-galactosidase gene fused to a cAMP-responsive p containing five repeats of the CRE element was obtained. Finally, conditio determined such that following transient transfection of the fusion gene cells and hormone treatment, adenylyl cyclase activity could be determi function of β-galactosidase activity using a rapid colorimetric assay in a plate format (Chen *et al.*, 1995). This rapid assay allows us to screen a mately 1000 compounds per day, in contrast to the 100 assays per day be performed by cAMP radioimmunoassay or by one of the more wide adenylyl cyclase assays (Salomon, 1991).

We began by first screening existing melanocortin peptide analogu viously examined using the classic frog sk n bioassay for activity at the

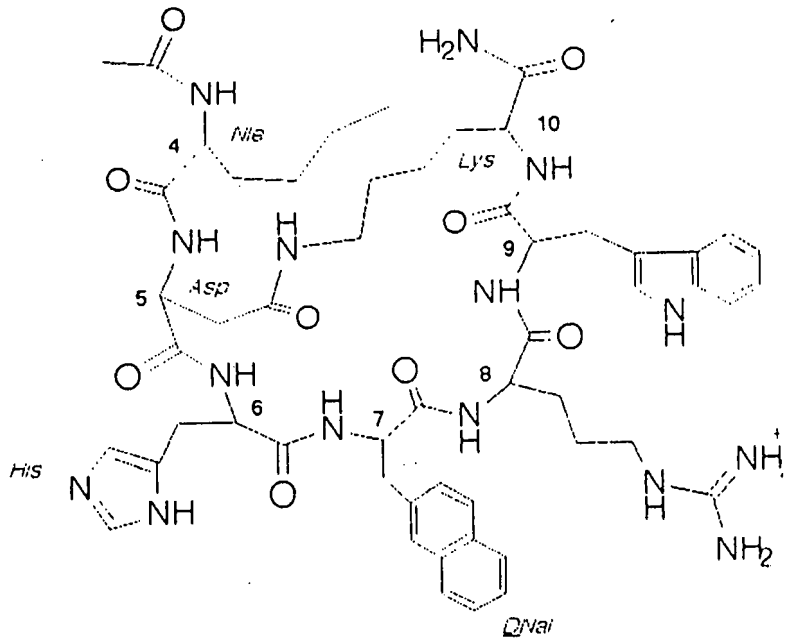

FIG. 14. Structure of SHU9119 (Ac-Nle⁴-c[Asp⁵, D-Nal (2)⁷, Lys¹⁰)] α-MSH(4–1 cyclic lactam derivative of α-MSH that is a potent antagonist of the MC3 and MC4 mc receptors.

(Shizume *et al.*, 1954), and rapidly identified a series of analogues with potent antagonist properties, the most potent of which can be seen in Figure 14 (for a detailed description, see Hruby *et al.*, 1995). This series of compounds is based upon the potent cyclic lactam analogue of α-MSH (Al-Obeidi *et al.*, 1989a,b). Like NDP-MSH, this compound is a potent agonist of the MC1, MC3, MC4, and MC5 receptors. Interestingly, it appears that replacement of the Phe in the His-Phe-Arg-Trp pharmacophore region with D-naphthylalanine (SHU9119) or para-iodophenylalanine (SHU8914) results in the production of potent and specific antagonists of the MC3 and MC4 receptors (Table V). These compounds are high-affinity competitive antagonists of the MC3 and MC4 receptors, but surprisingly are both full agonists of the MC1 and MC5 receptors (Fig. 15). SHU8914 retains significant partial agonist activity at the MC3-R and MC4-R while SHU9119 does not.

Recently, other groups have reported the identification of melanocortin antagonists. Adan *et al.* (1994) examined analogues of the linear $ACTH_{4-10}$ with modifications at positions 6–10. pA2 values the range of 6–8.6 were reported, with ($Pro^{8,10}$, Gly^{9})-$ACTH_{4-10}$ being the most potent with a pA2 value of 8.6 at the MC4-R. Interestingly, a linear $ACTH_{4-10}$ with a L-paraiodophenylalanine at position 7 was reported to have antagonist activity at the MC3, MC4, and MC5 receptors (pA2 = 7.4–8.4). Combinatorial peptide library approaches have been used to identify a melanocortin analogue (Met-Pro-D-Phe-Arg-D-Trp-Phe-Lys-Pro-Val-NH2) that can antagonize the *Xenopus* MC1-R with an IC_{50} of 11 nM (Jayawickreme *et al.*, 1994). Larger random combinatorial libraries were then used to identify a peptide, D-Trp-Arg-Leu-NH_2, that antagonized the human MC1-R with an IC_{50} of 0.6 μM (Quillan *et al.*, 1995).

TABLE V

EC_{50} (pM) and pA_2 Values for Phe^7-Substituted Ac-Nle^4-c[Asp^5, D-Phe^7, Lys^{10}]α-MSH(4-10)-NH_2 Compounds

	hMC1R	hMC3R	hMC4R	mMC5R
α-MSH	91 ± 69	669 ± 355	210 ± 57	807 ± 125
NDP-α-MSH	23 ± 7	132 ± 31	17 ± 18	not done
SHU9128 "(*p*-F1)Phe^7	16 ± 3	191 ± 9	19 ± 14	1360 ± 549
SHU9203 "(*p*-C1)Phe^7	5 ± 4	63 ± 26	18 ± 14	117 ± 70
SHU8914 "(*p*-I)Ph^7	55 ± 31	1134 ± 197 partial agonist $pA_2 = 8.3$	573 ± 357 partial agonist $pA_2 = 9.7$	684 ± 227 partial agonist
SHU9119 "(D-Nal)	36 ± 12	2813 ± 575 partial agonist $pA_2 = 8.3$	no activity $pA_2 = 9.3$	434 ± 260

[a] Indicates the halogen substitution at the *para* position of Phe^7.

[Reprinted with permission from *J. Med. Chem.* **38**, 3455. Copyright 1995, American Chemical Society.]

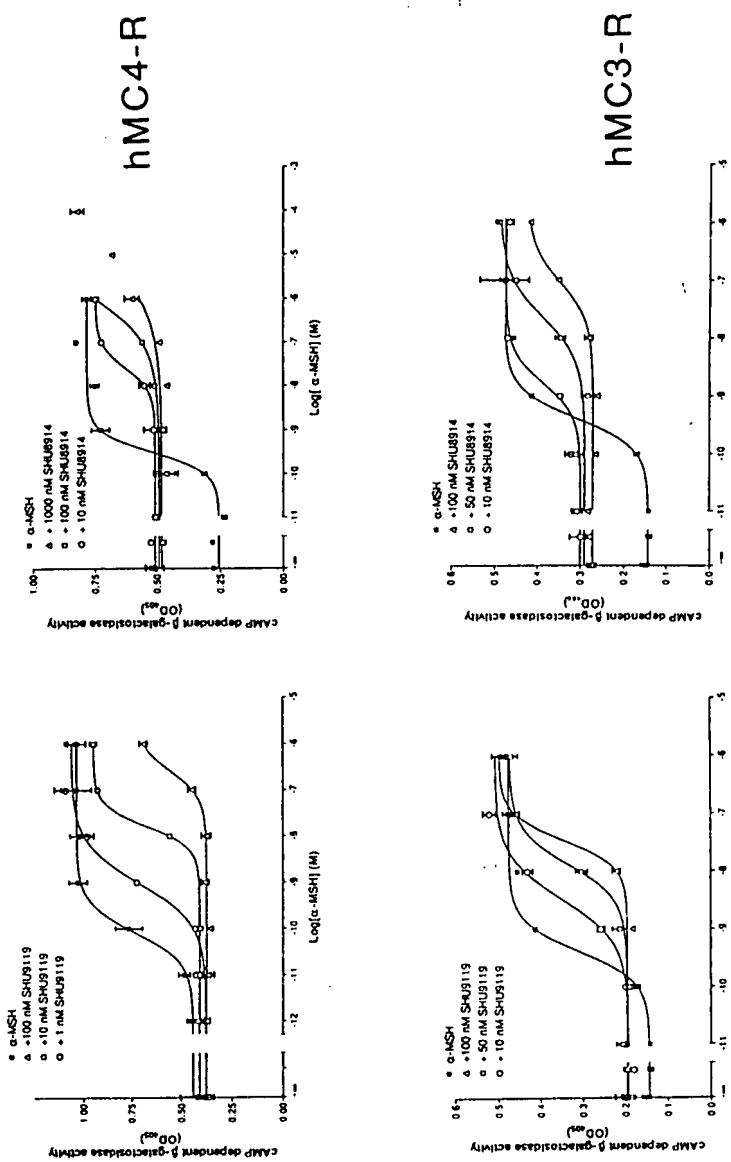

FIG. 15. Modification of the phenylalanine at position 7 of a cyclic lactam derivative of α-MSH results in high-affinity melanocortin antagonists. Dose-Response curves for antagonism of the MC3 and MC4 receptors by Ac-Nle^4-c[Asp^5, D-Nal (2)^7, Lys^{10}] α-MSH(4–10)NH_2 (SHU9119, left panels, top and bottom) and Ac-Nle^4-c[Asp^5, D-(*p*-I)Phe^7, Lys^{10}]α-MSH(4–10)NH_2 (SHU8914, right panels, top and bottom). Cell lines expressing the MC3 and MC4 receptors were stimulated with varying concentrations of α-MSH

Preliminary data show that these compounds will be very useful for the analysis of melanocortin receptor function *in vivo*. Experiments are currently underway to determine if centrally administered SHU9119 can affect feeding behavior or weight homeostasis, to test the hypothesis that antagonism of the MC4-R by *agouti* is the mechanism of induction of obesity by this peptide. While potent antagonists have not yet been found for the MC1 or MC5 receptors, substitution of Phe7 with bulky amino acid residues that retain aromatic character may be a way to eventually derive antagonists of these receptors as well.

VIII. Conclusions

Many mysteries concerning melanocortin action remain unsolved. For example, peripherally administered α-MSH induces eumelanin synthesis in skin and hair, yet hypophysectomized mice retain a darkly pigmented coat. How is eumelanin production by follicular melanocytes maintained in the absence of circulating α-MSH? Is it regulated by locally produced POMC peptides or perhaps via basal MC1-R activity? The products of at least three genes, *mahogany*, *mahoganoid*, and *umbrous*, are required for *agouti* action in pigmentation, and possibly obesity as well. What are these products and what are their roles?

Yet, progress has been made. The majority of the melanocortin receptors, perhaps all of them, have been cloned and characterized, and several groups are busily developing specific antagonists. Gene knockout experiments are also underway for the MC3-R, MC4-R, and MC5-R. Two biological activities have been demonstrated for the *agouti* peptide, antagonism of the MC1 and MC4 melanocortin receptors and elevation of intracellular Ca^{2+}, and readily testable hypotheses have been proposed for the mechanism of action of this peptide in pigmentation and obesity. The data reviewed here should convince the reader that some very useful tools have been developed in recent years for unraveling many of these remaining mysteries.

Note added in press: Valverde *et al.* (1995) have now reported the identification of nine coding polymorphisms in the human MC1-R, inclusive of the V92M and D84E changes reported here, that appear to be associated with light skin and red hair color in a study of British and Irish individuals. The new coding variants include D294H, A64S, T95M, V97I, F76Y, A103V, and L106Q.

ACKNOWLEDGMENTS

This work was supprted with funds to R.D.C. from the National Institutes of Health (AR42415, HD30236) and from the Lucille P. Markey Charitable Trust.

REFERENCES

Abdel-Malek, Z., Swope, V.B., Suzuki, I., Akcali, C., Harriger, M.D., Boyce, S.T., Urabe, K., and Hearing, V.J. (1995). *Proc. Natl. Acad. Sci. USA* **92**, 1789–1793.

Adan, R.A.H., Oosterom, J., Ludvigsdotter, G., Brakkee, J.H., Burbach, J.P.H., and Gispen, W.H. (1994). *Eur. J. Pharm.* **269**, 331–337.

Al-Obeidi, F., Castrucci, A.M.d.L., Hadley, M.E., and Hruby, V.J. (1989a). *J. Med. Chem.* **32**, 2[illegible] 2561.

Al-Obeidi, F., Hadley, M.E., Pettitt, B.-M., and Hruby, V.J. (1989b). *J. Am. Chem. Soc.* **111**, 3[illegible] 3416.

Baldwin, J. (1993). *EMBO J.* **12**, 1693–1703.

Barret, P., MacDonald, A., Helliwell, R., Davidson, G., and Morgan, P. (1994). *J. Mol. Endocr* **12**, 203–213.

Bateman, N. (1961). *J. Hered.* **52**, 186–189.

Bijlsma, W.A., Jennekens, F.G.I., Schotman, P., and Gispen, W.H. (1981). *Euro. J. Pharmacol* 73.

Boston, B.A., and Cone, R.D. (1996). *Endocrinology*, in press.

Buckley, D.I., and Ramachandran, J. (1981). *Proc. Natl. Acad. Sci. USA* **78**, 7431–7435.

Bultman, S.J., Michaud, E.J., and Woychik, R.P. (1992). *Cell* **71**, 1195–1204.

Calogero, A.E., Gallucci, W.T., Gold, P.W., and Chrousos, G.P. (1988). *J. Clin. Invest.* **82**, 767–

Cammas, F.M., Kapas, S., Barker, S., and Clark, A.J.L. (1995). *Biochem. Biophys. Res. Comm* **212**, 912–918.

Catania, A., and Lipton, J.M. (1993). *Endocr. Rev.* **14**, 564–576.

Chen, W., Shields, T.S., Stork, P.J.S., and Cone, R.D. (1995). *Analyt. Biochem.* **226**, 349–354.

Chhajlani, V., Muceniece, R., and Wikberg, J.E.S. (1993). *Biochem. Biophys. Res. Comm.* **195**, [illegible] 873.

Chhajlani, V., and Wikberg, J.E.S. (1992). *FEBS Lett.* **309**, 417–420.

Chowdhary, B.P., Gustavsson, I., Wikberg, J.E., and Chhajlani, V. (1995). *Cytogenet. Cell G* **68**, 79–81.

Clark, A.J.L., McLoughlin, L., and Grossman, A. (1993). *Lancet* **341**, 461–462.

Cohen, G.B., Oprian, D.D., and Robinson, P.R. (1992). *Biochemistry* **31**, 12592–12601.

Cone, R.D., and Mountjoy, K.G. (1993). *Trends in Endocrinol. Metab.* **4**, 242–247.

Conklin, B.R., and Bourne, H.R. (1993). *Nature* **364**, 110.

De Angelis, L., Cusella-De Angelis, M.G., Bouche, M., Vivarelli, E., Boitani, C., Molinaro, M., Cossu, G. (1992). *Devel. Biol.* **151**, 446–458.

Desarnaud, F., Labbe, O., Eggerickx, D., Vassart, G., and Parmentier, M. (1994). *Biochem. J.* 367–373.

DeWied, D., and Jolles, J. (1982). *Physiol. Rev.* **62**, 977–1059.

Eberle, A.N. (1988). "The Melanotropins. Chemistry, Physiology and Mechanisms of Action Karger Publishers, Basel, Switzerland.

Eberle, A.N., de Graan, P.N.E., Baumann, J.B., Girard, J., van Hees, G., and van de Veerdonk, F. (1984). *Yale J. Biol. Med.* **57**, 353–354.

Fathi, Z., Iben, L.G., and Parker, E.M. (1995). *Neurochem. Res.* **20**, 107–113.

Feng, J.D., Dao, T., and Lipton, J.M. (1987). *Brain Res.* **18**, 473–477.

Fuller, B.B., Lunsford, J.B., and Iman, D.S. (1987). *J. Biol. Chem.* **262**, 4024–4033.

Gantz, I., Shimoto, Y., Konda, Y., Miwa, H., Dickinson, C.J., and Yamada, T. (1994a). *Bioc Biophys. Res. Comm.* **200**, 1214–1220.

Gantz, I., Yamada, T., Tashiro, T., Konda, Y., Shimoto, Y., Miwa, H., and Trent, J.M. (19 *Genomics* **19**, 394–395.

Gantz, I., Konda, Y., Tashiro, T., Shimoto, Y., Miwa, H., Munzert, G., Watson, S.J., DelVall and Yamada, T. (1993a). *J. Biol. Chem.* **268**, 8246–8250.

Gantz, I., Miwa, H., Konda, Y., Shimoto, Y., Tashiro, T., Watson, S.J., DelValle, J., and Yam T. (1993b). *J. Biol. Chem.* **268**, 15174–15179.

Garrud, P., Gray, J.A., and DeWied, D. (1974). *Physiol. Psychol.* **112**, 109–119.

Gerst, J.E., Sole, J., Hazum, E., and Salomon, Y. (1988). *Endocrinology* **123**, 1792–1797.

Griffon, N., Mignon, V., Facchinetti, P., Diaz, J., Schwartz, J.-C., and Sokoloff, P. (1994). *Biochem. Biophys. Res. Comm.* **200**, 1007–1014.
Gruber, K.A., and Callahan, M.F. (1989). *Am. J. Phys.* **257**, R681-R694.
Halaban, R., Pomerantz, S.H., Marshall, S., and Lerner, A.B. (1984). *Arch. Biochem. Biophys.* **230**, 383–387.
Hearing, V.J., and Jimenez, M. (1987). *Int. J. Biochem.* **19**, 1141–1147.
Hnatowich, M.R., Queen, G., Stein, D., and LaBella, F.S. (1989). *Can. J. Physiol. Pharmacol.* **67**, 568–576.
Hoganson, G.E., Ledwitz-Rigby, F., Davidson, R.L., and Fuller, B.B. (1989). *Som. Cell. Mol. Genet.* **15**, 255–263.
Hruby, V.J., Lu, D., Sharma, S.D., Castrucci, A.L., Kesterson, R.A., Al-Obeidi, F.A., Hadley, M.E., and Cone, R.D. (1995). *J. Med. Chem.* **38**, 3454–3461.
Hunt, G., Todd, C., Kyne, S., and Thody, A.J. (1994). *J. Endocrinol.* **140**, R1-R3.
Jackson, E.J., Stolz, D., and Martin, R. (1976). *Horm. Metab. Res.* **8**, 452–455.
Jackson, I.J. (1993). *Nature* **362**, 587–588.
Jayawickreme, C.K., Quillan, J.M., Graminski, G.F., and Lerner, M.R. (1994). *J. Biol. Chem.* **269**, 29846–29854.
Johnson, R.A., and Salomon, Y. (1991). *Meth. in Enzymol.* **195**, 3–21.
Klebig, M.L., Wilkinson, J.E., Geisler, J.G., and Woychik, R.P. (1995). *Proc. Natl. Acad. Sci. USA* **92**, 4728–4732.
Klungland, H., Vage, D.I., Gomez-Raya, L., Adelsteinsson, S., and Lien, S. (1995). *Mamm. Genome* **6**, 636–639.
Konda, Y., Gantz, I., DelValle, J., Y., S., Miwa, H., and Yamada, T. (1994). *J. Biol. Chem.* **269**, 13162–13166.
Labbe, O., Desarnaud, F., Eggerickx, D., Vassart, G., and Parmentier, M. (1994). *Biochemistry* **33**, 4543–4549.
Lane, P.W., and Green, M.C. (1960). *J. Hered.* **51**, 228–230.
Little, C.C. (1957). "The Inheritance of Coat Colors in Dogs." Macmillan Publishing Company, New York.
Lu, D., Willard, D., Patel, I.R., Kadwell, S., Overton, L., Kost, T., Luther, M., Chen, W., Woychik, R.P., Wilkison, W.O., and Cone, R.D. (1994). *Nature* **371**, 799–802.
Lyon, M.F. (1961). *Nature* **190**, 372–373.
Magenis, R.E., Smith, L., Nadeau, J.H., Johnson, K.R., Mountjoy, K.G., and Cone, R.D. (1994). *Mamm. Genome* **5**, 503–508.
Malas, S., Peters, J., and Abbot, C. (1994). *Mammalian Genome* **5**, 577–579.
Manne, J., Argeson, A.C., and Siracusa, L.D. (1995). *Proc. Natl. Acad. Sci. USA* **92**, 4721–4724.
Michaud, E.J., Vugt, M.J.v., Bultman, S.J., Sweet, H.O., Davisson, M.T., and Woychik, R.P. (1994). *Genes & Devel.* **8**, 1463–1472.
Miller, M.W., Duhl, D.M.J., Vrieling, H., Cordes, S.P., Ollmann, M.M., Winkes, B.M., and Barsh, G.S. (1993). *Genes & Devel.* **7**, 454–467.
Motta, M., Mangili, G., and Martini, L. (1965). *Endocrinology* **77**, 392–395.
Mountjoy, K.G. (1994). *Mol. Cell. Endocrinol.* **102**, R7-R11.
Mountjoy, K.G., Mortrud, M.T., Low, M.J., Simerly, R.B., and Cone, R.D. (1994). *Mol. Endocrinol.* **8**, 1298–1308.
Mountjoy, K.G., Robbins, L.S., Mortrud, M.T., and Cone, R.C. (1992). *Science* **257**, 543–546.
Nes, N., Einarsson, E.J., Lohi, O., Jarosz, S., and Scheelje, R. (1988). "Beautiful Fur Animals and Their Colour Genetics." Scientifur, Glostrup, Denmark.
Oelofsen, W., and Ramachandran, J. (1983). *Arch. Biochem. Biophys.* **225**, 414–421.
Pathak, M.A., Fitzpatrick, T.B., Greiter, F., and Kraus, E.W. (1987). Preventive treatment of sunburn, dermatoheliosis, and skin cancer with sun-protective agents. In "Dermatology in General Medicine" (T.B. Fitzpatrick, A.Z. Eizen, K. Wolff, I.M. Freeberg, and K. F. Austen, 1507. McGraw-Hill, New York.
Pawelek, J. (1976). *J. Invest. Dermatol.* **66**, 201–209.
Perry, W.L., Hustad, C.M., Swing, D.A., Jenkins, N.A., and Copeland, N.G. (1995). *Genet* 267–274.
Quillan, J.M., Jayawickreme, C.K., and Lerner, M.R. (1995). *Proc. Natl. Acad. Sci. USA* 9 2898.
Robbins, L.S., Nadeau, J.H., Johnson, K.R., Kelly, M.A., Roselli-Rehfuss, L., Baack, E., M K.G., and Cone, R.D. (1993). *Cell* **72**, 827–834.
Robinson, P.R., Cohen, G.B., Zhukovsky, E.A., and Oprian, D.D. (1992). *Neuron* **9**, 719–7
Roselli-Rehfuss, L., Mountjoy, K.G., Robbins, L.S., Mortrud, M.T., Low, M.J., Tatro, J.B., E M.L., Simerly, R., and Cone, R.D. (1993). *Proc. Natl. Acad. Sci. USA* **90**, 8856–886
Salomon, Y. (1991). *Meth. Enzymology* **195**, 22–28.
Salomon, Y., Zohar, M., Dejordy, J.O., Eshel, Y., Shafir, I., Leiba, H., Garty, N.B., Schmidt Azrad, A., Shai, E., and Deganis, H. (1993). *Ann. N.Y. Acad. Sci.* **680** 364–377.
Sandman, C.A., Kastin, A.J., and Schaally, A.V. (1969). *Experientia* **25**, 1001–1002.
Schertler, G.F.X., Villa, C. and Henderson, R. (1993). *Nature* **362**, 770–772.
Schimmer, B.P., Kwan, W.K., Tsoa, J., and Qui, R. (1995). *J. Cell. Physiol.* **163**, 164–171.
Searle, A.G. (1968). "Comparative Genetics of Coat Colors in Mammals." Logos Press London.
Shizume, K., Lerner, A.B., and Fitzpatrick, T.B. (1954). *Endocrinology* **54**, 533–560.
Silvers, W.K. (1979). "The Coat Colors of Mice: A Model for Mammalian Gene Action ar action." Springer-Verlag, New York.
Silvers, W.K. (1958). *J. Exp. Zool.* **137**, 189–196.
Silvers, W.K., and Russel, E.S. (1955). *J. Exp. Zool.* **130**, 199–220.
Siracusa, L.D. (1994). *Trends in Genet.* **10**, 423–428.
Smith, A.I., and Funder, J.W. (1988). *Endocr. Rev.* **9**, 159–179.
Solca, F., Siegrist, W., Drozdz, R., Girard, J., and Eberle, A.N. (1989). *J. Biol. Chem.* **264**, 14280.
Strand, F.L., and Kung, T.T. (1980). *Peptides* **1**, 135–138.
Strand, F.L., Rose, K.J., Zuccarelli, L.A., Kume, J., Alves, S.E., Antonawich, F.J., and Garr (1991). *Physiol. Rev.* **71**, 1017–1046.
Suda, T., Yajima, F., Tomori, N., Sumitomo, T., Nakagami, Y., Ushiyama, T., Demura, Shizume, K. (1986). *Endocrinology* **118**, 459–461.
Taminaga, T., Fukata, J., Naito, Y., Funakoski, S., Fujii, N., and Imura, H. (1990). *J. End* **125**, 287–292.
Tatro, J.B. (1990). *Brain Res.* **536**, 124–132.
Tatro, J.B., and Reichlin, S. (1987). *Endocrinology* **121**, 1900–1907.
Tsigos, C., Arai, K., Hung, W., and Chrousos, G.P. (1993). *J. Clin. Invest.* **92**, 2458–2461.
Valverde, P., Healy, E., Jackson, I., Rees, J.L., and Thody, A.J. (1995). *Nature Genet.* **11**, 3.
Vamvakopoulos, N.C., Rojas, K., Overhäuser, J., Durkin, A.S., Nierman, A.C., and Chrous (1993). *Genomics* **18**, 454–455.
Vrieling, H., Duhl, D.M.J., Millar, S.E., Miller, K.A., and Barsh, G.S. (1994). *Proc. Natl. Ac USA* **91**, 5667–5671.
Wolff, G.L., Galbraith, D.B., Domon, O.E., and Row, J.M. (1978). *J. Hered.* **69**, 295–298.
Wong, G., and Pawelek, J. (1975). *Nature* **255**, 644–646.
Yen, T.T., Gill, A.M., Frigeri, L.G., Barsh, G.S., and Wolff, G.L. (1994). *FASEB J.* **8**, 479–
Zemel, M.B., Kim, J.H., Woychik, R.P., Michaud, E.J., Kadwell, S.H., Patel, I.R., and W W.O. (1995). *Proc. Natl. Acad. Sci. USA* **92**, 4733–4737.
Zhu, Q., and Solomon, S. (1992). *Endocrinology* **130**, 1413–1423.

DISCUSSION

Fred Stormshak: Some wild fur-bearing species undergo a coat color change in response to changes in photoperiod; i.e., from brown or black in spring or summer to white in fall and winter. Is this change in coat color from dark to white due to a block of the melanocortin receptor, reduction in melanocortin production, or some other mechanism?

Roger Cone: The seasonal coat color change seen in animals like the snowshoe rabbit, *Leptus americanus*, is unlikely to involve the MC1 receptor or agouti peptide. These molecules are regulators of the relative levels of phaeomelanin (red-yellow) versus eumelanin (brown-black) pigments. Thus for example, animals lacking functional MSH receptor, such as the red guinea pig, still have plenty of melanin in hair and skin. Animals that turn white in the winter must have a complete absence of melanins, possibly as a result of a total inhibition of tyrosinase. While I am unaware of the mechanism by which melanin synthesis is blocked, data in the rabbit points to gonadotropic hormone as the triggering factor.

Thomas Means: What are the mechanisms by which some of these receptors become constitutively active in the genetic models?

Roger Cone: We do not yet have a detailed molecular model for constitutive activation of the MSH receptor in the mouse, cow, or fox. The data we have collected at this point, however, do not support the original model that we proposed in which E92 maintains the receptor in a constrained state via an electrostatic interaction (Robbins *et al.*, 1992). First, the model would predict that substitution of any residue for the glutamic acid, with the possible exception of aspartic acid, would constitutively activate the receptor. This is not the case, suggesting that the insertion of a basic residue at position 92 is required for constitutive activation. Secondly, we have been unable to find any basic residues in the receptor that, when altered also, constitutively activate the receptor.

Larry Davis: Are there ever circulating levels of α-MSH in humans that are great enough to contribute melanocyte activity and pigmentation?

Roger Cone: Unlike other mammals examined, circulating levels of α-MSH are not generally detectable in man. Interestingly, the human MC1 receptor is one to two logs more sensitive to ACTH than is the mouse receptor, suggesting that ACTH is the melanotropic peptide in man. Of course, while pathophysiologically elevated levels of ACTH can produce hyperpigmentation in man, the role of normal pituitary-derived melanotropins in basal pigmentation is unclear. Hair pigmentation remains unchanged in the absence of pituitary function, suggesting that either basal MC1 receptor function or locally produced melanocortin peptides are responsible for the normal production, by follicular melanocytes, of eumelanin in the hair.

Larry Davis: Are there known variations in α-MSH levels?

Roger Cone: Abdel-Malek has recently shown that human melanocytes in culture do proliferate in response to α-MSH, which raises the important question that you have asked. One could imagine that constitutively active MC1 receptors might be involved in some stage of melanoma induction, just as activated TSH receptors are found in thyroid tumors. To my knowledge, a thorough examination of melanoma samples for MC1 receptor mutations has not been done. One observation, however, that may be relevant to the question is that no enhanced incidence of melanoma has been reported for any of the darker-pigmented animals, such as the Sombre mouse, that already express constitutively active MC1 receptors.

Obesity, diabetes, and neoplasia in yellow A^{vy}/- mice: ectopic expression of the *agouti* gene

TERENCE T. YEN*,[1] ANNE M. GILL*, LUCIANO G. FRIGERI,[†] GREGORY S. BARSH,[‡] AND GEORGE L. WOLFF[§,2]

*Lilly Research Laboratories, Eli Lilly & Co., Lilly Corporate Center, Indianapolis, Indiana 46285, USA; [†]Department of Molecular and Experimental Medicine, Scripps Research Institute, La Jolla, California 92037, USA; [‡]Department of Pediatrics and Howard Hughes Medical Institute, Stanford University School of Medicine, Stanford, California 94305-5428, USA; [§]Division of Nutritional Toxicology, National Center for Toxicological Research, Food and Drug Administration, U.S. Department of Health and Human Services, Jefferson, Arkansas 72079-9590, USA; and Departments of Biochemistry/Molecular Biology and Pharmacology/Toxicology, University of Arkansas for Medical Sciences, Little Rock, Arkansas 72205, USA

ABSTRACT The *viable yellow* A^{vy} mutation results in a mottled yellow mouse that is obese, slightly larger than its nonyellow sibs, and more susceptible to tumor formation in those tissues sensitized by the strain genome. The mutation exhibits variable expressivity resulting in a continuum of coat color phenotypes, from clear yellow to pseudoagouti. The mouse *agouti* protein is a paracrine signaling molecule that induces hair follicle melanocytes to switch from the synthesis of black pigment to yellow pigment. Molecular cloning studies indicate that the obesity and growth effects of the A^{vy} mutation result from ectopic expression of the normal *agouti* gene product. This review seeks to summarize the current state of knowledge regarding the obesity, stimulation of somatic growth, and enhancement of tumor formation caused by the A^{vy} mutation, and to interpret these pleiotropic effects in terms of the normal function of the *agouti* protein.—Yen, T. T., Gill, A. M., Frigeri, L. G., Barsh, G. S., and Wolff, G. L. Obesity, diabetes, and neoplasia in yellow A^{vy}/- mice: ectopic expression of the *agouti* gene. *FASEB J.* 8: 479-488; 1994.

Key Words: obesity · diabetes · neoplasia · yellow mouse · agouti locus

HISTORY OF THE A^{vy} MUTATION AT THE *AGOUTI* LOCUS IN THE MOUSE

The *viable yellow* (A^{vy}) mutation arose spontaneously in 1960 from the agouti (*A*) allele at the *agouti* locus in the C3H/HeJ strain (1). The *agouti* locus is located between loci *Hck-1* (hematopoietic cell kinase-1) and *Src-1* (Rous sarcoma virus proto-oncogene) in a section of mouse chromosome 2 that contains many mouse genes that have homologs (conserved synteny) on human chromosome 20q.

This locus determines the relative amounts of black (eumelanin) and yellow (phaeomelanin) pigment in the hairs. The species-type hair color pattern, "agouti," is common among mammals and is characterized by a subapical yellow band in black or brown hair; in mice heterozygous or homozygous for A^{vy} (hereafter A^{vy}/-), there is usually an excess of yellow pigment (see below). A^{vy} is one of four dominant *agouti* mutations associated with pleiotropic effects, the most prominent of which are obesity and increased somatic growth. In addition, A^{vy} and at least one other obesity-associated *agouti* allele, *lethal yellow* (A^{y}), are associated with increased susceptibility to diabetes (2) and to endogenously and exogenously induced hyperplasia, preneoplastic lesions, and neoplasms (3).

Most data reviewed here have been obtained with yellow VY/Wf-A^{vy}/*a* mice, in which case black *a/a* littermates served as non-A^{vy} controls. Alternatively, F_1 hybrids from matings of VY/Wf-A^{vy}/*a* mice with mice of another inbred strain, e.g., BALB/c-*A/A*, produce A^{vy}/*A* and agouti (*A/a*) mice, the latter serving as the non-A^{vy} controls.

The VY/Wf strain was developed at The Institute for Cancer Research, Philadelphia, from A^{vy}/*a* males and females of the first and third generations of backcrossing of C3H/HeJ- A^{vy} onto C57BL/6J and were obtained from The Jackson Laboratory, Bar Harbor, Maine, in 1962; thus, the strain includes 6.25%-25% C3H/HeJ genome and 75%-93.75% C57BL/6J genome. Breeding stock of the VY/Wf strain was provided to one of us (T.T.Y.) at Eli Lilly & Co., Inc. in 1970, rederived by cesarean section in 1985, and maintained as strain VY/WfL. Strain VY/Wf was brought to the National Center for Toxicological Research by G.L.W. in 1972. Litters were derived by cesarean section and fostered on C3H-MTV$^-$ dams in the NCTR breeding colony in 1977. The resulting VY/WffC3Hf/Nctr- A^{vy} strain is maintained in a SPF barrier-sustained environment.

THE *AGOUTI* GENE AND ITS ACTION

The *agouti* gene has recently been cloned (4, 5). It is normally expressed in the skin, the testes, and during embryonic development. The encoded protein is 131 amino acids in length and consists of a signal sequence, a central region that is highly basic, and a cysteine-rich carboxyl terminus. Multiple isoforms differ by the nature of their promoters and associated 5' untranslated exons and range in size from 697 nucleotides (nt)[3] to 792 nt, not including the polyA tail (Fig. 1*A*, Fig. 1*B*) (6).

---

[1]Present address: Department of Biochemistry and Molecular Biology, Indiana University School of Medicine, Indianapolis, IN 46202-5122, USA.

[2]To whom correspondence should be addressed, at: National Center for Toxicological Research, 3900 NCTR Rd., Jefferson, AR 72079, USA.

[3]Abbreviations: α-MSH, α-melanocyte stimulating hormone; IAP, intracisternal A particle; HF, high fat; HS, high sucrose; GTT, glucose tolerance test; MNNG, N-methyl-N'-nitro-N-nitrosoguanidine; nt, nucleotides.

0892-6638/94/0008-0479$01.50 © FASEB

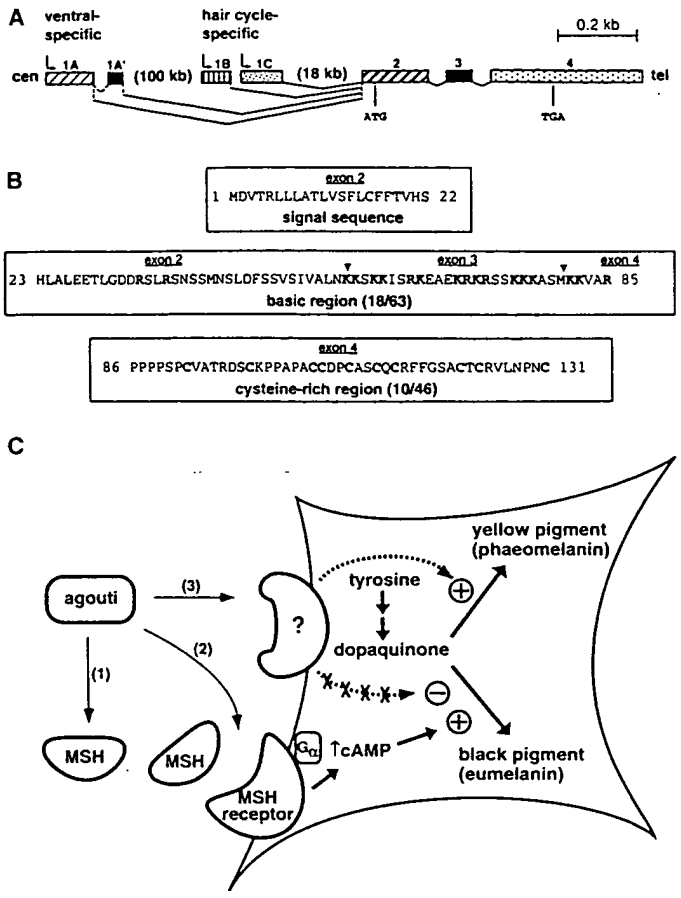

Figure 1. *Agouti* gene structure and action. *A)* Exon and intron structure reveal that the protein coding sequence is contained within exons 2, 3, and 4. Multiple isoforms of *agouti* mRNA differ in their 5' untranslated region and result from the use of different promoters and/or alternative splicing (6). A ventral-specific promoter results in isoforms that contain exon 1A or exons 1A and 1A', whereas a hair cycle-specific promoter results in isoforms that contain exon 1B or 1C. *B)* The amino acid sequence of the *agouti* protein contains a signal sequence, an amino-terminal basic domain with a high proportion of arginine and lysine residues, and a cysteine-rich carboxyl terminus. *C)* Possible mechanisms for *agouti* gene action, based on a secreted protein with a limited radius of action. Because the actions of α-MSH oppose and override those of *agouti* resulting in the synthesis of black pigment, the *agouti* protein may act by reducing the amount of active α-MSH available to the melanocyte; by interfering with activation of the melanocortin receptor; or by binding to its own receptor leading to an intracellular block to melanocortin receptor activation.

The *agouti* protein induces melanocytes within hair follicles to switch from synthesis of eumelanin (black pigment) granules to synthesis of phaeomelanin (yellow) granules, which become incorporated into a growing hair. A series of elegant transplantation studies (7; reviewed in ref 8) indicated that the gene product is produced by nonpigment cells and acts in a paracrine fashion, as it does not affect melanocytes in adjacent follicles or melanocytes in the interfollicular epidermis. These observations are consistent with recent studies which demonstrate that *agouti* expression within the hair follicle occurs only during the time of yellow pigment synthesis (4, 5). Although *agouti* RNA is also expressed in the testes and during embryonic development (6), there is no known function for the gene in these tissues; even null mutations in *agouti* have detectable effects only on coat color (4, 9).

The mechanism by which the *agouti* protein alters the function of melanocytes is not yet clear, although there are two different hypotheses (Fig. 1*C*) based on the opposing interactions between *agouti* and the 13 amino acid peptide α-melanocyte stimulating hormone (α-MSH). α-MSH causes melanocytes to switch from the synthesis of phaeomelanin to eumelanin (10), an effect that is mediated through a G_s-coupled seven transmembrane domain receptor that has recently been cloned (11). The α-MSH receptor on melanocytes is encoded by the *extension* (*E*) locus (12), and appears to be one member of a family of melanocortin receptors that also includes the ACTH receptor and at least two additional receptors expressed in the central nervous system (12–14). As expected, introduction of the α-MSH receptor into heterologous cells results in the stimulation of adenylate cyclase (11, 12). Exogenous α-MSH or exogenous dibutyryl-cAMP can override the effects of local agouti protein production (15), whereas loss-of-function mutations in the α-MSH receptor (*e*) result in the production of phaeomelanin regardless of the level of *agouti* expression (13, reviewed in ref 7). Therefore, it is possible that the *agouti* protein acts as an antagonist of the receptor to prevent α-MSH-induced stimulation of adenylate cyclase (16). Lack of a functional α-MSH receptor in *e/e* mice (13) failed to prevent A^y-induced obesity (17), indicating that this receptor is not required for *agouti*-associated obesity. Development of obesity in yellow mice is also independent of yellow pigment synthesis as demonstrated by complete inhibition of the latter by a gain-of-function mutation [*somber* (E^{so})] at the *extension* locus; totally black $A^y/a^e/E^{so}/E^+$ mice still become obese (18).

A second hypothesis proposes that *agouti* protein binds to its own receptor and interferes with the action of α-MSH at an intracellular level (19). A putative *agouti* receptor might couple to another G protein that inhibits adenylate cyclase, or affects other intracellular messengers such as calcium or phosphoinositol. Distinguishing between these two hypotheses for *agouti* gene action has important implications for understanding the molecular pathogenesis of A^{vy}-induced obesity and increased tumor susceptibility.

THE A^{vy} PHENOTYPE

Obese yellow $A^{vy}/-$ mice can be identified visually as early as 2–3 days after birth and, in contrast to mice homozygous for the recessive obesity mutations *ob* and *db*, have somewhat heavier muscles and longer bones than their non-A^{vy} sibs (reviewed in ref 20). No phenotypic differences between A^{vy}/a and A^{vy}/A^{vy} mice have been described.

Mottled $A^{vy}/-$ mice exhibit variegation with agouti and black patches or continuous and discontinuous transverse stripes on a yellow background. The pattern of transverse stripes is similar to that observed in animals that are mosaic or chimeric for a coat color mutation whose effects are mediated via the dermis (21). This suggests that A^{vy}-associated expression of *agouti* is unstable during early embryonic development, but stabilizes and is clonally propagated before the allocation of progenitor cells to dermal segments.

In general, effects of A^{vy} on nonpigment cells vary more or less concordantly with the coat color phenotype. Thus, yellow mice are obese and hyperinsulinemic, whereas pseudoagouti mice are lean and normoinsulinemic; however, the relative proportions of yellow pigment in mice with different degrees of mottling are *not* correlated with body weight. Even a small yellow area on an otherwise completely "pseudoagouti" mouse is often sufficient to predict that the animal likely will become obese and hyperinsulinemic, and thus will

not fit the definition of pseudoagouti (G. L. Wolff, unpublished observations).

MOLECULAR BASIS OF THE A^{vy} MUTATION

Northern analyses of tissues from adult yellow A^{vy}/a mice, using an *agouti* cDNA as probe, demonstrate expression of an RNA indistinguishable in size from the normal *agouti* RNAs, but in every tissue of the body rather than just in the skin and testes. This RNA is not detectable by Northern analysis in tissues of pseudoagouti A^{vy}/a mice (**Fig. 2**).

One of the most interesting aspects of A^{vy} is its variable expressivity with regard to coat color pattern, which is strongly influenced by the strain genome of the mother and by her *agouti* locus phenotype (22). Corresponding to the proportions of hair follicle melanocytes in which the *agouti* gene is expressed, $A^{vy}/-$ animals may be completely yellow (highest proportion), mottled (intermediate proportion), or pseudoagouti (lowest proportion). The phenotype of pseudoagouti animals is similar, but not identical, to the nonmutant agouti phenotype; rather than a subapical yellow band, individual hairs may exhibit a disordered arrangement of yellow pigment throughout the entire hair (23).

Molecular cloning studies indicate that the A^{vy}-specific RNA is chimeric, with a foreign 5' sequence derived from an intracisternal A particle (IAP) element (H. Vrieling, D. M. J. Duhl, K. A. Miller, G. T. Wolff, and G. S. Barsh, unpublished results). The 5' sequence is not translated, and is spliced to exons 2, 3, and 4 of the normal *agouti* gene (H. Vrieling et al., unpublished results). Thus, the A^{vy}-specific RNA encodes a normal *agouti* protein expressed in nearly every tissue of the body. These findings explain several genetic and biologic observations regarding A^{vy}.

The variable expressivity of A^{vy} can be explained most easily by epigenetic inactivation of regulatory sequences within the IAP, as germline reversion to A has not been observed. The variegation observed in mottled $A^{vy}/-$ mice indicates that gene inactivation occurs stochastically among precursor cells during embryonic development before hair follicle clones are laid down; after this time it is clonally inherited. This type of clonal inheritance might be maintained either by DNA methylation or by changes in chromatin conformation. Genetic studies (22) suggest that factors that influence A^{vy} gene inactivation depend on both strain background and parental origin.

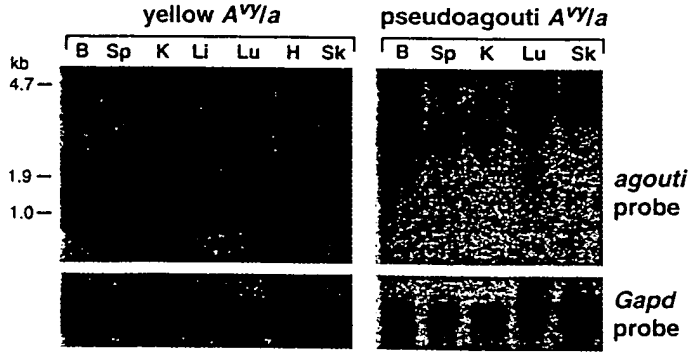

Figure 2. Molecular abnormalities in the A^{vy} mutation. Northern hybridization analysis of *agouti* expression in different tissues of adult yellow and pseudoagouti A^{vy}/a mice. Total RNA (30 μg) was isolated from brain (B), spleen (Sp), kidney (K), liver (Li), lung (Lu), heart (H), or skin (Sk) of yellow or pseudoagouti A^{vy}/a mice, fractionated on a formaldehyde-agarose gel, and transferred to a nylon membrane. The blot was hybridized with a probe that contained agouti coding sequences, stripped, and then rehybridized with a probe for the glyceraldehyde 3-phosphate dehydrogenase (Gapd) gene to control for amount of RNA present. Normally, *agouti* RNA is expressed only in the skin and the testes. Although there is no RNA detectable in pseudoagouti animals, their phenotype suggests a fine-grained mosaicism of *agouti* gene expression (see text).

The pseudoagouti phenotype is most easily explained by early inactivation of IAP regulatory sequences in every cell of the embryo, followed by partial reactivation in a small proportion of cells. An alternative explanation that the pseudoagouti phenotype represents inactivation in most, but not all, cells of the animal seems less likely given that pseudoagouti mice exhibit a fine-grained mosaicism rather than a single yellow stripe on an otherwise agouti animal.

THE OBESE-DIABETIC SYNDROME IN THE YELLOW $A^{vy}/-$ MOUSE

Obesity and diabetes are serious health hazards, not only by themselves, but also especially as risk factors for cardiovascular and respiratory diseases (24). In the U.S. 80% of type II diabetics are obese and about 20% of obese individuals are diabetic (25). Genetic rodent models of obesity and/or diabetes are important tools for elucidating the pathophysiology of these conditions and for testing new therapeutic approaches (26). The abnormalities in yellow $A^{vy}/-$ mice are markedly different from those caused by the recessive mouse obesity mutations *ob* (obese) and *db* (diabetes) and are reviewed in some detail.

Parabiosis of strain YS/Wf (27) yellow A^{y}/a with black *a/a* littermates of the same sex between 4 and 28 weeks of age failed to affect the body weight or fat content of either partner (28). These data indicate that the *agouti* protein does not circulate, at least not in sufficient quantity to induce obesity. This is in accord with the autocrine/paracrine mode of action of the *agouti* protein as suggested by its effects on hair follicle melanocytes and on cultured cells.

In contrast, parabiosis of fat *db/db* with lean nonmutant mice caused the lean partner to lose weight, become hypoglycemic, and die within 50 days of the surgery (29). When *ob/ob* mice were parabiosed with *db/db* partners, the *ob/ob* mice became hypoglycemic, lost weight, and died of starvation. Parabiosis of *ob/ob* with lean nonmutant mice decreased the food intake and slowed the weight gain of the *ob/ob* partners compared with these parameters in *ob/ob:ob/ob* parabionts (30). These results are interpreted as indicating that *ob/ob* mice are unable to produce enough of a postulated circulating satiety factor to regulate their food intake, whereas *db/db* mice produce sufficient satiety factor but cannot respond to it because of a defective satiety center.

In yellow A^{vy}/a or A^{y}/a mice, plasma corticosterone levels are not elevated above those in their nonyellow sibs, and adrenalectomy does not prevent development of obesity (reviewed in ref 3). In contrast, plasma corticosterone levels in *ob/ob* and *db/db* mice are elevated compared with their lean littermates (reviewed in ref 3).

Neither thyrotrophin, growth hormone, nor prolactin is involved in the development of obesity in either yellow or obese mice as the absence of these hormones in yellow dwarf (A^{y}/a *dw/dw*) mice and obese dwarf (*ob/ob dw/dw*) mice

failed to prevent adiposity (reviewed in ref 3). Indeed, the effects of the *agouti* protein in increasing lean body mass, as well as fat deposition, are still expressed in yellow hypophysectomized mice, even though to a lesser degree than in sham-operated mice (31, 32).

Hyperphagia

Yellow A^{vy}/- mice eat 10–36% more than their non-A^{vy} sibs, depending on genetic strain background (33–36). However, as in other genetic obesities in rodents, the degree of hyperphagia alone does not account for the fourfold increase of carcass triglyceride content of yellow A^{vy}/a mice (26%) compared with *a/a* controls (6%) (33). The results of the diet restriction experiment (34) discussed in a later section suggest that increased efficiency of calorie utilization also plays a role in the development of obesity. This was confirmed by measurements demonstrating a threefold greater efficiency in female yellow A^{vy}/A than in female agouti *A/a* (BALB/c × VY)F1 hybrid mice (35).

The effects of A^{vy} on body weight are apparent in mice fed a standard diet (4–6% fat), one with 10% fat (HF), and one with a high proportion of sucrose (HS). However, the effects of A^{vy} on insulin resistance and glucose metabolism are more pronounced with the HF and HS diets.

Both the HF and HS diets were more diabetogenic in female A^{vy}/A mice, as measured by an impaired glucose tolerance test (GTT), than the control diet. GTT impairment in A^{vy}/A mice was detected after 3 weeks of feeding; in contrast, the GTT of female *A/a* control mice was minimally affected (35).

Although hyperphagia in yellow A^{vy}/- mice is not necessary or sufficient to account for obesity, an intriguing observation, regarding a possible cause of hyperphagia is based on the effects of α-MSH compared with desacetyl-α-MSH. Bray et al. (36) found that the pituitary of yellow A^{vy}/a mice had a reduced α-MSH:desacetyl-α-MSH ratio. Because desacetylated α-MSH was more potent than α-MSH in stimulating food intake (37), reduced acetylation of α-MSH may play a role in A^{vy}-associated hyperphagia. Studies of adrenalectomized yellow mice showed that the effects of MSH peptides on food intake, weight gain, and fat storage were independent of, but interacted with, the effects of corticosterone (38). It will be interesting to determine whether desacetyl-α-MSH has an altered affinity for melanocortin receptors that may be involved in eating behavior.

Carcass triglyceride content

At 6 to 10 weeks of age, yellow A^{vy}/- mice exhibited twice the amount of carcass triglycerides per unit body weight compared with non-A^{vy} controls (33). By 5 months of age when their weights began to plateau, the carcass triglyceride content in yellow A^{vy}/a mice was about 26% of the body weight, 4.4-fold the amount compared with black *a/a* controls (33).

These observations are in contrast to C57BL/6J-*ob/ob* and C57BL/KsJ-*db/db* mice, which have a greater degree of obesity and an earlier onset. At 5 weeks of age, *db/db* and *ob/ob* mice already exhibited carcass triglyceride contents 3- and 4.5-fold those of their corresponding lean controls, and plateaued with triglyceride contents of 42% and 52%, respectively (33). These observations, in combination with morphometric data on adipocytes (39), led to the proposal that obesity of yellow A^{vy}/a mice is mostly hypertrophic, whereas the obesities of *ob/ob* and *db/db* mice are mostly hyperplastic (33).

Lipogenesis and lipolysis

One reason for the difference in the development of obesity between A^{vy}/a mice and *ob/ob* or *db/db* mice is the rate of hepatic lipogenesis (33). Although the lipogenic rate of A^{vy}/a mice was twice that of age-matched young black *a/a* mice and sixfold that of age-matched adult black *a/a* mice, the rates of A^{vy}/a mice were much lower at either age than those of *ob/ob* and *db/db* mice at corresponding ages (33). This may explain why yellow mice were more sensitive than *ob/ob* and *db/db* mice to antiobesity agents such as LY79771 (40). When treated with LY79771, body weights of yellow mice decreased, whereas those of *ob/ob* and *db/db* mice plateaued but were not reduced.

Regardless of its mechanism, an antiobesity agent perturbs the balance between energy intake and energy output until a new balance is established. In *ob/ob* and *db/db* mice and fatty *fa/fa* rats, antiobesity compounds arrest the development of obesity, but the very high hepatic lipogenic rate maintains the existing obesity and, hence, high body weight. In yellow mice, the hepatic lipogenic rate is higher than normal. However, in contrast to the rate in *ob/ob* and *db/db* mice and fatty *fa/fa* rats, it is not high enough to maintain the obesity during administration of LY79771, and thus drug treatment results in weight loss.

The sensitivity of yellow mice to antiobesity compounds is not restricted to β-agonists such as LY79771 and LY104119 (34). Other antiobesity compounds such as fluoxetine (41), a serotonin reuptake inhibitor that suppresses appetite, and ephedrine (42), which both suppresses appetite and stimulates thermogenesis, also reduced the body weight of yellow mice.

With regard to lipolysis, studies of isolated adipose tissue in vitro indicated that the basal lipolytic rate of adipose tissue from yellow A^{vy}/a mice was about half that of *a/a* mice (43), possibly due to the difference in the density of adipocytes as a function of different adipocyte size (39). Therefore, the response to lipolytic agents between yellow and black mice was normalized according to the respective basal rates. Measured by the release of free fatty acid and glycerol, the response of A^{vy}/a adipose tissue to epinephrine (43), theophylline (43), and the β agonists LY79771 (44) and LY104119 (34) was lower than normal. However, the response of A^{vy}/a adipose tissue to dibutyryl cyclic AMP was normal (43).

These observations suggest that yellow A^{vy}/a mice have a defect in the signaling mechanisms responsible for generating and/or maintaining intracellular cyclic AMP in adipocytes. This was confirmed by measuring total cyclic AMP concentrations in the adipose tissue and incubation medium in the presence of LY79771 (44) and LY104119 (34). This signaling deficiency in adipose tissue provides a striking parallel to the effect of *agouti* in pigment cells. Although the cyclic AMP-coupled lipolytic defect is a contributing factor to the obesity of yellow A^{vy}/a mice, it may not result from the direct action of the mutation as it is also present in obese *ob/ob* and *db/db* mice (45) and in obese A^{y}/a mice (43).

Thermogenesis

An important determinant of energy balance and regulation of body weight is nonshivering thermogenesis, which occurs in brown adipose tissue under the control of the sympathetic nervous system (46). The accumulation of tissue dopamine resulting from the inhibition of dopamine β-hydroxylase by 1-cyclohexyl-2-mercaptoimidazole is one method of measuring sympathetic tone that reflects the relative level of nonshivering thermogenesis (47).

Normally, heart, liver, and interscapular brown adipose tissue exhibit a marked diurnal rhythm of dopamine accumulation, reaching a peak just before the initiation of the light cycle. In A^{vy}/a mice this rhythm was dampened in the liver and brown adipose tissue but not in the heart (48). Concordantly, whole body thermogenesis of yellow A^{vy}/a mice, measured with a gradient layer calorimeter, was about 75% that of *a/a* mice (34). As in the case of lipogenesis and lipolysis, changes in thermogenesis are also present in rodent obesity caused by other single gene mutations (46).

When yellow A^{vy}/a mice were forced to lose weight by restricting food intake to 80% of the ad libitum level, whole body thermogenesis decreased, presumably as a compensatory mechanism (34). Subsequently, thermogenesis increased to its preweight loss rate, but no further weight loss ensued. However, a subsequent 20% diet restriction (64% of ad libitum) caused further weight loss, but no change in thermogenesis, before the weight stabilized for the second time. These observations suggest that the change in thermogenesis is insufficient to account for the changes in body weight, and instead suggest that alterations in fuel efficiency account for the observed regulation of body weight.

It seems likely that fuel efficiency increased after the first weight loss experience and thus the same level of thermogenesis was maintained in spite of lower energy intake. Regulation, leading to increased fuel efficiency, could occur by a variety of different mechanisms and may be integrated by the hypothalamus (49). The fact that yellow mice are able to stabilize their weights at different levels of energy intake indicates that their hypothalamic control of energy homeostasis is intact but the set point for the equilibrium is high.

The reduced thermogenesis could be corrected by β-agonists such as LY79771 (50) and LY104119 (34). This, together with the ability of these compounds to stimulate lipolysis in these mice (34, 44, 50), resulted in weight loss.

Hyperinsulinemia and pancreatic islet hyperplasia and hypertrophy

Unlike *db/db* mice that are hyperinsulinemic at 10 days of age (51) and *ob/ob* mice in which hyperinsulinemia is detectable by 4 weeks of age (52), A^{vy}/A (BALB/c × VY)F_1 mice did not become hyperinsulinemic until about 6 weeks of age (53) and exhibited a sexual dimorphism in this characteristic as well as in the degree of hyperglycemia. By 2 months of age, plasma insulin concentrations in female yellow A^{vy}/a mice were 4-fold those of controls, whereas those in comparable male mice were 10-fold those of *a/a* control mice (2). By the time the obesity of A^{vy}/a mice peaked at 6 months of age, both male and female mice had plasma insulin levels more than 20-fold those of male and female black *a/a* mice, with female A^{vy}/a mice usually having the highest concentrations (2, 54).

Plasma insulin data from strain VY/WfL yellow A^{vy}/a and black *a/a* mice younger than 5 weeks of age are not available. However, longitudinal studies of pancreatic insulin and glucagon contents and pancreatic islet morphometrics have been performed in two separate experiments. In one study, pancreatic islets of strain VY/WfL male and female A^{vy}/a and *a/a* mice were measured and counted at 21 days and at 3, 6, and 12 months of age (T. T. Yen and G. Williams, unpublished data). No hyperplasia or hypertrophy of islets was observed in either male or female yellow mice at 21 days, but both were present at 3 months. In another study, the number of β cells was higher in male A^{vy}/A (BALB/c × VY)F1 hybrid mice than in male *A/a* mice at 21 days of age; however, neither the insulin or glucagon contents per unit weight of pancreas nor the mean total islet areas differed between A^{vy}/A and *A/a* mice (55). These data suggest that morphological changes precede biochemical changes in pancreatic islets.

A gender difference existed in islet size. At 6 months of age, the mean islet size of female *a/a* mice was 10-fold that of comparable male mice (2). Regardless of the gender difference, 6-month-old male and female A^{vy}/a mice had islet sizes approximately twice as large as the corresponding *a/a* mice (T. T. Yen and G. Williams, unpublished data). Although quantitative mouse to mouse correlations are not available, it appears that female A^{vy}/a mice are more hyperinsulinemic and have a higher degree of islet hyperplasia and hypertrophy than male A^{vy}/a mice.

Hyperinsulinemia and lipogenesis

To define the temporal interactions among obesity, hyperinsulinemia, and the activities of six hepatic lipogenic enzymes (glucose-6-phosphate dehydrogenase, 6-phosphogluconate dehydrogenase, malic enzyme, citrate cleavage enzyme, acetyl CoA carboxylase, fatty acid synthetase), a developmental study was conducted in A^{vy}/a and *a/a* mice at 2, 3, 5, and 8 months of age (56). Yellow $A^{vy}/-$ mice are especially suitable for dissecting the temporal relationships among these parameters because their obesity develops relatively slowly.

In yellow mice, the specific activity of malic enzyme correlated positively with body weight, liver weight, plasma insulin level, and age. The specific activities of citrate cleavage enzyme and 6-phosphogluconate dehydrogenase correlated positively with age, body weight, and liver weight. However, when adjusted for insulin level, correlations between other parameters disappeared, indicating that elevated plasma insulin level was a common factor that correlated with the increase of body and liver weight and with specific activities of malic enzyme and citrate cleavage enzyme. Correlation does not prove that hyperinsulinism is the cause of obesity in yellow $A^{vy}/-$ mice, but does suggest that it plays a central role in its development.

Hyperglycemia

Although obesity poses an increased risk for diabetes, not all obese people develop diabetes and not all diabetics are obese (25). This suggests that development of obesity and diabetes can be influenced by independent factors (57). Many obese human subjects exhibit only impaired glucose tolerance (58) and do not progress to a diabetic state (59) because both insulin resistance and β cell defects are required to precipitate type II diabetes (60). This is also true for the genetic rodent obesities (61), including A^{vy} (2). Yellow $A^{vy}/-$ mice exhibit hyperinsulinism and insulin resistance, but the development of overt hyperglycemia depends on physiological factors that differ with strain background, gender, and diet.

A case in point is that male and female yellow A^{vy}/a mice with identical strain background are obese, hyperinsulinemic, insulin resistant, and glucose intolerant; however, only the males are hyperglycemic. Most female yellow mice are normoglycemic or, if their blood glucose levels are elevated, the elevation is slight. Administration of dexamethasone induces hyperglycemia in female yellow mice (62), reminiscent of the diabetogenic effects of glucocorticoids in humans (63). It can be reversed by ciglitazone, a compound that improves insulin sensitivity (62). The induction of hyperglycemia in female A^{vy}/a mice is concomitant with the induction of hepatic estrone sulfotransferase (64), an enzyme that inactivates estrogens, supporting the hypothesis that estrogens confer protection against the development of diabetes (61).

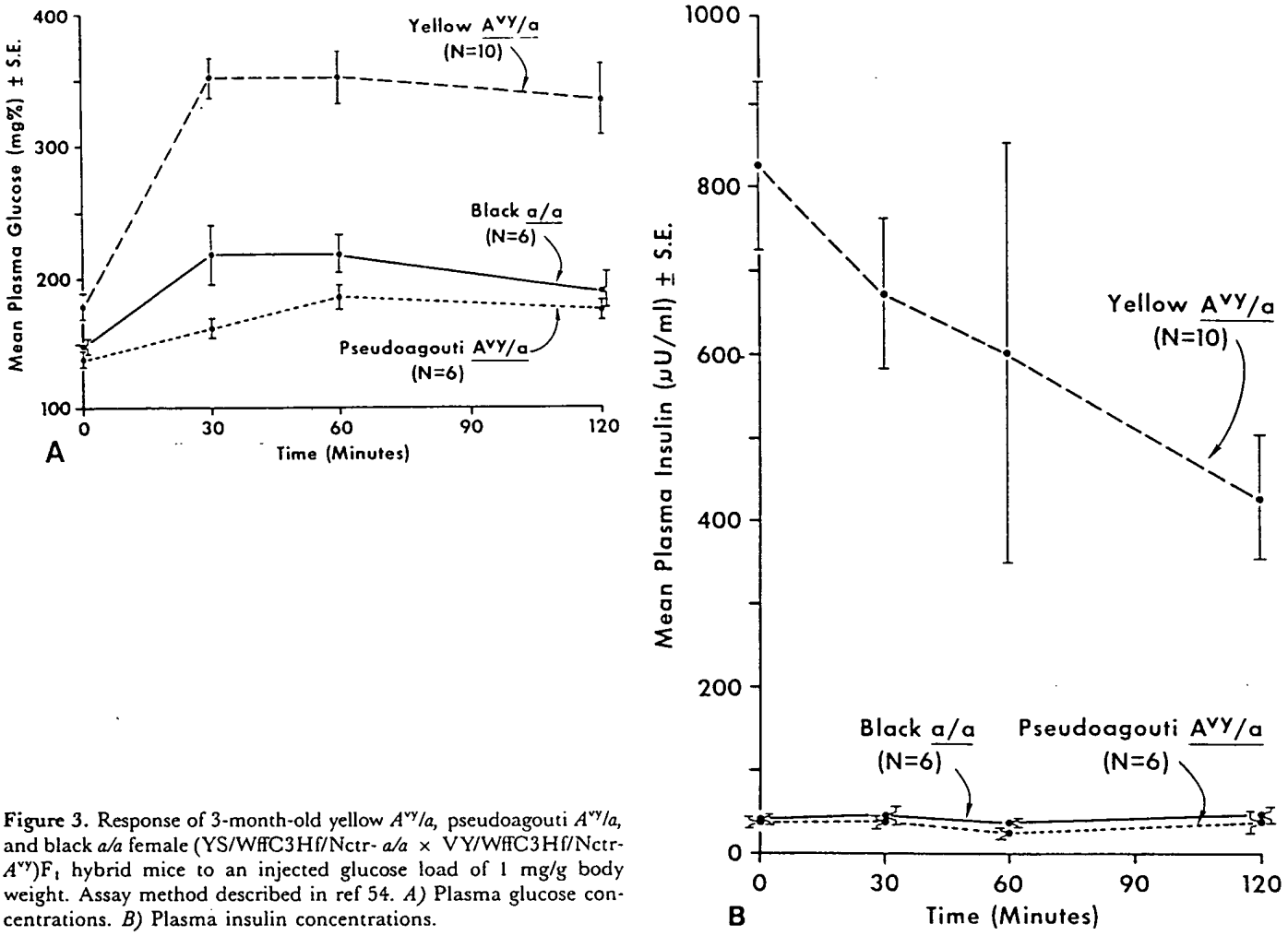

Figure 3. Response of 3-month-old yellow A^{vy}/a, pseudoagouti A^{vy}/a, and black *a/a* female (YS/WffC3Hf/Nctr-*a/a* × VY/WffC3Hf/Nctr-A^{vy})F_1 hybrid mice to an injected glucose load of 1 mg/g body weight. Assay method described in ref 54. *A)* Plasma glucose concentrations. *B)* Plasma insulin concentrations.

Insulin resistance

The insulin resistance of yellow $A^{vy}/-$ mice has been quantitated directly in vivo and in vitro. The former was measured by the ability of exogenous insulin to lower fasting blood glucose or to improve glucose tolerance (2). The latter was determined in isolated adipose tissue by the ability of insulin to stimulate glucose metabolism (2) or to suppress hormone-stimulated lipolysis (65). In general, both types of measurements show increased insulin resistance in 6- to 7-month-old yellow $A^{vy}/-$ mice compared with *a/a* mice (2). The degree of resistance is relatively greater in males compared with females, and parallels the sexual dimorphism in hyperglycemia. Maximal responses to insulin could not be elicited in either in vivo or in vitro systems, suggesting that insulin resistance in these mice is due to postreceptor defects (2, 53). Direct assays of insulin resistance in vivo in yellow mice younger than 6–7 months have not yet been performed; however, glucose metabolism in adipose tissue showed some insulin resistance in 2-month-old male yellow A^{vy}/a mice; this coincided with the earliest age at which hyperinsulinemia was observed (2). To discern the cause and effect relationship between hyperinsulinemia and insulin resistance will require analyses in even younger mice.

Compounds that improve insulin sensitivity without decreasing body weight, such as ciglitazone (54) and Tanabe-174 (66), were able to normalize blood glucose and plasma insulin without causing weight loss. This suggests that hyperinsulinism and insulin resistance are not required to maintain obesity in yellow A^{vy}/a mice. Although insulin is lipogenic, antilipolytic, and thermogenic, hyperinsulinism and insulin resistance may play only a permissive, rather than a primary, role in the maintenance of obesity. On the other hand, insulin resistance does play a pivotal role in the expression of hyperglycemia.

PLEIOTROPY AND THE LEAN PSEUDOAGOUTI A^{vy}/a PHENOTYPE

As noted earlier, *agouti* mRNA could not be detected by Northern analysis in tissues of pseudoagouti A^{vy}/a mice. These mice are similar in body weight to control black *a/a* mice. They also have normal glucose and insulin levels, and respond normally to a glucose load (**Fig. 3***A*, Fig. 3*B*). Their rates of glucose oxidation and conversion of glucose to lipid are higher than those in the obese yellow A^{vy}/a mice and resemble those of the *a/a* mice (67). However, these mice do not represent a complete reversion to the nonmutant phenotype, as indicated by detailed analysis of their hair color pattern (23) and by their response to the tumor promoter lindane (see next section).

Comparison of the responses of the pseudoagouti with the yellow A^{vy}/a and black *a/a* mice makes it possible to discriminate between those physiologic, pathologic, and metabolic responses to particular agents associated with obesity

and those that are modulated by a presumed very low or mosaic expression of the *agouti* gene (68). For example, lung and liver tumor formation occurred in the lindane-treated pseudoagouti as well as in the yellow A^{vy}/a mice, but *not* in the black *a/a* littermates. In contrast, A^{vy}/a mice differ in some components of immunocompetence from pseudoagouti A^{vy}/a and black *a/a* mice, but the pseudoagouti and black mice do not differ from each other (69). Likewise, in the lindane study (70, see below) the yellow A^{vy}/a females experienced 50% mortality between 17 and 24 months of age, regardless of treatment group, whereas the pseudoagouti and black females experienced only half as great mortality, i.e., 24% and 23%.

GROWTH REGULATION, HYPERPLASIA, AND NEOPLASIA

Enhancement of somatic growth by the A^{vy} and A^{y} genes and their influence on development of hyperplasia, preneoplastic lesions, and neoplasms were reviewed previously (20), as was utilization of these characteristics in carcinogenicity/toxicity bioassays (71). In general, the effects of A^{vy} on tumor development are rather subtle compared with other oncogenes. Endogenously ("spontaneous") or exogenously induced tumors or hyperplastic precursor lesions may develop in a wide variety of epithelial and mesenchymal tissues in yellow $A^{vy}/-$ and $A^{y}/-$ animals, depending on the strain background and treatment with specific carcinogens (W. E. Heston and co-workers, reviewed in ref 3 and 20).

Specific effects of A^{vy} on tumor incidence in mice with genomes susceptible or resistant to liver tumor formation are illustrated by the results of two studies. In one study yellow A^{vy}/A and agouti *A/a* male mice with a *susceptible* (C3H × VY)F1 genome were fed a phenobarbital-supplemented diet for 1 year (72). No difference in the incidence (18%) of single hepatocellular adenomas was observed between the genotypes. However, *multiple* adenomas appeared in 36% of the yellow mice, but in only 5% of the agouti sibs.

In the second study yellow A^{vy}/a, pseudoagouti A^{vy}/a, and black *a/a* female mice with the (YS × VY)F1 genome, which is relatively *resistant* to liver tumor development, were fed a diet supplemented with lindane (γ-hexachlorocyclohexane) for 24 months (70). The black *a/a* females were completely resistant to the compound, no formation of hepatocellular tumors or lung tumors above the background incidence (<5%) being observed. In contrast, hepatocellular adenoma incidence in treated yellow mice was increased 27% above background and 6% above background in treated pseudoagouti females. Lung tumor incidence was increased 15% above background in the yellow mice and 7% in the pseudoagouti mice.

Increased somatic growth in yellow mice indicates an effect of the *agouti* protein on an unknown process (or processes) of growth regulation in the animal. The cumulative data from chronic bioassays of the response of A^{vy}/a mice to various toxicants suggest that the presence of *agouti* protein in susceptible tissues also affects growth regulation at the cellular level and appears to potentiate/facilitate processes involved in cell transformation to hyperplasia and neoplasia. In addition, the anabolic tissue environments in yellow mice stimulate tumor growth.

The effects of A^{vy} on cell transformation in vitro have been examined in two different studies with apparently opposite results. In one study, established cell lines from A^{vy}/a fibroblasts exhibited elevated levels of spontaneous focus formation compared with cell lines from *a/a* mice of the same strains (73). In another study, primary fibroblasts from A^{vy}/a mice exhibited lower levels of spontaneous and N-methyl-N'-nitro-N-nitrosoguanidine (MNNG)-induced transformation compared with control fibroblasts from *a/a* mice (74). The apparent difference between the results of the two studies may reflect the different experimental protocols and/or the use of primary fibroblasts vs. established cell lines.

In summary, expression of A^{vy} results in increased tumor susceptibility by itself and in combination with classical tumor promoters, both in genetically susceptible as well as in genetically resistant strain backgrounds. It is significant that, even though *agouti* expression could not be detected by Northern analysis in pseudoagouti mice, there is nonetheless a slight increase in tumor formation in this phenotype.

POSSIBLE MECHANISMS FOR A^{vy}-INDUCED OBESITY AND FUTURE DIRECTIONS

The A^{vy}-specific RNA codes for a normal *agouti* protein. Similarly, three other obesity-associated *agouti* mutations also result from the ubiquitous expression of chimeric RNAs, which each encode a normal *agouti* protein (H. Vrieling et al., unpublished results). These observations suggest that A^{vy}-induced obesity results from ectopic activation of a signaling pathway that is used normally by hair follicle melanocytes, and leads to two alternative hypotheses (16, 19) based on possible mechanisms for *agouti* signaling in hair follicles (Fig. 4*A*).

If the *agouti* protein normally antagonizes the action of α-MSH at its melanocyte receptor (melanocortin-1 receptor) (Fig. 4*B*), then ectopic *agouti* expression is likely to antagonize the effects of α-MSH and related compounds at other melanocortin receptors, of which three have been cloned. None of the four cloned melanocortin receptors is expressed in the liver, in the pancreas, or in adipocytes. Therefore, if *agouti*-induced obesity is caused by melanocortin antagonism, A^{vy}-associated defects in lipolysis, lipogenesis, insulin sensitivity, and insulin overproduction are all likely to be consequences, rather than causes, of A^{vy}-induced obesity. Under this scenario, likely targets for *agouti* in nonpigment cells are expression of the melanocortin-3 and 4 receptors in the hypothalamus, which might lead to alterations in thermogenesis, eating behavior, and/or release of corticotrophic releasing factor. As described above, alterations in each of these components characterize all the rodent genetic obesities including A^{vy}. However, in no case does the magnitude of a particular alteration appear to be sufficient to account for the degree of obesity observed (reviewed in ref 26).

A second hypothesis proposes that *agouti* binds to its own receptor in melanocytes, and that the same or a similar receptor is present on nonpigment cells in most tissues, including brain, and can account for the plethora of physiologic derangements observed in yellow $A^{vy}/-$ mice (Fig. 4*C*). This hypothesis is attractive given the parallels between adenylate cyclase metabolism in adipocytes and melanocytes of A^{vy}/a animals. It could also explain why morphologic alterations in pancreatic islets apparently precede biochemical and physiologic derangements (55), assuming that *agouti* receptors are present on islet cells or their precursors.

Two avenues of research are likely to be helpful in distinguishing between these alternatives. The construction of transgenic animals in which *agouti* is placed under the control of tissue-specific promoters should indicate whether obesity can be induced by expression of *agouti* in potential target organs such as adipocytes or the pancreas. Development of an

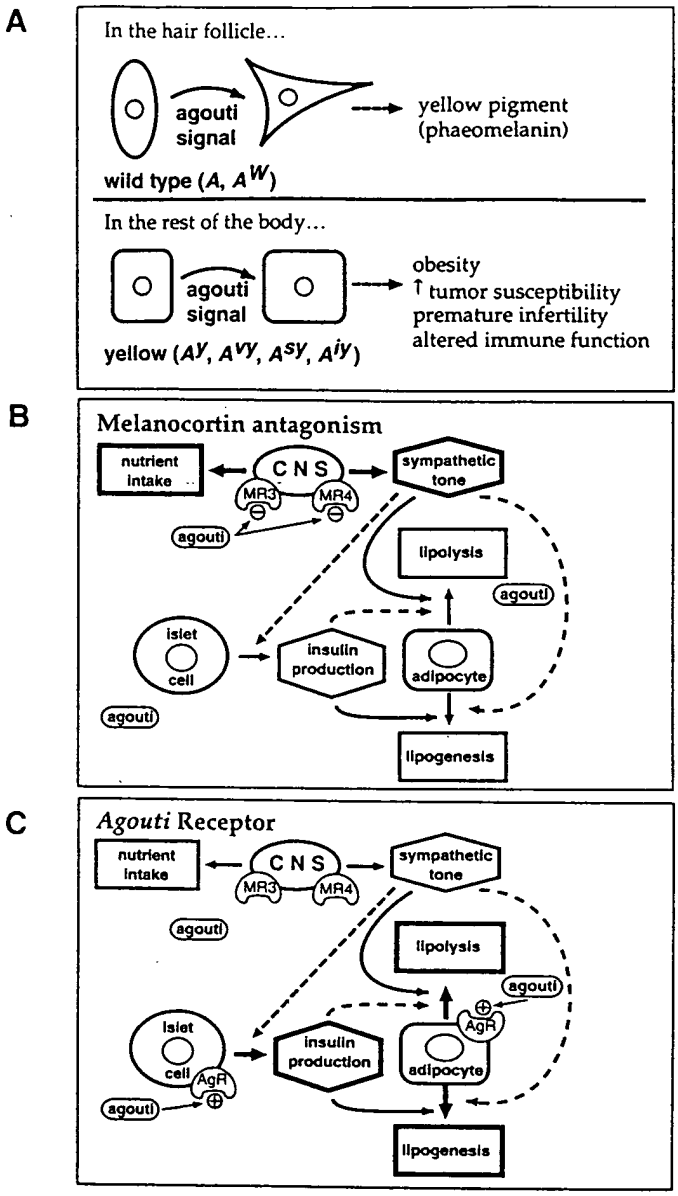

Figure 4. Possible mechanisms of *agouti*-induced obesity. *A)* Ectopic expression of the *agouti* protein in nearly every tissue explains similarities in the pleiotropic effects of A^{vy} and A^{y}. *Agouti* is also expressed ectopically in the dominant *agouti* mutants *sienna yellow* (A^{sy}) and *intermediate yellow* (A^{iy}) (24). A^{sy} and A^{iy} produce obesity but have not been characterized with regard to tumor susceptibility, immune abnormalities, or glucose metabolism. *B)* If *agouti* acts by antagonizing the effects of melanocortins, the MR3 and MR4 receptors in the hypothalamus and other portions of the brain are likely target sites to explain A^{vy}-associated obesity. In this case, alterations in nutrient intake and a reduction in sympathetic tone may be primary events (indicated in boldface). Adrenergic agonists generally produce decreased insulin production and lipogenesis (indicated by the dotted lines) and increased lipolysis (indicated by solid line); therefore, changes in energy balance, hyperinsulinism, and insulin resistance that occur in *agouti*-induced obesity would be secondary to a reduction in adrenergic tone. None of the four melanocortin receptors is expressed at significant levels in adipocytes, although low levels of the MR3 receptor can be detected in rat pancreas. *C)* If *agouti* acts by binding to an as yet unidentified receptor (AgR) expressed in islet cells and/or adipocytes, a direct and primary effect on insulin production and adipocyte metabolism would parallel the effects of *agouti* on G protein-coupled signal transduction in pigment cells. In this case, hyperphagia and altered thermogenesis would be a secondary response. A putative *agouti* receptor might also be expressed in the central nervous system.

in vitro assay for a soluble *agouti* protein should allow testing for antagonism to melanocortin receptor activation and/or to identify an agouti receptor using cell biologic approaches.

CONCLUSION

After almost 50 years of attempts to understand the physiologic/metabolic bases of the "yellow mouse syndrome," cloning and sequencing of the *agouti* gene and definition of the regulation of its expression have made conceptual and experimental integration of the molecular and physiologic aspects of the function of the *agouti* locus a practical possibility. Such studies should lead to a better understanding of the cellular metabolic dysregulations that give rise to obesity, diabetes, and neoplasia. FJ

This review is dedicated to the memory of Margaret M. Dickie who first described the A^{vy} mutation and provided the breeding stock from which Strain VY was developed. We thank K. B. Delclos and D. L. Greenman for constructive critiques of the manuscript.

REFERENCES

1. Dickie, M. M. (1962) A new viable yellow mutation in the house mouse. *J. Hered.* 53, 4-86
2. Yen, T. T., Bue, J. M., and Gill, A. M. (1990) The obese-diabetic syndrome of the viable yellow mouse and pharmacological interventions. In *Frontiers in Diabetes Research. Lessons from Animal Diabetes III.* (Shafrir, E., ed) pp. 294-299
3. Wolff, G. L., Roberts, D. W., and Galbraith, D. B. (1986) Prenatal determination of obesity, tumor susceptibility, and coat color pattern in viable yellow (A^{vy}/a) mice. *J. Hered.* 77, 151-158
4. Bultman, S. J., Michaud, E. J., and Woychik, R. P. (1992) Molecular characterization of the mouse agouti locus. *Cell* 71, 1195-1204
5. Miller, M. W., Duhl, D. M. J., Vrieling, H., Cordes, S. P., Ollmann, M. M., Winkes, B. M., and Barsh, G. S. (1993) Cloning of the mouse *agouti* gene predicts a secreted protein ubiquitously expressed in mice carrying the *lethal yellow* mutation. *Genes & Dev.* 7, 454-467
6. Vrieling, H., Duhl, D. M. J., Millar, S. E., Miller, K. A., and Barsh, G. S. (1994) Differences in dorsal and ventral pigmentation result from temporal- and region- specific expression of alternative isoforms of the mouse *agouti* gene. *Proc. Natl. Acad. Sci. USA* In press
7. Silvers, W. K. (1958) An experimental approach to action of genes at the *agouti* locus in the mouse. III. Transplants of newborn A^{w}-, *A*-, and a^{t}-*skin to* A^{y}-, A^{w}-, *A*-, and *aa* hosts. *J. Exp. Zool.* 137, 189-196
8. Silvers, W. K. (1979) The agouti and extension series of alleles, umbrous, and sable. In *The Coat Colors of Mice,* pp. 6-44, Springer Verlag, New York
9. Barsh, G. S., and Epstein, C. J. (1989) Physical and genetic characterization of a 75-kilobase deletion associated with a^{l}, a recessive lethal allele at the mouse *agouti* locus. *Genetics* 121, 811-818
10. Geschwind, I. (1966) Change in hair color in mice induced by injection of αMSH. *Endocrinology* 79, 1165-1167
11. Mountjoy, K. G., Robbins, L. S., Mortrud, M. T., and Cone, R. D. (1992) The cloning of a family of genes that encode the melanocortin receptors. *Science* 257, 1248-1251.
12. Robbins, L. S., Nadeau, J. H., Johnson, K. R., Kelly, M. A., Roselli-Rehfuss, L., Baack, E., Mountjoy, K. G., and Cone, R. D. (1993) Pigmentation phenotypes of variant extension locus alleles result from point mutations that alter MSH receptor function. *Cell* 72, 827-834
13. Gantz, I., Konda, Y., Tashiro, T., Shimoto, Y., Miwa, H., Munzert, G., Watson, S. J., Delvalle, J., and Yamada, T. (1993) Molecular cloning of a novel melanocortin receptor. *J. Biol. Chem.* 268, 8246-8250
14. Gantz, I., Miwa, H., Konda, Y., Shimoto, Y., Tashiro, T., Watson, S. J., Delvalle, J., and Yamada, T. (1993) Molecular cloning, expression, and gene localization of a 4th melanocortin receptor. *J. Biol. Chem.* 268, 15174-15179
15. Tamate, H. B., and Takeuchi, T. (1964) Action of the *e* locus of mice in the response of phaeomelanic hair follicles to alpha-melanocyte stimulating hormone in vitro. *Science* 224, 1241-1242
16. Jackson, I. (1993) Molecular genetics. Colour-coded switches. *Nature (London)* 362, 587-588
17. Lamoreaux, M. L. (1973) A study of gene interactions using coat color mutants in the mouse and selected mammals. Ph.D. thesis, University of Maine, Orono

18. Wolff, G. L., Galbraith, D. B., Domon, O. E., and Row, J. M. (1978) Phaeomelanin synthesis and obesity in mice: interaction of the viable yellow (A^{vy}) and sombre (e^{so}) mutations. *J. Hered.* 69, 295-298
19. Conklin, B. R., and Bourne, H. R. (1993) Mouse coat color reconsidered. *Nature (London)* 364, 110
20. Wolff, G. L. (1987) Body weight and cancer. *Am. J. Clin. Nutr.* 45, 168-180
21. Mintz, B. (1970) Gene expression in allophenic mice. In *Control Mechanisms in the Expression of Cellular Phenotypes* (Padykula, H. A., ed) pp. 15-42, Academic, New York
22. Wolff, G. L. (1978) Influence of maternal phenotype on metabolic differentiation of agouti locus mutants in the mouse. *Genetics* 88, 529-539
23. Galbraith, D. B., and Wolff, G. L. (1974) Aberrant regulation of the agouti pigment pattern in the viable yellow mouse. *J. Hered.* 65, 137-140
24. Turner, R. C. (1992) The role of obesity in diabetes. *Int. J. Obesity* 16 (Suppl. 2) S43-S46
25. Salan, L. B. (1987) Obesity and non-insulin-dependent diabetes mellitus. In *Recent Advances in Obesity Research: V* (Berry, E. H., Blondheim, S. H., Blondhjeim, H. E., and Shafrir, E., eds) pp. 26-32, John Libbey, London
26. Johnson, P. R., Greenwood, M. R. C., Horwitz, B. A., and Stern, J. S. (1991) Animal models of obesity: genetic aspects. *Annu. Rev. Nutr.* 11, 325-353
27. Wolff, G. L., and Pitot, H. C. (1973) Influence of background genome on enzymatic characteristics of yellow ($A^{y}/-$, $A^{vy}/-$) mice. *Genetics* 73, 109-123
28. Wolff, G. L. (1963) Growth of inbred yellow ($A^{y}a$) and non-yellow (aa) mice in parabiosis. *Genetics* 48, 1041-1058
29. Coleman, D. L., and Hummel, K. P. (1969) Effects of parabiosis of normal with genetically diabetic mice. *Am. J. Physiol.* 217, 1298-1304
30. Coleman, D. L. (1973) Effects of parabiosis of obese with diabetes and normal mice. *Diabetologia* 9, 294-298
31. Plocher, T. A., and Powley, T. L. (1976) Effect of hypophysectomy on weight gain and body composition in the genetically obese yellow (A^{y}/a) mouse. *Metabolism* 25, 593-602
32. Salem, M. A. M., Lewis, U. J., Haro, L. S., Kishi, K., McAllister, D. L., Seavey, B. K., Bee, G., and Wolff, G. L. (1989) Effects of hypophysectomy and the insulin-like and anti-insulin pituitary peptides on carbohydrate metabolism in yellow A^{vy}/A (BALB/c × VY)F_1 hybrid mice. *Proc. Soc. Exp. Biol. & Med.* 191, 408-419
33. Yen, T. T., Allan, J. A., Yu, P. L., Acton, M. A., and Pearson, D. V. (1976) Triacylglycerol contents and in vivo lipogenesis of *ob/ob*, *db/db*, and A^{vy}/a mice. *Biochim. Biophys. Acta* 441, 213-220
34. Yen, T. T., McKee, M. M., and Stamm, N. B. (1984) Thermogenesis and weight control. *Int. J. Obesity* 8 (Suppl. 1) 65-78
35. Frigeri, L. G., Wolff, G. L., and Teguh, C. (1988) Differential responses of yellow A^{vy}/A and agouti A/a (BALB/c × VY) F-1 hybrid mice to the same diets: glucose tolerance, weight gain, and adipocyte cellularity. *Int. J. Obesity* 12, 305-320
36. Bray, G. A., Shimizu, H., Retzios, A. D., Shargill, N. S., and York, D. A. (1988) Reduced acetylation of melanocyte stimulating hormone (MSH): a biochemical explanation for the yellow obese mouse. In *Obesity in Europe 88* (Bjorntorp, P., and Rossner, S., eds) pp. 259-270, John Libbey, London
37. Shimizu, H., Shargill, N. S., Bray, G. A., Yen, T. T., and Gesellchen, P. D. (1989) Effects of MSH on food intake, body weight and coat color of the yellow obese mouse. *Life Sci.* 45, 543-552
38. Shimizu, H., Shargill, N. S., and Bray, G. A. (1989) Adrenalectomy and response to corticosterone and MSH in the genetically obese yellow mice. *Am. J. Physiol.* 256, R494-R500
39. Johnson, P. R., and Hirsch, J. (1972) Cellularity of adipose depots in six strains of genetically obese mice. *J. Lipid Res.* 13, 2-11
40. Shaw, W. N., Schmiegel, K. K., Yen, T. T., Toomey, R. E., Meyers, D. B., and Mills, J. (1981) LY79771: a novel compound for weight control. *Life Sci.* 29, 2091-2101
41. Yen, T. T., Wong, D. T., and Bemis, K. G. (1987) Reduction of food consumption and body weight of normal and obese mice by chronic treatment with fluoxetine: a serotonin reuptake inhibitor. *Drug. Dev. Res.* 10, 37-45
42. Yen, T. T., McKee, M. M., and Bemis, K. G. (1981) Ephedrine reduces weight of viable yellow obese mice (A^{vy}/a). *Life Sci.* 28, 119-128
43. Yen, T. T., Steinmetz, J., and Wolff, G. L. (1970) Lipolysis in genetically obese and diabetes-prone mice. *Horm. Metab. Res.* 2, 200-203
44. Yen, T. T., McKee, M. M., Stamm, N. B., and Bemis, K. G. (1983) Stimulation of cyclic AMP and lipolysis in adipose tissue of normal and obese A^{vy}/a mice by LY79771, a phenethanolamine, and stereoisomers. *Life Sci.* 32, 1515-1522
45. Steinmetz, J., Lowry, L., and Yen, T. T. T. (1969) An analysis of the lipolysis in vitro of obese-hyperglycemic and diabetic mice. *Diabetologia* 5, 373-378
46. Himms-Hagen, J. (1989) Brown adipose tissue thermogenesis and obesity. *Prog. Lipid Res.* 28, 67-115
47. Fuller, R. W., and Perry, K. W. (1982) Dopamine accumulation after dopamine β-hydroxylase inhibition in rat hearts as an index of norepinephrine turnover. *Life Sci.* 31, 563-570
48. Yen, T. T., Fuller, R. W., Hemrick-Luecke, S., and Dininger, N. B. (1988) Effects of LY104119, a thermogenic weight-reducing compound, on norepinephrine concentrations and turnover in obese and lean mice. *Int. J. Obesity* 12, 59-67
49. Anderson, G. H., Li, E. T. S., and Glanville, N. T. (1984) Brain mechanisms and the quantitative and qualitative aspects of food intake. *Brain Res. Bull.* 12, 167-173
50. Yen, T. T. (1984) The antiobesity and metabolic activities of LY79771 in obese and normal mice. *Int. J. Obesity* 8, 69-78
51. Coleman, D. L., and Hummel, K. P. (1974) Hyperinsulinemia in preweaning diabetes (*db*) mice. *Diabetologia* 10, 607-610
52. Joosten, H. F. P., and van der Kroon, P. H. W. (1974) Enlargement of epididymal adipocytes in relation to hyperinsulinemia in obese hyperglycemic mice (*ob/ob*). *Metabolism* 23, 59-66
53. Frigeri, L. G., Wolff, G. L., and Robel, G. (1983) Impairment of glucose tolerance in yellow (A^{vy}/A) (BALB/c × VY) F-1 hybrid mice by hyperglycemic peptide(s) from human pituitary glands. *Endocrinology* 113, 2097-2105
54. Gill, A. M., and Yen, T. T. (1991) Effects of ciglitazone on endogenous plasma islet amyloid polypeptide and insulin sensitivity in obese-diabetic viable yellow mice. *Life Sci.* 48, 703-710
55. Warbritton, A., Gill, A. M., Yen, T. T., Bucci, T., and Wolff, G. L. (1994) Pancreatic islet cells in pre-obese yellow $A^{vy}/-$ mice: relation to adult hyperinsulinemia and obesity. *Proc. Soc. Exp. Biol. & Med.* In press
56. Yen, T. T., Greenberg, M. M., Yu, P., and Pearson, D. V. (1976) An analysis of the relationship among obesity, plasma insulin, and hepatic lipogenic enzymes in "viable yellow obese" mice (A^{vy}/a). *Horm. Metab. Res.* 8, 159-166
57. Barrett-Connor, E. (1989) Epidemiology, obesity, and non-insulin-dependent diabetes mellitus. *Epidemiol. Rev.* 11, 172-181
58. Lillioja, S., Mott, D. M., Howard, B. V., Bennett, P. H., Yki-Jarvinen, H., Freymond, D., Nyomba, B. L., Zurlo, F., Swinburn, B., and Borgardus, C. (1988) Impaired glucose tolerance as a disorder of insulin action. *New Engl. J. Med.* 318, 1217-1225
59. Shuman, C. R. (1988) Diabetes mellitus: definition, classification, and diagnosis. In *Diabetes Mellitus* (Galloway, J. A., Potvin, J. H., and Shuman, C. R., eds) pp. 2-13, Eli Lilly, Indianapolis
60. DeFronzo, R. A., Bonadonna, R. C., and Ferrannini, E. (1992) Pathogenesis of NIDDM. A balanced review. *Diabetes Care* 15, 318-368
61. Leiter, E. H. (1993) Obesity genes and diabetes induction in the mouse. *Crit. Rev. Food Sci. Nutr.* 33, 333-338
62. Yen, T. T., Gill, A. M., Powell, J. G., and Sampson, B. M. (1992) Ciglitazone prevents and reverses dexamethasone-induced hyperglycemia in female viable yellow mice. *Int. J. Obesity* 16, 923-933
63. Wajngot, A. S., Giacca, A., Grill, V., Vranic, M., and Efendic, S. (1992) The diabetogenic effects of glucocorticoids are more pronounced in low-than in high-insulin responders. *Proc. Natl. Acad. Sci. USA* 89, 6035-6039
64. Gill, A. M., Leiter, E. H., Powell, J. G., Chapman, H. D., and Yen, T. T. (1994) Dexamethasone-induced hyperglycemia in obese A^{vy}/a (viable yellow) female mice entails preferential induction of hepatic estrogen sulfotransferase. *Diabetes* In press
65. Yen, T. T., and Steinmetz, J. A. (1972) Lipolysis of genetically obese and/or hyperglycemic mice with reference to insulin response of adipose tissue. *Horm. Metab. Res.* 4, 331-337
66. Yen, T., Bue-Valleskey, J., Burkhart, D., Dininger, N., Gill, A., Gold, G., Johnson, T., Myers, S., Shaw, W., Short, W., Tinsley, F., Williams, G., Williams, V., and Yakubu-Madus, F. (1993) The efficacy and adverse effects of a potent insulin sensitivity enhancer: LY282449 (Tanabe-174). *Proc. Eur. Assn. Study Diabetes* 698 (abstr.)
67. Yen, T. T. T., Lowry, L., Steinmetz, J., and Wolff, G. L. (1970) Physiologic and genetic influences on regulation of glucose metabolism in adipose tissue of mice. *Horm. Metab. Res.* 2, 161-165
68. Wolff, G. L. (1991) Obesity, cancer and the viable yellow (A^{vy}/a) mouse: discrimination among pathophysiologic effects of the expression of the A^{vy}/a genotype in obese and lean mice. In *Progress in Obesity Research 1990*, Chap. 70, pp. 445-448
69. Roberts, D. W., Wolff, G. L., and Campbell, W. L. (1984) Differential effects of the mottled yellow and pseudoagouti phenotypes on immunocompetence in A^{vy}/a mice. *Proc. Natl. Acad. Sci. USA* 81, 2152-2156
70. Wolff, G. L., Roberts, D. W., Morrissey, R. L., Greenman, D. L., Allen, R. R., Campbell, W. L., Bergman, H., Nesnow, S., and Frith, C. H. (1987) Tumorigenic responses to lindane in mice: potentiation by a

dominant mutation. *Carcinogenesis* 8, 1889–1897
71. Wolff, G. L. (1993) Multiple levels of response in carcinogenicity bioassays: regulational variation among viable yellow (A^{vy}/-) mice. *J. Exp. Anim. Sci.* 35, 221–231
72. Wolff, G. L., Morrissey, R. L., and Chen, J. J. (1986) Amplified response to phenobarbital promotion of hepatotumorigenesis in obese yellow A^{vy}/A (C3H × VY) F-1 hybrid mice. *Carcinogenesis* 7, 1895–1898
73. Hsiao, W. L., Wendy, Barsh, G. S., Wolff, G. L., and Fan, H. (1991) High level of spontaneous transformation in newly established mouse cell lines carrying the viable yellow mutation (A^{vy}). *Proc. Am. Assn. Cancer Res.* 32, 160
74. Furst, A. S., and Becker, F. F. (1991) Suppression of in vitro chemical transformation by the carcinogenesis-promoting, viable yellow gene A^{vy} *Carcinogenesis* 12, 1157–1160

Antagonism of Central Melanocortin Receptors in Vitro and in Vivo by Agouti-Related Protein

Michael M. Ollmann,* Brent D. Wilson,* Ying-Kui Yang, Julie A. Kerns, Yanru Chen, Ira Gantz, Gregory S. Barsh†

Expression of Agouti protein is normally limited to the skin where it affects pigmentation, but ubiquitous expression causes obesity. An expressed sequence tag was identified that encodes Agouti-related protein, whose RNA is normally expressed in the hypothalamus and whose levels were increased eightfold in *ob/ob* mice. Recombinant Agouti-related protein was a potent, selective antagonist of Mc3r and Mc4r, melanocortin receptor subtypes implicated in weight regulation. Ubiquitous expression of human *AGRP* complementary DNA in transgenic mice caused obesity without altering pigmentation. Thus, Agouti-related protein is a neuropeptide implicated in the normal control of body weight downstream of leptin signaling.

Analysis of mouse obesity mutations has helped define regulatory circuits that govern energy expenditure (*1*). In mice carrying certain alleles of the *Agouti* coat color gene such as *lethal yellow* (A^y) or *viable yellow* (A^{vy}), pleiotropic effects including a yellow coat, obesity, and increased body length are caused by ubiquitous expression of chimeric transcripts encoding a normal Agouti protein (*2–4*). Agouti is a paracrine signaling molecule (*5*) that affects pigmentation by antagonism of the melanocortin 1 receptor (Mc1r) (*6, 7*), one of five related heterotrimeric GTP-binding protein–coupled receptors named for their ability to respond to α-melanocyte stimulating hormone (α-MSH) and adrenocorticotrophic hormone (ACTH) (*8*). Expression and action of Agouti is normally limited to the skin (*3, 5*), but recombinant Agouti protein will also antagonize Mc2r and Mc4r (*6, 9*), expressed primarily in the adrenal gland and the central nervous system (CNS), respectively (*8, 10*).

Using a characteristic pattern of cysteine spacing from the COOH-terminal region of Agouti to search an expressed sequence tag database, we isolated a gene from 129/sv mice and from humans that encodes a protein nearly identical in size and genomic structure to *Agouti* that we named *Agouti-related protein* (*Agrp*) (Fig. 1A). The same gene was recently described by Shutter *et al.* as *Agouti-related transcript* (*11*). Reverse transcriptase–polymerase chain reaction (RT-PCR) and Northern (RNA) hybridization experiments demonstrated that *Agrp* RNA was expressed primarily in the adrenal gland and the hypothalamus (Fig. 1, B and C). To investigate functional overlap between *Agrp* and *Agouti*, we examined whether the steady-state level of *Agrp* RNA would be altered by ectopic expression of Agouti in A^y/a animals. Northern hybridization analysis of hypothalamic and adrenal gland RNA from A^y/a or coisogenic *a/a* animals revealed an ≈fivefold reduction of *Agrp* RNA in the hypothalamus of A^y/a animals (Fig. 1C). We also measured the levels of hypothalamic *Agrp* RNA in *ob/ob* animals and found an ≈eightfold increase relative to coisogenic controls. In the adrenal gland, levels of *Agrp* RNA in A^y/a and nonmutant animals were below the level of detection, but could easily be detected in *ob/ob* animals.

To determine whether AGRP antagonizes melanocortin signaling, we used the baculovirus expression system to produce conditioned media containing recombinant human AGRP, and measured antagonist activity using a *Xenopus* melanophore cell line developed by Lerner and colleagues (*12*). Melanophores provide a rapid and sensitive bioassay for melanocortin agonists and antagonists because pigment granule dispersion induced by α-

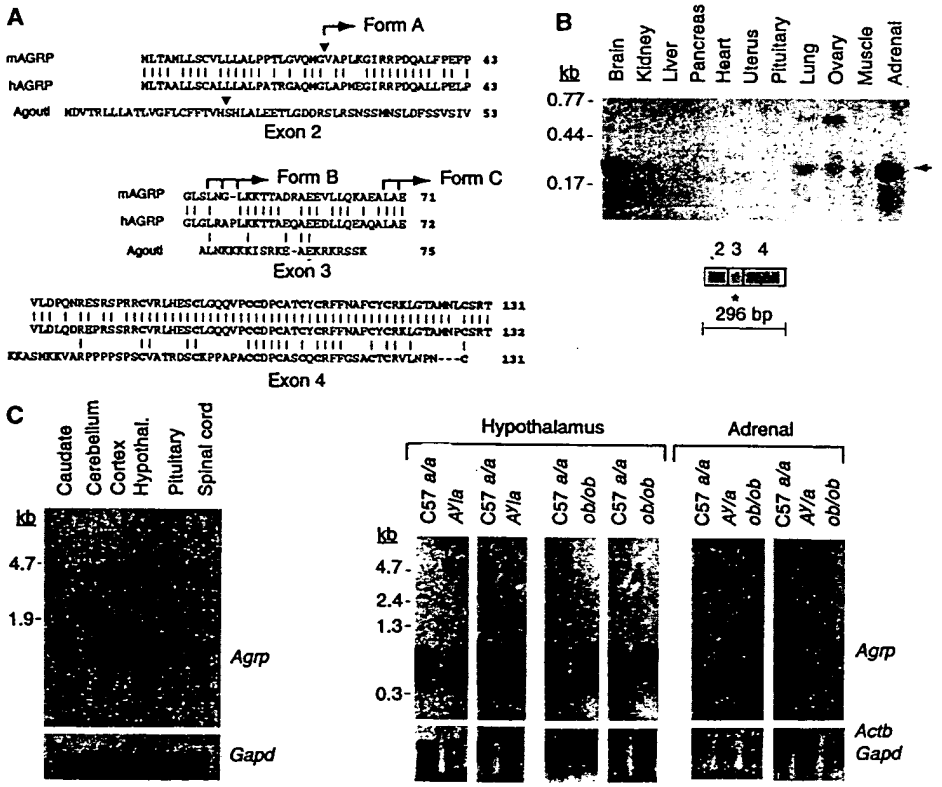

Fig. 1. Structure and expression of *Agrp*. (**A**) Comparison of mouse and human AGRP sequences with that of mouse Agouti. Arrowheads indicate signal sequence cleavage sites; arrows indicate different forms of recombinant AGRP. Abbreviations for the amino acid residues are as follows: A, Ala; C, Cys; D, Asp; E, Glu; F, Phe; G, Gly; H, His; I, Ile; K, Lys; L, Leu; M, Met; N, Asn; P, Pro; Q, Gln; R, Arg; S, Ser; T, Thr; V, Val; W, Trp; and Y, Tyr. Cysteine residues are in bold. (**B**) RT-PCR assay for mouse *Agrp* RNA (*23*). (**C**) Northern hybridization assay for mouse *Agrp* RNA in brain tissues (9 μg, left) or in hypothalamus and adrenal glands of A^y/a and *ob/ob* mice (5 μg, right); each lane represents RNA from a single animal. Relative ratios of *Agrp* RNA determined with a PhosphorImager were based on signal from an exon 4 cDNA probe compared with *Actb* and *Gapd* control probes hybridized to the same blot.

M. M. Ollmann, B. D. Wilson, J. A. Kerns, Y. Chen, G. S. Barsh, Departments of Pediatrics and Genetics and the Howard Hughes Medical Institute, Stanford University School of Medicine, Stanford, CA 94305, USA.
Y.-K. Yang and I. Gantz, Department of Surgery, University of Michigan School of Medicine, Ann Arbor, MI 48109–0682, USA.

*These authors contributed equally to this work.
†To whom correspondence should be addressed at Beckman Center B271A, Stanford University School of Medicine, Stanford, CA 94305–5323, USA. E-mail: gbarsh@cmgm.stanford.edu.

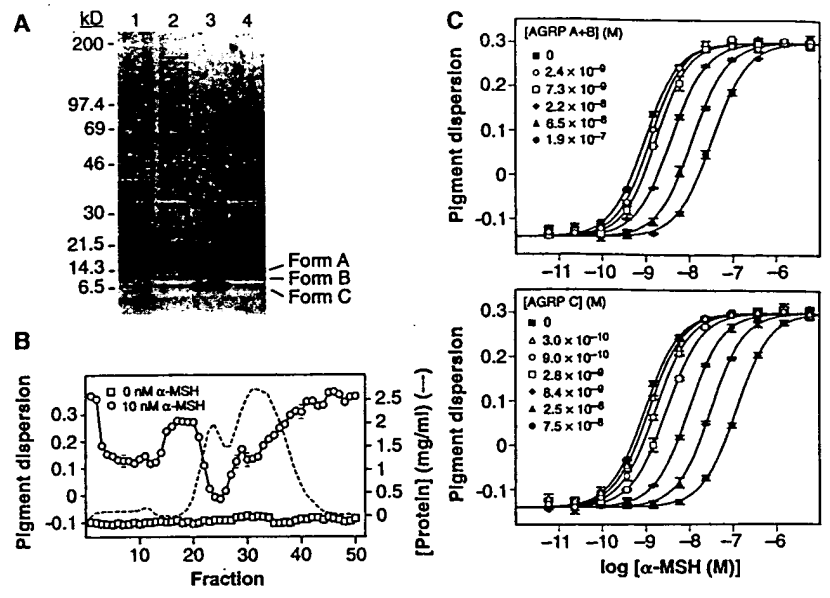

Fig. 2. AGRP activity in *Xenopus* melanophores. (**A**) One microgram of protein from serial steps in the purification procedure analyzed by silver-stained 4 to 20% SDS–polyacrylamide gel electrophoresis. Two liters of conditioned media (lane 1) was applied to a Blue Sepharose Fast Flow Column, then eluted with 40 mM CAPS (pH 10.8), 2.5 M NaCl. Fractions with α-MSH antagonist activity (lane 2) were concentrated (Centriprep 3), buffer-exchanged into 40 mM CAPS (pH 10.8), 20 mM NaCl, applied to a HiTrap Q anion-exchange column, then eluted with a 20 to 800 mM NaCl gradient in 40 mM CAPS (pH 10.8). (**B**) Major peaks of α-MSH antagonist activity in the flow-through (fractions 2 to 13, lane 3) and in fractions 20 to 26 (lane 4) were dialyzed into storage buffer [20 mM Pipes (pH 6.8), 50 mM NaCl]. NH_2-terminal sequencing of the two predominant bands in each peak revealed mature AGRP and two heterogeneous smaller forms as indicated. AGRP purity, estimated by densitometry of a 10-μg sample loaded on a 10% Tricine gel stained with ProBlue, was used to calculate effective concentrations of 40 and 11 μM for form A+B (lane 4) and form C (lane 3), respectively. (**C**) Quantitative α-MSH dose-response analysis of different Agrp forms measured at equilibrium conditions 180 min after addition of AGRP and α-MSH. In the 96-well melanophore assay (*12*), pigment dispersion is calculated as $(A_{650}$ final $- A_{650}$ initial$)/A_{650}$ final, where A_{650} is the absorbance at 650 nm. Data points represent mean ± SEM of triplicate samples.

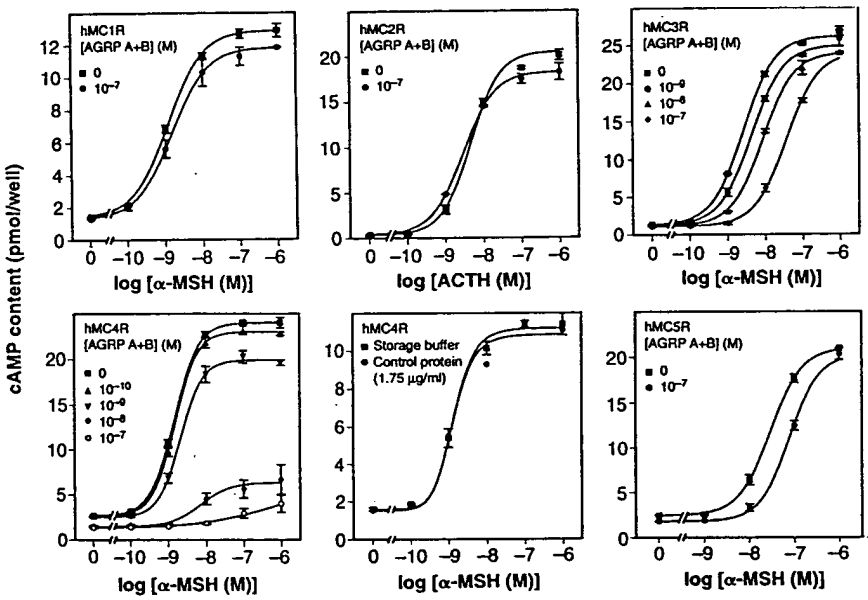

Fig. 3. Effects of AGRP on human melanocortin receptors. 293 cells (hMC1R, hMC3R, hMC4R, or hMC5R) or OS3 cells (hMC2R) stably transfected with the indicated receptor were preincubated with the indicated amounts of AGRP for 30 min; various amounts of α-MSH or ACTH were added for 30 min in the presence of 0.2 mM isobutylmethylxanthine, and total cAMP accumulation was determined on duplicate wells (*9*). Data points represent the mean ± SEM of 2 to 3 independent experiments. As a control for proteins other than AGRP, conditioned media from insect cells infected with an unrelated baculovirus were loaded and eluted from a Blue Sepharose column with conditions identical to those used for AGRP, dialyzed into storage buffer (490 μg/ml), then used at a dilution identical to that used to prepare 100 nM AGRP form A+B. Nanomolar concentrations of AGRP form A+B antagonize the hMC3R and hMC4R but do not meet criteria for competitive antagonism (*15*); therefore, K_B values cannot be calculated.

MSH can be measured in microtiter plates as a change in optical density (*12*). Using the ability of conditioned media to inhibit α-MSH–induced pigment dispersion, we partially purified multiple forms of AGRP that cofractionate with α-MSH antagonist activity by Blue Sepharose and anion-exchange chromatography (Fig. 2). One peak of α-MSH antagonist activity contained mature AGRP with the signal sequence removed (form A) and a mixture of three AGRP fragments cleaved after residues 46, 48, or 50 (form B). The second major peak contained AGRP fragments cleaved after residues 69 or 71 (form C).

Partially purified AGRP forms A+B and form C are potent, specific antagonists of α-MSH–induced pigment dispersion in *Xenopus* melanophores, with calculated antagonist dissociation constant (K_B) values of 7.0 and 1.2 nM, respectively (Fig. 2C). AGRP did not inhibit pigment granule dispersion in the absence of α-MSH and did not inhibit pigment granule dispersion induced by forskolin, a direct activator of adenylate cyclase (*13*).

To examine the selectivity of AGRP for human melanocortin receptors, we added various concentrations of AGRP form A+B to cell lines that had been stably transfected with each of the five different receptor subtypes, then measured the ability of α-MSH or ACTH to induce adenosine 3′,5′-monophosphate (cAMP) accumulation. At concentrations up to 100 nM, AGRP had no effect on hMC1R or hMC2R, and only slightly inhibited hMC5R (Fig. 3). By contrast, AGRP concentrations of 1 nM or more caused a dose-dependent inhibition of α-MSH–induced cAMP accumulation mediated by hMC3R and hMC4R.

Because AGRP form C can antagonize α-MSH in melanophores (Fig. 2) or in Mc4r-transfected cells (*13*), the COOH-terminal cysteine-rich region is probably sufficient for biologic activity, as is the case for Agouti (*14*). Sequence comparison of AGRP and Agouti highlights a short region of similarity beginning with the third Cys residue, CCDPCAXCXCRFF, that may contain determinants required for melanocortin antagonism (Fig. 1A). Nonetheless, the exact biochemical mechanism by which these proteins act is not clear. Most evidence favors competitive antagonism,

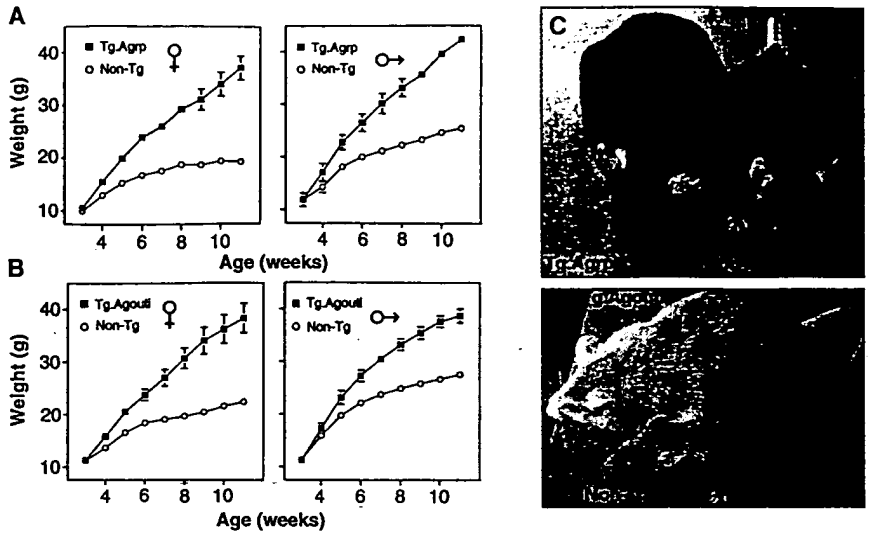

Fig. 4. Effects of AGRP or human Agouti in transgenic mice. A β-actin human *AGRP* cDNA construct nearly identical to one described previously for human Agouti (*24*) was injected into F_2 (C57BL/6J × CBA/J) embryos. One of six F_0 founders (*17*) was bred to C57BL/6J animals. At 11 weeks of age, F_1 transgenic animals (females: $n = 4$; males: $n = 3$) weighed significantly more than nontransgenic littermates (females: $n = 6$, $P = 0.00005$; males: $n = 6$; $P = 0.00002$). The time of onset and level of weight gain caused by the AGRP transgene (**A**) were similar to those caused by the Agouti transgene (**B**), but the AGRP transgene had no effect on pigmentation (**C**). Data points represent the mean ± SEM.

whereby α-MSH and Agouti (or AGRP) bind to mutually exclusive sites on melanocortin receptors (*14*). The effects of AGRP on melanophores are consistent with competitive antagonism, because increasing amounts produced a proportionate and parallel displacement of the α-MSH dose-response curve without affecting maximal signaling (Fig. 2C). For the hMC4R, however, AGRP concentrations of 10 and 100 nM produced a decrease in basal levels of cAMP accumulation, as well as a decrease in the maximal level of α-MSH–induced cAMP accumulation (Fig. 3), neither of which is consistent with competitive antagonism (*15*). It has been proposed that some effects of Agouti are mediated by alterations in calcium flux (*16*), an intriguing finding given the similarity in cysteine spacing between Agouti, AGRP, and certain calcium channel antagonists (*4*). It is possible that Agouti or AGRP does not bind directly to melanocortin receptors or binds to more than one cell surface protein, uncertainties that may be resolved by studies of Agouti and AGRP binding.

To determine whether or not Agouti and AGRP have comparable effects in vivo, we constructed transgenic mice in which the human *AGRP* cDNA was controlled by the ubiquitously expressed β-actin promoter. Weight gain of six independent transgenic founders was significantly increased over nontransgenic littermates (*17*), and a transgenic line was established. Among F_1 animals carrying the β-actin AGRP transgene, increased weight gain was detectable at 4 weeks of age, reached levels 100 or 70% above that of nontransgenic females or males, respectively, and was nearly indistinguishable from that caused by a β-actin Agouti transgene (Fig. 4). Body length and food consumption were also increased by the AGRP transgene (*17*). By contrast, none of 15 animals carrying the AGRP transgene exhibited a difference in coat color from their nontransgenic littermates (Fig. 4). Thus, although AGRP mimics the effect of Agouti on weight gain, body length, and food consumption, it has no effect on pigmentation.

Given the eightfold increase of hypothalamic expression in *ob/ob* mice, we propose that *Agrp* normally regulates body weight via central melanocortin receptors, analogous to the relation between Agouti and the Mc1r for regulation of pigmentation. Huszar *et al.* (*18*) have shown that Mc4r-deficient animals develop obesity and metabolic derangements that mimic those in $A^y/-$ mice, which suggests that obesity caused by ubiquitously expressed *Agrp* or *Agouti* is mediated largely by Mc4r. However, AGRP may also be a physiologic ligand of Mc3r (Fig. 3), which has been implicated in Agouti-induced obesity (*19*) and whose CNS expression (*20*) more closely matches that of *Agrp*. In the brain, *Agrp* RNA is localized primarily to the arcuate nucleus and median eminence (*11*), but unlike Agouti, which has a very small sphere of action in vivo (*3*), AGRP may diffuse more widely, particularly if it is processed to a smaller COOH-terminal form in vivo. AGRP is also produced by the adrenal gland but does not affect hMC2R and therefore may act at a more distant site.

What advantages do endogenous receptor antagonists such as Agouti or AGRP offer for homeostatic regulation? In the case of melanocortins, which activate five receptors to varying extents, an antagonist limited in its tissue distribution or biochemical specificity, or both, allows individual regulation of receptor subtype signaling. Melanocortin receptors were identified on the basis of their response to the agonist α-MSH (*6*), but physiologic signaling via Mc1r is regulated mainly by alterations in levels of the antagonist, Agouti. Similarly, regulation of Mc3r or Mc4r signaling could be mediated primarily by changes in Agrp expression rather than proopiomelanocortin, the precursor of α-MSH and ACTH. Agouti or AGRP, or both, may also transduce a signal via melanocortin receptors independent of melanocortin binding (*21*), consistent with the effects we observed on basal levels of cAMP accumulation.

Leptin deficiency lies upstream of *Agrp* expression, directly or indirectly, but other signaling systems implicated in energy balance (*22*) may also regulate *Agrp* expression. Additional studies based on gene targeting may help to place *Agrp* in a genetic pathway for feeding behavior, which should be useful in understanding and developing treatments for disorders of body weight regulation.

REFERENCES AND NOTES

1. Y. Zhang *et al.*, *Nature* **372**, 425 (1994); L. A. Tartaglia *et al.*, *Cell* **83**, 1263 (1995); K. Noben-Trauth, J. K. Naggert, M. A. North, P. M. Nishina, *Nature* **380**, 534 (1996); J. K. Naggert *et al.*, *Nature Genet.* **10**, 135 (1995).
2. D. M. J. Duhl, H. Vrieling, K. A. Miller, G. L. Wolff, G. S. Barsh, *Nature Genet.* **8**, 59 (1994); E. J. Michaud *et al.*, *Genes Dev.* **8**, 1463 (1994).
3. W. K. Silvers, in *The Coat Colors of Mice* (Springer-Verlag, New York, 1979), pp. 6–44.
4. J. Manne, A. C. Argeson, L. D. Siracusa, *Proc. Natl. Acad. Sci. U.S.A.* **92**, 4721 (1995).
5. S. J. Bultman, E. J. Michaud, R. P. Woychik, *Cell* **71**, 1195 (1992); M. W. Miller *et al.*, *Genes Dev.* **7**, 454 (1993).
6. D. S. Lu *et al.*, *Nature* **371**, 799 (1994).
7. L. S. Robbins *et al.*, *Cell* **72**, 827 (1993).
8. K. G. Mountjoy, L. S. Robbins, M. T. Mortrud, R. D. Cone, *Science* **257**, 1248 (1992).
9. Y. K. Yang *et al.*, *Mol. Endocrinol.* **11**, 274 (1997).
10. I. Gantz *et al.*, *J. Biol. Chem.* **268**, 15174 (1993); K. G. Mountjoy, M. T. Mortrud, M. J. Low, R. B. Simerly, R. D. Cone, *Mol. Endocrinol.* **8**, 1298 (1994).
11. J. R. Shutter *et al.*, *Genes Dev.* **11**, 593 (1997).
12. J. M. Quillan, C. K. Jayawickreme, M. R. Lerner, *Proc. Natl. Acad. Sci. U.S.A.* **92**, 2894 (1995); N. Potenza and M. R. Lerner, *Pigment Cell Res.* **5**, 372 (1992).
13. M. M. Ollmann, Y.-K. Yang, B. D. Wilson, I. Gantz, G. S. Barsh, unpublished observations.
14. D. H. Willard *et al.*, *Biochemistry* **34**, 12341 (1995); S. G. Blanchard *et al.*, *ibid.*, p. 10406.
15. T. P. Kenakin, *Can. J. Physiol. Pharmacol.* **60**, 249 (1982).
16. M. B. Zemel *et al.*, *Proc. Natl. Acad. Sci. U.S.A.* **92**, 4733 (1995); J. H. Kim *et al.*, *FASEB J.* **10**, 1646 (1996).

17. Individually caged mice had free access to standard Chow and were treated in accordance with Stanford guidelines. At 11 weeks of age, female F_0 animals weighed 30.5, 35.5, and 41.9 g, and male F_0 animals weighed 32.4, 34.8, and 43 g—significantly more than nontransgenic littermates (females: 21.1 ± 2.0 g, n = 10, P = 0.02; males: 26 ± 2.0 g, n = 5, P = 0.03, student's t test). At 15 weeks of age, body length of F_1 transgenic animals (10.5 ± 0.1 cm, n = 4) was more than that of nontransgenic littermates (9.18 ± 0.2 cm, n = 10, P = 0.0002). Food consumption measured over a 7-day period at 12 weeks of age for F_1 transgenic animals (27.9 ± 5.4 g, n = 4) was more than that of nontransgenic littermates (21.9 ± 2.8 g, n = 5, P = 0.03).
18. D. Huszar *et al.*, *Cell* **88**, 131 (1997).
19. W. Fan, B. A. Boston, R. A. Kesterson, V. J. Hruby, R. D. Cone, *Nature* **385**, 165 (1997); L. L. Kiefer *et al.*, *Biochemistry* **36**, 2084 (1997).
20. L. Roselli-Rehfuss *et al.*, *Proc. Natl. Acad. Sci. U.S.A.* **90**, 8856 (1993); I. Gantz *et al.*, *J. Biol. Chem.* **268**, 8246 (1993).
21. W. Siegrist *et al.*, *J. Recept. Signal Transd. Res.* **17**, 75 (1997); G. Hunt and A. J. Thody, *J. Endocrinol.* **147**, R1 (1995); C. Sakai *et al.*, *EMBO J.* **16**, 3544 (1997).
22. J. C. Erickson, G. Hollopeter, R. D. Palmiter, *Science* **274**, 1704 (1996); D. Qu *et al.*, *Nature* **380**, 243 (1996); M. Spina *et al.*, *Science* **273**, 1561 (1996).
23. RNA (1 μg) was amplified by RT-PCR with the oligonucleotides 5′-ATGCTGACTGCAATGTTGCTG-3′ and 5′-GGTAC[illegible]CAAGCAG-3′; identity of the 296–base pair product was confirmed by hybridization with a [illegible] oligonucleotide, 5′-CTGCAGAAGGCAG[illegible]-3′.
24. B. D. Wilson *et al.*, *Nature Genet.* **4**, 223 (1995).
25. We thank M. Lerner, [illegible], and F. Chehab for advice and reagents. Supported by NIH grants EY07106 and [illegible] to M.M.C., J.A.K., and B.D.W. This work was supported in part by a Veterans Administration [illegible] and by grants from the NIH to the University of Michigan (P30DK-34933) and to G.S.B. (D[illegible]); and as an Associate Investigator of the Howard Hughes Medical Institute.

16 May 1997; accepted [illegible] August 1997

NF-AT Activation Induced by a CAML-Interacting Member of the Tumor Necrosis Factor Receptor Superfamily

Götz-Ulrich von Bülow and Richard J. Bram*

Activation of the nuclear factor of activated T cells transcription factor (NF-AT) is a key event underlying lymphocyte action. The CAML (calcium-modulator and cyclophilin ligand) protein is a coinducer of NF-AT activation when overexpressed in Jurkat T cells. A member of the tumor necrosis factor receptor superfamily was isolated by virtue of its affinity for CAML. Cross-linking of this lymphocyte-specific protein, designated TACI (transmembrane activator and CAML-interactor), on the surface of transfected Jurkat cells with TACI-specific antibodies led to activation of the transcription factors NF-AT, AP-1, and NFκB. TACI-induced activation of NF-AT was specifically blocked by a dominant-negative CAML mutant, thus implicating CAML as a signaling intermediate.

We identified proteins that can interact with CAML in a two-hybrid screen (*1*, *2*). To determine if any of these CAML-binding proteins affected signaling in T cells, we examined their ability to modulate activity of the Ca^{2+}-dependent transcription factor NF-AT (*3*). Overexpression of the two-hybrid clones in Jurkat T cells revealed that expression of one clone (encoding the TACI protein) led to activation of NF-AT, suggesting that TACI may lie in the same signaling pathway as CAML. The deduced amino acid sequence of TACI (Fig. 1A) (*4*) includes a single hydrophobic region (residues 166 to 186) that has features of a membrane-spanning segment. Analysis of the protein sequence (*5*) predicted extracellular exposure for the NH_2-terminus with a cytoplasmic COOH-terminus. Although TACI lacks an NH_2-terminal signal sequence, the presence of an upstream stop codon indicates that the complete open reading frame is contained within the clone (*6*). The predicted cell-surface location of TACI was confirmed in intact Cos-7 cells transfected with an expression plasmid encoding TACI with an NH_2-terminal FLAG epitope tag. Staining with monoclonal antibody to FLAG revealed TACI localized to the cell surface (Fig. 2A). TACI is therefore a type III transmembrane protein with an extracellular NH_2-terminus in the absence of a cleaved signal sequence (*7*). Inspection of the TACI protein sequence also revealed two repeated regions (residues 33 to 66 and 70 to 104) that are 50% identical. A PROSITE motif search (*8*) identified this repeated region as a cysteine-rich motif characteristic of the tumor necrosis factor receptor (TNFR) superfamily. Comparison of TACI with other members of TNFR superfamily (Fig. 1B) demonstrates the similarity between these domains, with the best match to cysteine-rich domains of DR3 (also known as Wsl-1, Apo-3, or TRAMP) (*9*).

Northern blot analysis of TACI mRNA demonstrated a 1.4-kb transcript expressed in spleen, small intestine, thymus, and peripheral blood lymphocytes, suggesting that a single TACI transcript is present in both T and B lymphocytes (Fig. 2B). Specific antibody staining of peripheral blood cells with a polyclonal antibody to TACI (*10*) revealed the presence of TACI on the surface of B cells, but not resting T cells (Fig. 2C). Because expression of other TNFR members such as [illegible] is increased after activation of T lymphocytes (*11*) and because TACI appears to be expressed in thymocytes, we examined T cells activated with ionomycin and phorbol ester. Such treatment of T cells induced the synthesis of cell-surface TACI in 54% of CD2-positive cells within 48 hours (Fig. 2D). This subset was equally distributed between CD4 and CD8 cells. Stimulation of interleukin-2 (IL-2)–dependent T cells with antibodies to CD3 and CD2 also induced expression of TACI. A reverse transcriptase–polymerase chain reaction assay revealed TACI message in resting B cells but not in T cells, unless they were activated (*6*).

Neither TACI mRNA nor protein could be detected in untransfected Jurkat cells expressing the SV40 large T-antigen (TAg), either unstimulated or treated with phorbol myristyl acetate (PMA) and ionomycin (*6*). To assess the effect of TACI on NF-AT activity in T cells, we transiently expressed the protein in TAg Jurkat cells along with a secreted alkaline phosphatase reporter driven by the NF-AT–binding sequences from the IL-2 promoter (*12*, *13*, *14*). TACI overexpression could partially replace the requirement for PMA and ionomycin in this assay for maximal activation of the NF-AT reporter. The addition of antibodies to TACI to the cells increased NF-AT activation up to sevenfold (Fig. 3A), demonstrating that TACI responds to cross-linking at the cell surface. This affinity-purified antibody to TACI had no effect on control transfected cells. To further verify the specificity of the response, we transfected cells with an NH$_2$-terminal FLAG-epitope–tagged TACI expression plasmid and incubated them with the M2-FLAG monoclonal antibody (*15*). This treatment gave a similar increase in NF-AT activity (Fig. 3A). The degree of NF-AT activation varied among different experiments because of transfection efficiency, but was typically 40 to 100% of the maximal re-

G.-U. von Bülow, Department of Experimental Oncology, St. Jude Children's Research Hospital, 332 North Lauderdale, Memphis, TN 38105, USA.
R. J. Bram, Departments of Experimental Oncology and Hematology/Oncology, St. Jude Children's Research Hospital, 332 North Lauderdale, and Department of Pediatrics, University of Tennessee, Memphis, TN 38105, USA.
*To whom correspondence should be addressed. E-mail: richard.bram@stjude.org

space and periaxonal collar[5,14-16]. In contrast, P_0 ear later, are present in compacted myelin and are myelin compaction[15,17-20]. The *Krox-20* mutation ppears to block Schwann cell differentiation after ctivation and engulfing of the axon but before spiral-on and activation of P_0 and MBP. This phenotype is very milar to the defect observed when differentiating Schwann cells are exposed to antibodies directed against galactocerebroside[21] (GalC), the major glycolipid of the myelin sheath. It differs, however, from the lesions associated with mutations affecting genes encoding major myelin proteins[19,20,22]. Our data therefore suggest that *Krox-20* is involved directly or indirectly, in the activation of late myelin genes, although it is not clear whether the absence of late myelin proteins constitutes the cause or the consequence of the differentiation block. Finally, this block is likely to be responsible for the augmentation in the number of Schwann cells by increased proliferation and/or survival. □

Received 20 June; accepted 9 September 1994.

1. Lemke, G. *Glia* **7**, 263–271 (1993).
2. Chavrier, P. *et al. EMBO J.* **7**, 29–35 (1988).
3. Chavrier, P. *et al. EMBO J.* **9**, 1209–1218 (1990).
4. Schneider-Maunoury, S. *et al. Cell* **75**, 1199–1214 (1993).
5. Trapp, B. D. & Quarles, R. H. *J. Cell biol.* **92**, 877–882 (1982).
6. Greenfield, S., Brostoff, S., Eylar, E. H. & Morell, P. *J Neurochem.* **20**, 1207–1216 (1973).
7. Kies, M. W., Murphy, J. B. & Alvord, E. C. in *Chemical Pathology of the Nervous System* (ed. Folch-Pi, J.) 197 (Pergamon, London, 1961).
8. Wilkinson, D., Bhatt, S., Chavrier, P., Bravo, R. & Charnay, P. *Nature* **337**, 461–464 (1989).
9. Jessen, K. R. *et al. Neuron* **12**, 509–527 (1994).
10. Gabe, M. *Techniques histologiques* (ed. Masson) 468 (Masson, Paris, 1968).
11. Uyemura, K., Tobari, C. & Hirano, S. *Biochim. biophys. Acta* **214**, 190–197 (1970).
12. Brockes, J. P., Fields, K. L. & Raff, M. C. *Brain Res.* **165**, 105–118 (1979).
13. Bunge, M. B., Bunge, R. P., Kleitman, N. & Dean, A. C. *Devl Neurosci.* **11**, 348–360 (1989).
14. Trapp, B. D., Quarles, R. H. & Suzuki, K. *J. Cell biol.* **99**, 594–605 (1984).
15. Trapp, B. D. *J. Cell Biol.* **107**, 675–685 (1988).
16. Li, C. *et al. Nature* **369**, 747–750 (1994).
17. Giese, K. P., Martini, R., Lemke, G., Soriano, P. & Schachner, M. *Cell* **71**, 565–576 (1992).
18. Filbin, M. T., Walsh, F. S., Trapp, B. D., Pizzey, J. A. & Tennekoon, G. I. *Nature* **344**, 871–872 (1990).
19. Kirschner, D. A. & Ganser, A. L. *Nature* **283**, 207–210 (1980).
20. Kimura, M. *et al. Proc. natn. Acad. Sci. U.S.A.* **86**, 5661–5665 (1989).
21. Owens, G. C. & Bunge, R. P. *Glia* **3**, 118–124 (1990).
22. Henry, E. W. & Sidman, R. L. *Science* **241**, 344–346 (1988).
23. Levi, G., Crossin, K. & Edelman, G. M. *J. Cell Biol.* **105**, 2359–2372 (1987).
24. Chomczynski, P. & Sacchi, N. *Analyt. Biochem.* **162**, 156–159 (1987).

ACKNOWLEDGEMENTS. P.T. and S.S.-M. contributed equally to this work. We thank B. Trapp for the gift of anti-P_0, anti-MAG and anti-P_2 antibodies, P. Brophy and F. Lachapelle for the gifts of anti-MAG and anti-MBP antibodies, respectively, M. Wassef and C. Sotelo for critical comments on the manuscript, D. Pham-Dinh, P. Cameron-Curry, N. Baumann and B. Zalc for helpful discussions. This work was supported by grants from INSERM, MRT, EEC, ARC, LNFCC, AFM and AISM. The financial support of Telethon (Italy) to the project 'Molecular modulation of cell adhesion and cytoskeletal molecules during neuromuscular development and regeneration' is gratefully acknowledged.

Agouti protein is an antagonist of the melanocyte-stimulating-hormone receptor

Dongsi Lu*, Derril Willard†, Indravadan R. Patel†, Sue Kadwell†, Laurie Overton†, Tom Kost†, Michael Luther†, Wenbiao Chen*, Richard P. Woychik‡, William O. Wilkison†§ & Roger D. Cone*

* Vollum Institute for Advanced Biomedical Research, Oregon Health Sciences University, Portland, Oregon 97201, USA
† Division of Molecular Sciences, Glaxo Research Institute, Research Triangle Park, North Carolina 27709, USA
‡ Biology Division, Oak Ridge National Laboratory, Oak Ridge, Tennessee 37831-8077, USA

THE genetic loci *agouti* and *extension* control the relative amounts of eumelanin (brown–black) and phaeomelanin (yellow–red) pigments in mammals[1]: *extension* encodes the receptor for melanocyte-stimulating hormone (MSH)[2] and *agouti* encodes a novel 131-amino-acid protein containing a signal sequence[3,4]. Agouti, which is produced in the hair follicle[5], acts on follicular melanocytes[6] to inhibit α-MSH-induced eumelanin production, resulting in the subterminal band of phaeomelanin often visible in mammalian fur. Here we use partially purified agouti protein to demonstrate that agouti is a high-affinity antagonist of the MSH receptor and blocks α-MSH stimulation of adenylyl cyclase, the effector through which α-MSH induces eumelanin synthesis. Agouti was also found to be an antagonist of the melanocortin-4 receptor[7,8], a related MSH-binding receptor. Consequently, the obesity caused by ectopic expression of agouti in the lethal yellow (A^y) mouse[9] may be due to the inhibition of melanocortin receptor(s) outside the hair follicle.

Two models have been proposed for the mechanism by which agouti protein inhibits stimulation of melanogenesis by α-MSH: (1) agouti is a negative regulator of the cyclic AMP signalling pathway acting through a unique agouti receptor[10], or (2) agouti is a competitive antagonist of α-MSH[11]. We produced recom-

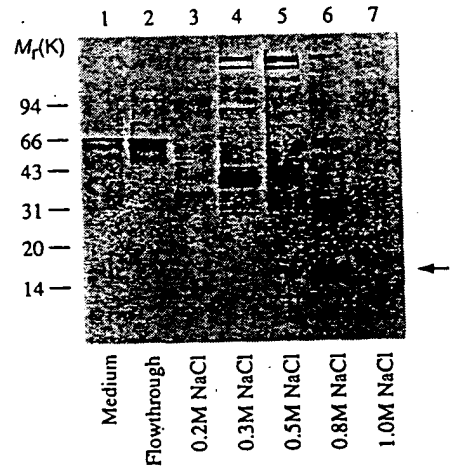

FIG. 1 Production and purification of recombinant agouti polypeptide. A 614-bp *Xbal/Pstl* fragment of the full-length mouse agouti cDNA was subcloned into a *Xbal/Pstl*-digested baculovirus expression vector pAcMP3 (PharMingen, San Diego). Virus was produced using standard methods[22]. 1 μg of each sample was electrophoresed on a 4–20% Tris-glycine gel (Novex, San Diego) and visualized by ProBlue (Integrated Separation Systems, MA) staining. The agouti protein eluted with the 0.8 M-NaCl wash. The 18.5K agouti species (arrow) was not observed in media infected with wild-type virus, and was demonstrated, after elution from the gel, to contain agouti by N-terminal sequencing. Lanes: 1, 48 h post-infection medium from pAcMP3-M.agouti-infected cells; 2, flow-through from Poros-20 HS column; 3–7, NaCl elutions from Poros-20 HS column. Arrow indicates authentic agouti protein.
METHODS. *T. ni* cells were infected at an MOI of 2 with pAcMP3-M.agouti virus or control virus and media were collected 48 h post-infection. This medium was directly loaded onto a Poros-20 HS cation-exchange column (PerSeptive Biosystems, MA) and bound protein eluted with NaCl concentrations from 0.2–1.0 M. The 0.8 M fraction was dialysed into 50 mM NaCl, 20 mM PIPES, pH 6.5, and then diluted for assay. Agouti concentrations were estimated from gel electrophoresis and amino-acid analysis of purified protein. Media controls consisted of unrelated baculovirus supernatants collected 48 h post-infection and purified by NaCl elution of a Poros-20 HS column as for agouti.

To whom correspondence should be addressed.

binant agouti protein using the baculovirus expression system in order to test these hypotheses. The band indicated by the arrow in Fig. 1 was absent from *Trichiplusia* cells not infected with the agouti/baculovirus vector, and its identity as the *agouti* gene product was verified by N-terminal sequencing (data not shown). Agouti pooled from the 0.8 M NaCl elution shown in this preparation was estimated to be 75% pure, resulting in an effective agouti concentration of ~0.14 mg ml^{-1}.

Agouti action was examined initially on the B16F10 murine melanoma cell line[12]. Agouti (0.7 nM) shifted the half-maximal effective concentration (EC_{50}) for stimulation of adenylyl cyclase by α-MSH in these cells from 1.7 ± 0.24 nM to 13.4 ± 3.3 nM (data not shown). To characterize agouti action further, we examined the effects of agouti on the MSH receptor (MSH-R) and other G-protein-coupled receptors stably transfected into the human embryonic kidney 293 cell[8,13,15]. α-MSH had no effect on the cAMP pathway in untransfected 293 cells, demonstrating the absence of endogenous melanocortin receptors in this cell line (Fig. 2*a*). Furthermore, addition of agouti (0.7 nM) had no effect on the basal adenylyl cyclase levels. Agouti also had no effect on the ability of thyroid-stimulating hormone (TSH) to bind to its receptor and stimulate adenylyl cyclase in TSH-R-transfected 293 cells (Fig. 2*b*). As the TSH-R couples to the same G protein as do the melanocortin receptors, G_S, this experiment shows that agouti acts upstream of G_S in the cAMP signalling pathway.

In contrast, the same concentration of agouti protein produced a significant shift in the adenylyl cyclase/functional coupling curve of the murine MSH-R expressed in 293 cells (Fig. 3*a*). Control supernatants from baculovirus-infected cells at the same total protein concentration had no effect. Agouti protein (0.7 nM) increased the EC_{50} for activation of adenylyl cyclase from $1.5 \pm 1.1 \times 10^{-9}$ to $2.2 \pm 1.2 \times 10^{-8}$ M, but did not alter the maximally induced activity of the receptor. The apparent K_i value calculated from four independent experiments was $3.2 \pm 2.6 \times 10^{-10}$ M. A dose-response curve demonstrated increasing inhibition of the murine MSH-R by agouti at concentrations from below 10^{-9} M up to 10^{-6} M (Fig. 3*b*). The human MSH receptor was also inhibited by agouti but only at much higher protein concentrations (Fig. 3*c*). It is conceivable that, unlike its murine counterpart, human agouti is antagonist of the human MSH-R. But as the wi[illegible] a high-pigmentation phenotype is not commonly observed [illegible]d-type possible that agouti no longer antagonizes MSH-R [illegible] in m the human hair follicle. [illegible]un

The ability of agouti to shift the MSH-R functional coup curve without affecting maximal receptor activation sugge that agouti was acting as a competitive antagonist. To investi this further, the ability of the protein to compete with ano melanocortin peptide for binding to the mouse MSH-R examined. Adrenocorticotropic hormone (ACTH), which c tains the α-MSH peptide in its first 13 amino acids, can radiolabelled at Tyr 23 without loss of potency and binds to same site on the melanocortin receptors as does α-MSH[7,1 Competition binding experiments were performed with [1] labelled $ACTH_{1-39}$ and the M-3 subclone of the Cloudman m ine melanoma cell line. This cell line was used because of the h density of MSH receptors expressed on the plasma membr (10,000–50,000), in contrast to the MSH-R-transfected 293 ce which were estimated to express under 1,000 MSH receptors cell (data not shown). ACTH bound the MSH-R with a of $6.3 \pm 13.3 \times 10^{-8}$ M, within the range of previously repor values[12] (Fig. 3*d*). Using a single-site model, agouti prot blocked 50% of specific ACTH binding to the MSH recep at a concentration of 1.2 ± 0.7 ng ml^{-1} ($K_i = IC_{50}$ (half-maxim inhibitory concentration) $= 6.6 \pm 3.8 \times 10^{-10}$ M) (Fig. 3*e*). Sin lar results were obtained when a synthetic radiolabelled α-MS analogue (Nle_4, D-Phe_7-α-MSH) was used as the radiolabell ligand (data not shown). As a control, baculovirus supernata from *T. ni* cells infected with a baculovirus construct containi an unrelated gene insert was purified as described for agou This protein had no activity in this assay (Fig. 3*e*) or on α-MS stimulation of adenylyl cyclase in MSH-R-transfected 293 ce (data not shown).

So far there are five members of the melanocortin recept family, MC1-R (MSH-R)[14,16], MC2-R (ACTH-R)[1] MC3-R[15,17], MC4-R[7,8] and MC5-R[18,19]. No functions have y been described for the latter three members of the family, b the MC3-R and MC4-R are expressed primarily in the centr nervous system in brain nuclei involved in neuroendocrine an

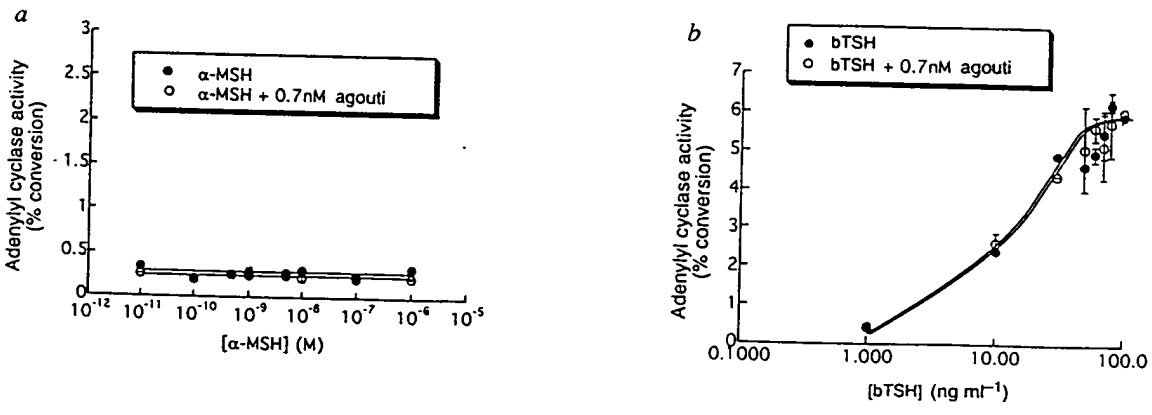

FIG. 2 Agouti does not affect basal or TSH-R-stimulated adenylyl cyclase activity. *a*, Adenylyl cyclase assay showing no effect of agouti on basal levels of this enzyme in untransfected 293 cells. α-MSH treatment also elicits no response, demonstrating the absence of endogenous melanocortin receptors in this cell line. *b*, Adenylyl cyclase assay showing no effect of agouti protein on the cAMP signalling pathway following activation by bovine thyroid-stimulating hormone (TSH) of adenylyl cyclase in 293 cells transfected with human TSH-receptor.

METHODS. Agouti protein was prepared as Fig. 1. Two independent preparations of agouti yielded similar results. 293 cells (5×10^5) and 293 cells expressing human TSH-R were preloaded with 5 μCi ^{3}H-adenine for 1.5 h at 37 °C in a 5% CO_2 incubator. Cells were stimulated with varying concentrations of α-MSH (*a*) or bovine TSH (*b*) in the presence or absence of 0.7 nM agouti for 40 min in cyclase assay incubation medium (Dulbecco's modified Eagle's medium containing 0.1 mg ml^{-1} bovine serum albumin and 0.1 mM isobutylmethylxanthine). Medium was aspirated and 2.5% perchloric acid containing 0.1 mM cAMP was used to stop the incubation. Adenylyl cyclase activity was calculated by determining the per cent conversion of ^{3}H-adenine to ^{3}H-cAMP as described[23,24]. Correlation of cAMP accumulation measured in this assay with actual adenylyl cyclase activity is made under the assumption that isobutymethylxanthine effectively blocks cAMP degradation. Data represent means and standard deviations from triplicate data points.

autonomic control. Surprisingly, agouti was also found to be a potent antagonist of α-MSH activation of the MC4-R (Fig. 4*a*). Once again, the protein appeared to act like a competitive antagonist, not significantly interfering with maximal activation of the receptor. The same concentration of agouti (0.7 nM) did not antagonize activation of the MC3 or MC5 receptors, and the MC5-R was unaffected even at 100 nM agouti concentrations (Fig. 4*b*, *c*).

Our results show that agouti is a high-affinity antagonist of the MSH-R, and of at least one of the other melanocortin receptors. Agouti appears to function as a competitive antagonist, inhibiting agonist binding to the MSH-R. This unique bifunctional regulation of the MSH-R by α-MSH and agouti allows for fine spatial and temporal regulation of eumelanin and phaeomelanin synthesis. These findings also provide a context for understanding the complex interactions of agouti and extension (MSH-R)

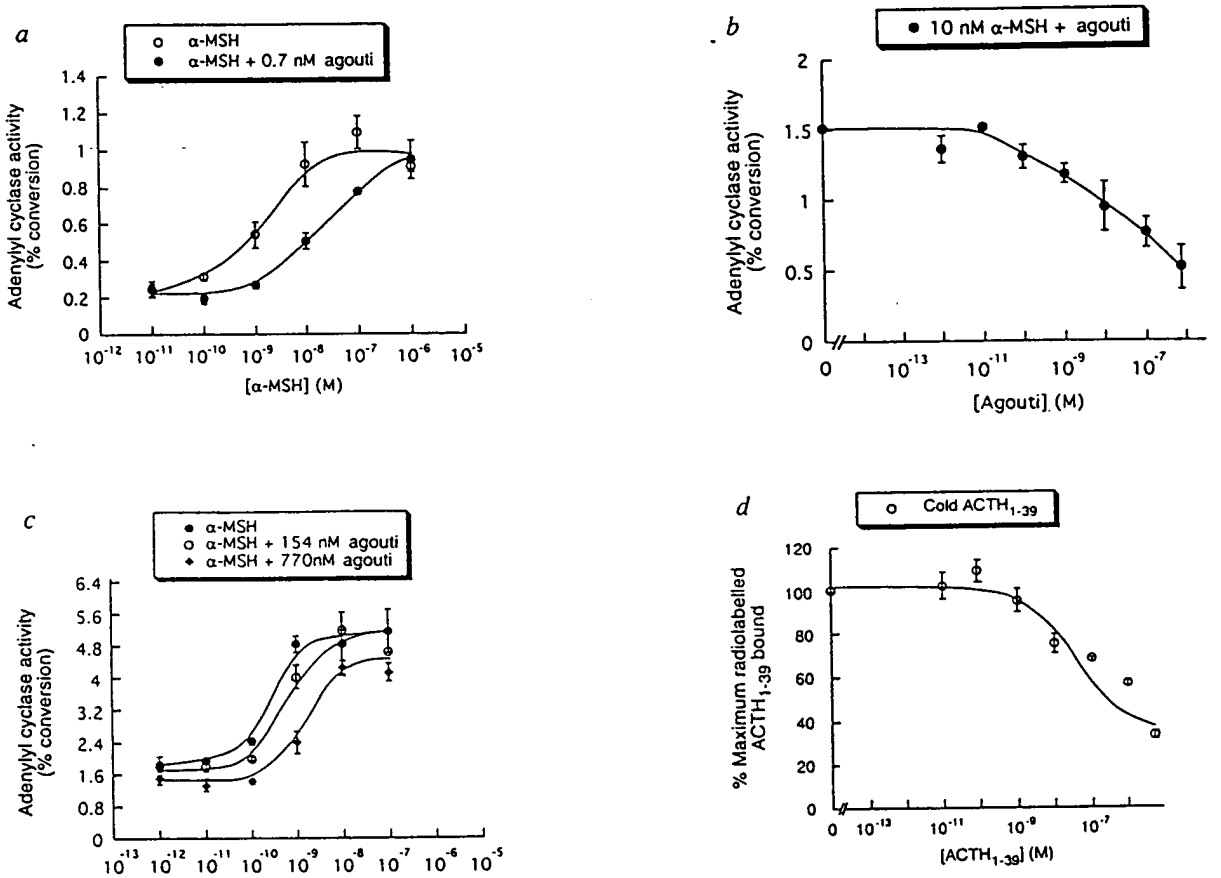

FIG. 3 Agouti is an antagonist of α-MSH at the murine MSH receptor. *a*, Agouti inhibits activation of the mMSH-R by α-MSH in stably transfected 293 cells, as monitored by stimulation of adenylyl cyclase. *b*, Agouti inhibition of murine MSH-R activation is dose-responsive. mMSH-R expressing 293 cells were stimulated with 10 nM α-MSH in the presence of agouti (10^{-12}–7×10^{-7} M). *c*, Agouti inhibits activation of human MSH-R at high protein concentrations. No inhibition of MSH-R activation by 0.7 nM agouti was observed. EC_{50} values were $2.3 \pm 0.8 \times 10^{-10}$ M (no agouti), $8.8 \pm 2.1 \times 10^{-10}$ M (154 nM agouti), and $1.1 \pm 1.5 \times 10^{-9}$ M (770 nM agouti). *d*, Competition binding demonstrates murine MSH-R expression in the Cloudman M-3 melanoma cell line. *e*, Competition binding demonstrates agouti protein blocks ^{125}I-labelled $ACTH_{1-39}$ binding to mouse MSH-R. Baculovirus supernatants from SF9 cells infected with a virus containing an unrelated gene insert were purified in parallel with agouti protein and did not block ^{125}I-labelled $ACTH_{1-39}$ binding to MSH-R up to 0.01 μg ml^{-1}. Values are shown as protein concentrations to compare agouti with control protein. METHODS. *a*–*c*, Adenylyl cyclase activity was measured as for Fig. 2. EC_{50} values were calculated using GraphPad InPlot version 4.0. *d*, *e*, Competition binding with radiolabelled ACTH has been described[25]: 1×10^6 cells were washed twice with binding medium and incubated in binding medium containing 9×10^{-11} M ^{125}I-labelled $ACTH_{1-39}$ (200,000 c.p.m.; Amersham) and different concentrations of agouti, control protein or cold ACTH for 2 h at 22 °C. Cells were then washed, lysed and counted as before[25] and data were analysed using the Kaleidagraph software package. Nonspecific binding, determined as the amount of radioactivity bound at 10^{-5} M cold ACTH, was 10% of the total counts bound.

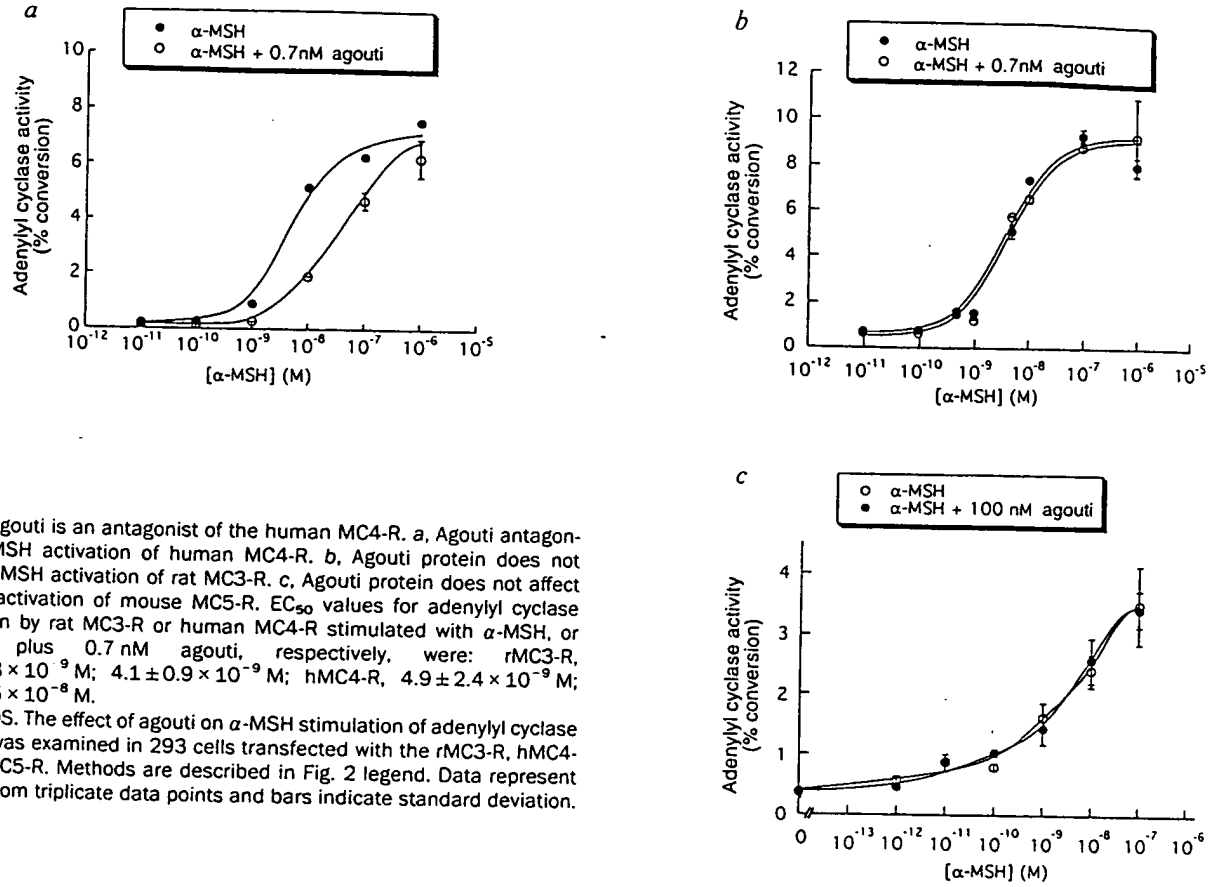

FIG. 4 Agouti is an antagonist of the human MC4-R. *a*, Agouti antagonizes α-MSH activation of human MC4-R. *b*, Agouti protein does not affect α-MSH activation of rat MC3-R. *c*, Agouti protein does not affect α-MSH activation of mouse MC5-R. EC_{50} values for adenylyl cyclase activation by rat MC3-R or human MC4-R stimulated with α-MSH, or α-MSH plus 0.7 nM agouti, respectively, were: rMC3-R, $4.2 \pm 0.8 \times 10^{-9}$ M; $4.1 \pm 0.9 \times 10^{-9}$ M; hMC4-R, $4.9 \pm 2.4 \times 10^{-9}$ M; $3.3 \pm 0.5 \times 10^{-8}$ M.
METHODS. The effect of agouti on α-MSH stimulation of adenylyl cyclase activity was examined in 293 cells transfected with the rMC3-R, hMC4-R or mMC5-R. Methods are described in Fig. 2 legend. Data represent means from triplicate data points and bars indicate standard deviation.

responsible for many mammalian coat colour variants, such as the variable black and tan markings in the German shepherd, resulting from combinations of two *extension* (E^m, E) and three *agouti* (A^a, a^y, a^t) alleles[20].

Because agouti also antagonizes MC4-R function, ectopic overexpression of agouti may lead to obesity in the lethal yellow mouse (A^y) through pathological antagonism of melanocortin receptor(s) expressed outside the hair follicle. Although no agouti pigmentation phenotype has ever been reported in humans, a gene encoding a conserved human agouti protein has been found[21] and so may have a physiological role. □

Received 13 June; accepted 15 September 1994.

1. Silvers, W. K. *The Coat Colors of Mice: A Model for Mammalian Gene Action and Interaction* (Springer, New York, 1979).
2. Robbins, L. S. *et al. Cell* **72**, 827–834 (1993).
3. Bultman, S. J., Michaud, E. J. & Woychik, R. P. *Cell* **71**, 1195–1204 (1992).
4. Miller, M. W. *et al. Genes Dev.* **7**, 454–467 (1993).
5. Silvers, W. K. & Russel, E. S. *J. exp. Zool.* **130**, 199–220 (1955).
6. Lamoreux, M. L. & Mayer, T. C. *Devl Biol.* **46**, 160–166 (1975).
7. Gantz, I. *et al. J. biol. chem.* **268**, 15174–15179 (1993).
8. Mountjoy, K. G. *et al. Molec. Endocr.* **8**, 1298–1308 (1994).
9. Dickerson, G. E. & Gowen, J. W. *Science* **105**, 496–498 (1947).
10. Conklin, B. R. & Bourne, H. R. *Nature* **364**, 110 (1993).
11. Jackson, I. J. *Nature* **362**, 587–588 (1993).
12. Siegrist, W. *et al. J. Rec. Res.* **8**, 323–343 (1988).
13. Frazier, A. L. *et al. Molec. Endocr.* **4**, 1264–1276 (1990).
14. Mountjoy, K. G. *et al. Science* **257**, 543–546 (1992).
15. Roselli-Rehfuss, L. *et al. Proc. natn. Acad. Sci. U.S.A.* **90**, 8856–8860 (1993).
16. Chhajlani, V. & Wikberg, J. E. S. *FEBS Lett.* **309**, 417–420 (1992).
17. Ganz, I. *et al. J. biol. Chem.* **268**, 8246–8250 (1993).
18. Chhajlani, V., Muceniece, R. & Wikberg, J. E. S. *Biochem. biophys. Res. Commun.* **195**, 866–873 (1993).
19. Desarnaud, F. *et al. Biochem. J.* **299**, 367–373 (1994).
20. Little, C. C. *The Inheritance of Coat Colors in Dogs* (Macmillan, New York, 1957).
21. Kwon, H. Y. *et al. Proc. natn. Acad. Sci. U.S.A.* (in the press).
22. Summers, M. D. & Smith, G. E. *Texas Agric. exp. St. Bull.* 1555 (1987).
23. Salomon, Y. *Meth. Enz.* **195**, 22–28 (1991).
24. Johnson, R. A. & Salomon, Y. *Meth. Enzym.* **195**, 3–21 (1991).
25. Rainey, W. E., Viard, I. Saez, J. M. *J. biol. Chem.* **264**, 21474–21477 (1989).

ACKNOWLEDGEMENTS. This work was supported by NIH grants (R.D.C.), and by the Office of Health and Environmental Research, US Department of Energy, under contract with Martin Marietta Energy Systems, Inc. (R.P.W.). We thank J. Weiel, P. DeLacey, and K. Lewis for their help and M. Furth and T. Kenakin for discussion.

Inefficient gene transfer by adenovirus vector to cystic fibrosis airway epithelia of mice and humans

Barbara R. Grubb, Raymond J. Pickles, Hong Ye, James R. Yankaskas, Ralph N. Vick, John F. Engelhardt*, James M. Wilson*, Larry G. Johnson & Richard C. Boucher

CF/Pulmonary Research and Treatment Center, University of North Carolina at Chapel Hill, Chapel Hill, North Carolina 27599-7020, USA
* Institute of Human Gene Therapy, University of Pennsylvania, Philadelphia, Pennsylvania 19104-4268, USA

THE success of adenoviral vectors for gene therapy of lung disease in cystic fibrosis (CF) depends on efficient transfer of the complementary DNA encoding the correct version of the cystic fibrosis transmembrane regulator (CFTR) to the affected columnar epithelial cells lining the airways of the lung. Pre-clinical studies *in vitro* suggest that low doses of adenovirus vectors carrying this CFTR cDNA can correct defective Cl^- transport in cultured human CF airway epithelia[1]. Here we use mice carrying the disrupted CF gene[2] to test the efficacy of this transfer system *in vivo*. We find that even repeated high doses can only partially (50%) correct the CF defect in Cl^- transport *in vivo* and do not correct the Na^+ transport defect at all. We investigated this discrepancy between the *in vivo* and *in vitro* transfer efficiency using CF mouse

Horm Res 1992;37(suppl 3):74–87

R. Wanke[a]
E. Wolf[b]
W. Hermanns[a]
S. Folger[a]
T. Buchmüller[c]
G. Brem[b]

[a] Veterinary Pathology and
[b] Molecular Animal Breeding, University of Munich, FRG, and
[c] Department of Internal Medicine, University of Ulm, FRG

The GH-Transgenic Mouse as an Experimental Model for Growth Research: Clinical and Pathological Studies

Key Words
Bone growth
Gene transfer
Glomerulosclerosis
Growth hormone
Hepatocarcinogenesis
Transgenic mouse
Visceromegaly

Abstract
The objectives and the methodology of mammalian gene transfer are discussed and findings in growth hormone (GH) transgenic mice are reported to illustrate the potential offered by genetically designed animal models for investigations in various areas of biomedical research. Transgenic mice expressing hybrid genes composed of either human or bovine GH coding sequences fused to the mouse metallothionein I promoter show high serum levels of heterologous GH, increased growth rates and final adult size, decreased life expectancy and a variety of pathological changes.

Introduction

Two mice, one twice as large as the other, graced the cover of the 16th December, 1982 issue of *Nature*. The significant difference in body size between the two individuals was the result of the introduction of a DNA fragment containing the promoter of the mouse metallothionein I (MT) gene fused to the structural gene of rat growth hormone (rGH) into the mouse genome [1]. This was not the first report on a successful gene transfer experiment in mammals. The first animals carrying experimentally introduced foreign DNA were produced in 1974 by microinjecting simian virus 40 DNA into the cavity of murine blastocysts [2]. Nevertheless, the GH transgenic mouse played a key role in the history of mammalian gene transfer and attracted considerable attention from scientists as well as the popular press. Not only was it possible to alter an animal's genotype in a stable fashion, but the phenotype could also be influenced and the giant transgenic mouse became a highly visible manifestation of the potential offered by gene transfer.

The term 'transgenic' was coined by Gordon and Ruddle in 1981 [3] and is used to describe animals that have foreign DNA integrated into their somatic cells and their germ line as a consequence of the experimental introduction of DNA [4, 5]. The introduction of foreign genes into the mammalian genome was immediately recognized as an important scientific achievement and many institutions adopted the methodology of gene transfer during the past decade. Most gene transfer work has focused on the mouse. However, in 1985, gene transfer was extended to other mammalian species [6, 7] and DNA integration has

R. Wanke, MD
Institut für Tierpathologie
Universität München
Veterinärstrasse 13
D-W-8000 München 22 (FRG)

since been achieved in rat [8], rabbit, pig, sheep, goat, and cattle [for review, see 9–11]. The ability to produce alterations in the host mammalian genome in a functional and stable manner has tremendous potential for advancing research into many fields very rapidly. At present, three main areas of application of transgenic animals may be distinguished: (1) biomedical sciences, (2) agriculture, and (3) biotechnology (genetic farming).

The last few years have witnessed an extraordinary increase in the use of transgenic animals in biomedical research. Gene transfer experimentation has presented a powerful new tool for identifying endogenous genes and has provided an excellent means of clarifying questions on gene integration, and the regulation, as well as the consequences, of gene expression in the context of the whole organism. Various approaches have been used to generate transgenic animal models for human diseases. The most widely used strategy consists of the expression of a gene added to the genome of the host mammal to cause an elevated level of the transgene product either in the circulation or in a particular cell type. Another approach includes interruption of the correct expression of an endogenous gene [for review see 5, 12–16]. From an agricultural standpoint, gene transfer is concerned with the introduction of economically important traits into the genome of farm animals [10, 11]. The objective of genetic farming is using transgenic animals to synthesize large quantities of medically relevant proteins (e.g. human coagulation factors that cannot be produced in their active form by microorganisms). Regulatory elements capable of targeting transgene expression to the mammary gland are of special interest in this context [10, 17, 18].

Methods of Gene Transfer in Mice

Three different methods are currently being used to introduce foreign genes into the mouse genome: (1) the direct microinjection of gene constructs into pronuclei of fertilized one-cell eggs; (2) the transduction of foreign DNA by retroviral vectors into embryos at various stages of development, and (3) the use of genetically transformed pluripotential teratocarcinoma cells or embryonic stem cells as vehicles. The most prevalent technique for introducing genes into the germ line is the pronuclear microinjection of cloned genes into zygotes. This method involves several steps including the superovulation of donor mice, the recovery of single cell embryos from the oviducts, the microinjection of 1–2 pl of a DNA solution containing several hundred copies of the gene construct per picoliter into the male pronuclei of zygotes, and the transfer of microinjected embryos into synchronized recipients. Detailed descriptions of this procedure are given elsewhere [19–21]. The main advantage of the microinjection technique is that gene integration mostly occurs before the first DNA replication cycle. The percentage of somatic and germ line mosaicism (20–30%) is, therefore, relatively low [19]. Further advantages of DNA microinjection are its reproducible efficiency in the range of a few percent of transgenic animals per zygotes injected [16, 19] and the possibility of introducing large gene constructs of up to at least 50 kb [22]. A disadvantage of this method is the random integration of gene constructs with respect to both the chromosomal integration site and the number of copies integrated [4].

By contrast, retroviral vectors allow efficient insertion of single copies of a gene construct as a consequence of the retroviral integration mechanisms [23]. Although technically simple, the use of retroviruses and retroviral vectors has not found widespread application so far. This may be due to the size limitations for transduced DNA, to a higher rate of mosaic founder animals as compared to the microinjection technique, to a possible interference of retroviral DNA sequences with expression of genes that it carries, and to the risk of recombination between retroviral vectors and endogenous retroviral sequences.

Pluripotential stem cell lines, isolated either from teratocarcinoma tumours or from pre-implantation stage mouse embryos, provide another route of inserting foreign genes into the mouse germ line [for review see 24]. Pluripotential stem cells are transformed in vitro and then incorporated into the blastocoele cavity of blastocysts or aggregated with eight-cell embryos to produce transgenic chimaeras. Via transfected cells that have populated the germ line of a chimaeric mouse the experimentally introduced DNA can be transmitted to descendants which then will carry the transgene in every cell. The advantage of this method is the possibility of screening the stem cells for gene integration or even for gene expression in vitro before manipulating them into an embryo. The chance of altering the genome by homologous recombination therefore arises [25]. This technique has already been applied to study the function of a peptide belonging to the growth hormone family. DeChiara et al. [26] disrupted the mouse insulin-like growth factor II (IGF II) gene by gene targeting in embryonic stem cells and used them to establish chimaeric mice. Germ line transmission of the inactivated IGF II gene from male chimaeras resulted in heterozygous offspring that were significantly smaller than their embryonic stem cell-derived wild-type

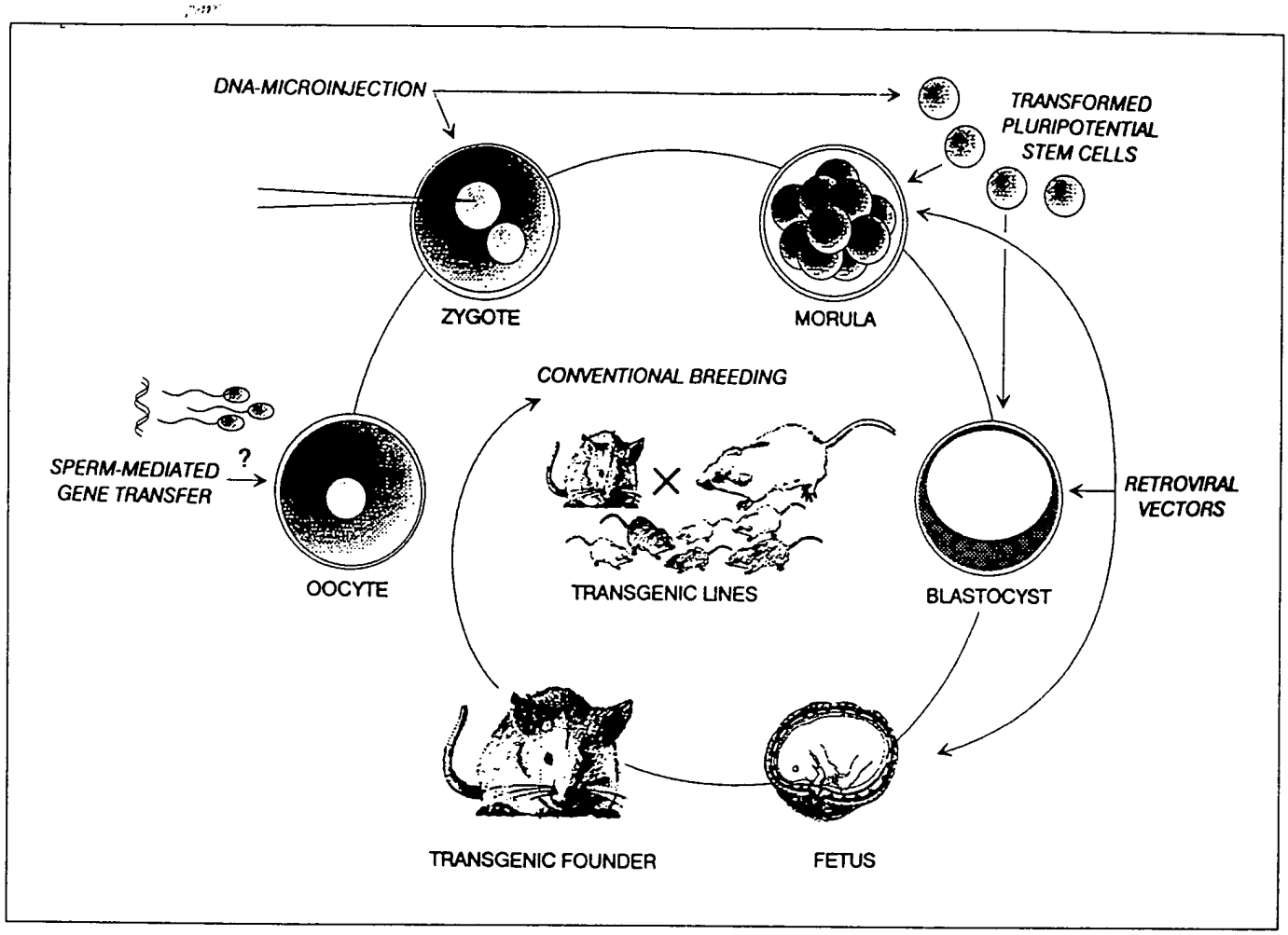

Fig. 1. Methods of gene transfer in mice.

littermates. However, when the disrupted gene was transmitted maternally, the heterozygous progeny were phenotypically normal. Homozygous mutants displayed the same phenotype as growth-deficient heterozygous siblings [27]. These results demonstrated that the mouse IGF II gene is subject to parental imprinting.

A report of a remarkably simple method of sperm-mediated gene transfer was published by Lavitrano et al. [28]. These workers incubated mouse spermatazoa for 15 min in an isotonic solution containing plasmid DNA and used them for in vitro fertilization. 30% of the 250 born offspring were reported to be transgenic. However, other groups of investigators have been unable to repeat this experiment successfully [29, 30]. Figure 1 shows the most important techniques of gene transfer in mice together with the stages of embryonic development they are used at.

Tests after Gene Transfer – Establishment of Transgenic Lines

Gene transfer experiments aiming at the addition of a functional gene to the murine genome via pronuclear microinjection are currently finding the most widespread application and include a series of subsequent tests. After the animals that develop from microinjected zygotes have been born, those individuals carrying the foreign DNA must be identified. This is commonly done at 3 weeks of age, when the pups have been weaned and marked for identification purposes. A small piece of tail provides enough DNA to confirm the presence of the inserted gene by various DNA hybridization techniques. Expression of a transgene foreign to the recipient's genome can be determined by various methods. Total RNA extracted from tissue samples can be subjected to Northern blot analysis

with a probe complementary to the relevant mRNA to determine transgene transcription. Various protein analysis techniques are applied for detecting translation of the transgene encoded RNA. Quantitation of foreign proteins which are either secreted into the bloodstream or produced by exocrine glands (e.g. the mammary gland) easily allows estimation of the level of transgene expression in a live animal. In situ hybridization and immunohistochemistry make it possible to identify the site of expression in tissue sections at the level of RNA or protein, respectively.

Biological effects of transgene expression are examined in clinical and pathological studies. Germ line integration is detected by breeding. Transgenic animals derived from microinjected zygotes commonly have integrated multiple copies of the fusion gene at one chromosomal location. Since there is no corresponding allele on the homologous chromosome, transgenic founders are defined to be hemizygous rather than heterozygous. Transgenes are inherited as Mendelian traits, i.e., when mating a hemizygous transgenic founder with a normal animal, one expects 50% of the offspring to be transgenic. The percentage may be higher if the transgenic founder animal contains two or more integration sites which segregate independently [31]. On the other hand, the number of transgenic descendants may be extremely low if germ line mosaicism has occurred [32]. The term genetic mosaicism refers to individuals that derive from a single zygote but consist of cell populations carrying different genetic information. About one third of transgenic founder mice produced by the pronuclear microinjection technique exhibit somatic and/or germ line mosaicism as a result of integration of the foreign DNA after the initial replication cycle of the endogenous DNA [9, 23]. The final consideration concerns the possibility of disrupting an endogenous gene by the insertion of foreign DNA. Most insertional mutations are probably transmitted in a recessive manner and thus only become apparent in homozygous individuals obtained by interbreeding of hemizygous animals. Inactivation of an endogenous gene by insertion of a transgene can cause embryonic lethality or developmental abnormalities in the homozygous state. Insertional mutagenesis thereby offers a potential means of studying developmental processes and hereditary disorders at a molecular level. Using the foreign DNA of known sequence as a marker it is possible to identify the disrupted and yet uncharacterized endogenous gene. Recombinant DNA containing the human GH gene has been used to investigate the mutagenic potential of DNA transfection [33, 34].

Mice Harbouring Transgenes of the Growth Hormone Family

Since the first GH transgenic mice were generated in 1982 [1], a variety of genes coding for peptides involved in the regulation of growth have been introduced into the mouse genome, including human growth hormone releasing factor (GRF), rat (r), human (h), bovine (b), ovine (o) GH, and human insulin-like growth factor I (IGF I). Both rGH or hGH genes driven by their homologous promoters have been introduced into mice. However, the foreign GH genes were not expressed under the control of their own regulatory DNA sequences [33, 35]. The regulation of mammalian gene expression is still poorly understood. Among the multitude of factors controlling gene expression regulatory regions containing promoter sequences, enhancer sequences, or a combination of both appear to be the most important *cis*-acting elements [15].

The difficulties in expressing certain genes in transgenic mice have led to an approach in which a regulatory region of one gene has been fused to the protein coding region of another gene (i.e. the usual regulatory region is replaced by a heterologous one). This procedure may be referred to as 'gene design' and offers the potential for developmental timing and tissue-specific transgene expression. Furthermore a number of promoters allow modulation of gene expression by hormonal or other external stimuli. The choice of a particular regulatory sequence is dependent on the experimental purposes. Regulatory sequences may be distinguished that either direct expression of hybrid genes in a wide variety of tissues or target transgene expression to particular cell types. Promoters of both categories have been used to drive foreign GH genes in transgenic mice.

MTGH Transgenic Mice

The mouse MT promoter has been used preferentially to induce expression of various GH transgenes in mice (MTGH transgenic mice). The endogenous MT gene is regulated transcriptionally by various factors, such as heavy metal ions, glucocorticoids and other endogenous stimuli, and can be considered as a housekeeping gene, because it is expressed in a wide variety of tissues. However, the extent of MT gene expression varies markedly from tissue to tissue, with the liver being the major site of metallothionein synthesis [23, 36]. Given that transgenes are expressed, one of the salient questions is whether the foreign genes are regulated properly. Endogenous MT

genes are expressed both prenatally and postnatally in animals as well as humans [37, 38]. Similarly, expression of MT promoter driven GH genes has been detected before birth from day 13 of gestation onward in transgenic mice which will thereby develop immunological tolerance to the foreign peptide hormones [36, 39, 40]. The addition of zinc or cadmium to the drinking water dramatically increased serum GH levels in MTGH transgenic mice, thereby demonstrating that the property of heavy metal inducibility of the MT promoter is retained in the hybrid gene [36]. However, the expectation that the expression of a foreign GH gene under the control of the MT promoter might parallel that of the endogenous MT gene was not fully realized, indicating that the MT promoter is influenced by other factors (e.g. the site of integration of the fusion gene copies and tissue environment) [23].

We investigated transgenic mice expressing either MThGH or MTbGH fusion genes. Details on the production of the MThGH transgenic animals and the fusion gene used for pronuclear microinjection have been reported elsewhere [6, 31]. Both MThGH transgenic founders and progeny carrying the fusion gene in a hemizygous state have been included in our studies. The MTbGH transgenic counterparts were obtained by subsequent mating of transgenic mice (originally generated and kindly provided by T.E. Wagner, The Edison Biotechnology Center, Athens, Ohio, USA) with mice of an outbred population derived from the NMRI strain [41]. The integration of the MThGH or the MTbGH fusion gene, respectively, was detected by Southern or slot blot analysis [31, 42].

Serum Levels of Foreign GH

Expression of the MThGH transgene was quantified by measuring hGH in the serum using a commercially available immunoradiometric assay (Hybritech Tandem-R® hGH assay) based on a double monoclonal antibody technique [43]. Serum hGH levels of transgenic mice belonging to three different lines ranged between 1,200 and 900,000 ng/ml when no heavy metal ions were applied to further stimulate MThGH transgene expression, and thereby dramatically exceeded physiological murine GH levels which correspond to less than 90 ng/ml of serum in normal mice [44, 45]. The MTbGH transgenic mice expressed the foreign GH gene at markedly lower levels when compared to their MThGH transgenic counterparts. Serum concentration of bGH was quantified by radioimmunoassay [46], and did not exceed 1,400 ng/ml in the MTbGH transgenic mice investigated so far.

Data pertaining to the level of expression of MTGH fusion genes in transgenic mice reported in the literature vary considerably and have recently been summarized elsewhere [47, 48]. Among the variety of factors that influence transgene expression, the site of transgene insertion in the genome plays an important role in its expression [23]. Germ line transmission of transgenes thereby offers the potential to select different lines of transgenic mice that express GH fusion genes at low or at high basal levels. These lines might be very helpful to further elucidate effects of GH. Short-term and long-term studies were carried out on MThGH transgenic mice to evaluate the course of hGH serum levels which showed undulating fluctuations with values as a whole being permanently increased [47]. Determination of hGH in serum samples taken at 60-min intervals over a 7-hour period indicated continuous secretion of the foreign GH in these animals. Physiological profiles of circulating GH in adult mice are characterized by episodic fluctuations, and exhibit sex-dependent differences. Sexually dimorphic secretory patterns of GH have been found, in rodents, to be an important factor in determining the expression of several sex-specific phenotypes. Transgenic mice exhibiting a continuous mode of GH secretion offer the opportunity to investigate the possible involvement of the secretory rhythm of GH in both physiological and pathological states [49, 50]. The possible role of altered GH secretory patterns for the growth-promoting effect of GH in male and female transgenic mice has been discussed elsewhere [51].

Consequences of MTGH Transgene Expression in Mice

Effects on Reproductive Function

The expression of GH transgenes under the transcriptional control of the MT promoter causes a variety of both phenotypic and pathomorphological alterations. Furthermore, transgenic female mice expressing MThGH fusion genes were found to be almost invariably sterile and their male counterparts exhibited reduced fertility [35, 47, 52]. Transplantation of ovaries of transgenic mice into non-transgenic females was successfully used to circumvent the reproductive problems in MThGH transgenic female mice and demonstrated the potential ability of these animals to shed normal eggs [53]. Reduced fertility was also observed in transgenic female mice expressing either

Table 1. Comparison of sequence homology, expressed as percentage, in the primary structure of GH

	hGH	bGH	oGH	pGH	rGH	mGH
hGH	*	66.3%	65.8%	67.9%	65.8%	66.3%
bGH	64	*	99.5%	90.5%	87.9%	87.4%
oGH	65	1	*	90.0%	87.4%	86.8%
pGH	61	18	19	*	94.7%	94.7%
rGH	65	23	24	10	*	98.4%
mGH	64	24	25	10	3	*

Numbers of different amino acids.

h = Human; b = bovine; o = ovine; p = porcine; r = rat; m = mouse.

MTrGH or MTbGH hybrid genes [35, 54]. In contrast, the fertility of MToGH transgenic female mice was almost unimpaired [55] despite bGH and oGH being different in only one amino acid (table 1). MTGRF transgenic mice which have elevated serum levels of endogenous GH did not exhibit perturbations of fertility [44]. Furthermore, transgenic female mice expressing human placental GH variant (hGH·V) gene regulated by the MT promoter can reproduce, although hGH·V, similarly to hGH, is both somatotropic and lactotropic in rodents [54]. Transgenic mice carrying various GH genes thereby can serve as appropriate models for unravelling the effects of GH on reproductive functions.

Effects on Body Weight, Skeletal Growth, and Organ Weights

Stimulation of body growth is the most obvious phenotypic effect of MTGH transgene expression in mice. Similar maximum body weights of about twice normal have been achieved with expression of various heterologous GH genes in transgenic mice. This finding indicates that growth promoting effects of GH in mice do not depend on a highly homologous peptide. In table 1 the primary structures of human [56], bovine [57], ovine [58], porcine [59], rat [60] and murine GH [61] are compared. Furthermore, no correlation was detected between the level of circulating heterologous GH and the degree of increase in body weight. For instance, MThGH transgenic mice exhibited similar maximum growth ratios compared to controls when serum concentration of hGH corresponded to either less than 10 ng/ml or was several 1,000-fold higher. Data on growth promotion and serum GH levels in MTGH transgenic mice have been reviewed elsewhere [47, 48]. Despite prior onset of MTGH transgene expression, marked differences in body growth between transgenic and non-transgenic mice are not evident until about 3 weeks of age [39, 47]. This observation is consistent with the concept that GH does not play a major role in the control of fetal and newborn growth [for review see 62]. Between 3 and 13 weeks of age MTGH transgenic mice display significantly increased growth rates, reflected in a markedly steeper slope of the growth curves of transgenic mice compared with those of controls (fig. 2). Thus, the period of rapid weight gain is similar for both transgenic and non-transgenic mice (i.e. the differences due to MTGH transgene expression are in the amount, not the timing, of body growth) [51, 63]. A peculiar phenomenon noted in MThGH transgenic mice with high serum levels of hGH is the absence of sex-related differences in body growth [47]. Growth curves and maximum body weights of male and female MThGH transgenic mice are almost identical (fig. 2).

A variety of factors come into question to explain the absence of body weight sexual dimorphism in these transgenic animals. One of the factors involved may be the continuous mode of hGH secretion. This has been discussed elsewhere in detail [51]. However, male and female MTbGH transgenic mice exhibit differences in body growth (fig. 2) despite continuously high serum levels of bGH [unpubl. observations] and similar results have been obtained with MTrGH transgenic mice [39]. Therefore, differences in the biological activities of various GH species have to be taken into account. On the other hand, MThGH transgenic mice with low serum concentrations of hGH (less than 10 ng/ml) display accelerated growth and sex-related differences in body weight [unpubl. observations], indicating that the level of GH transgene expression may play an important role. Taken together, further attempts are necessary to identify the mechanisms causing either absence or presence of body weight sexual dimorphism in MTGH transgenic mice exhibiting stimulation of body growth.

Expression of MTGH transgenes in mice not only results in increased body weight but its influence is also

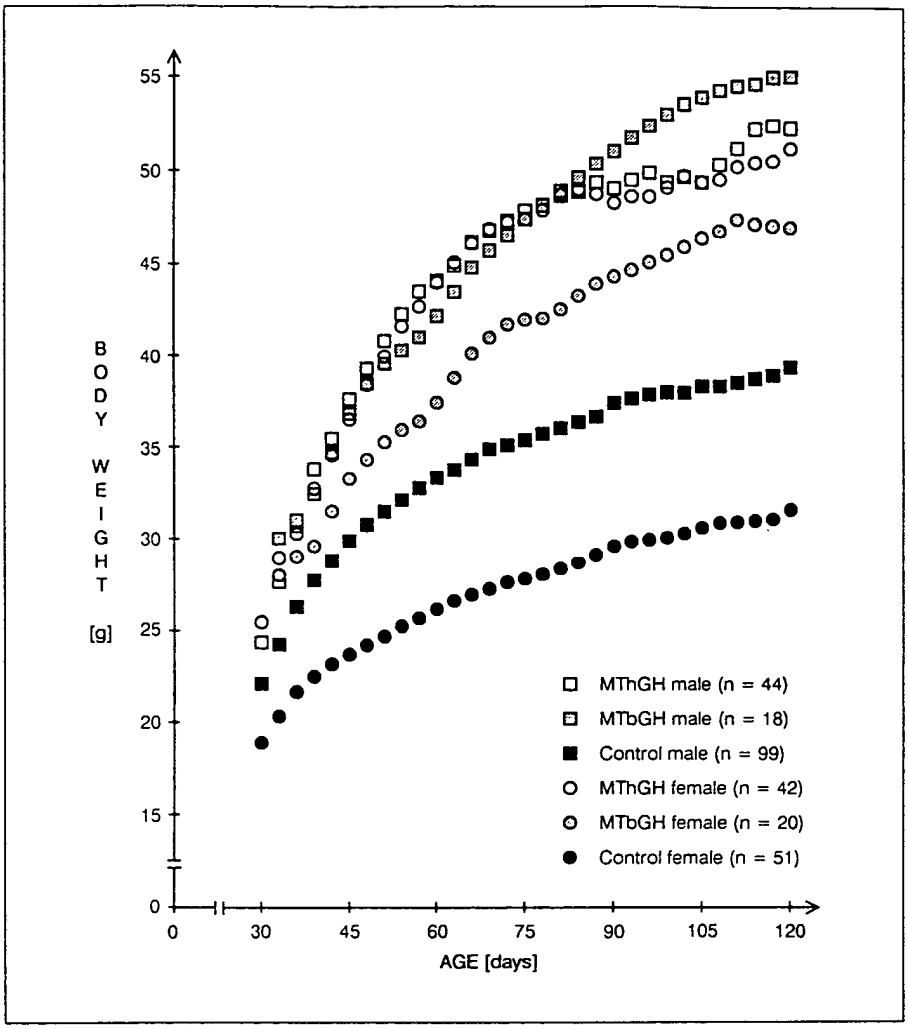

Fig. 2. Mean body weight gain of MThGH transgenic mice, MTbGH transgenic mice, and controls.

reflected in external body dimensions and skeletal dimensions (fig. 3). Detailed analyses carried out on both MThGH [51, 64, 65] and MTrGH [63, 66] transgenic mice revealed that the transgenic mice exhibit body and skeletal proportions which are significantly different from those of adult controls. Disproportionate skeletal gigantism was found in adult MThGH transgenic mice [64]. With the exception of only a few skeletal measurements, absolute bony dimensions of MThGH transgenic mice were significantly larger than those of sex-matched controls. Differences pertaining to individual bony measurements ranged from 3 to 32% in male and from 6 to 28% in female mice, respectively. Comparisons of the skeletal dimensions relative to body weight revealed that the cube roots of maximum body weight related skeletal dimensions of male and female MThGH transgenic mice commonly were smaller than those of sex-matched controls. The extent of stimulation of bone growth exhibited sex-related differences. In male MThGH transgenic mice, growth of long tubular bones was as a rule characterized more by bony apposition than by lengthening, whereas in transgenic females longitudinal growth exceeded the thickening of the diaphysis of the long bones (with the exception of the radius – an early maturing bone). Various hormones influence skeletal growth, but GH is the only recognized hormone that can cause excessive stimulation of longitudinal bone growth. A controversial question is whether GH exerts its growth promoting effect directly or indirectly by regulating the circulating level of IGF I. The somatomedin hypothesis implies that GH stimulates the hepatic synthesis of IGF I, which then mediates the actions of GH in an endocrine manner. The findings that IGF I is produced in many tissues and that such production also is GH stimulated have changed the

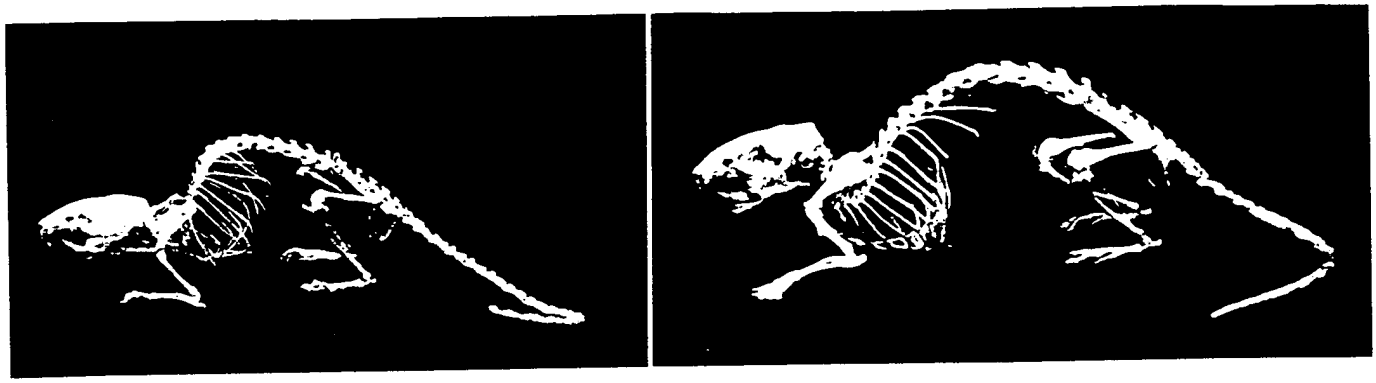

Fig. 3. Skeletal gigantism in an adult MThGH transgenic mouse (right). For comparison the skeleton of a non-transgenic littermate control is shown (left) at the same magnification.

concept of IGF I action from primarily endocrine to dominatingly paracrine or autocrine. Recent reports suggest that GH stimulates longitudinal bone growth both directly – by stimulating the differentiation of epiphyseal growth plate precursor cells – and indirectly – by increasing the responsiveness ot the differentiating cells to IGF I and enhancing the local production of IGF I that stimulates the clonal expansion of differentiating chondrocytes via the endocrine or paracrine mechanisms [for review see 67, 68]. Findings in MTIGF I transgenic mice indicate that elevated serum levels of IGF I per se are not sufficient to stimulate skeletal growth. Mice expressing this transgene had 1.5-fold higher concentrations of IGF I in their serum than non-transgenic controls. Enhancement of body weight gain was not apparent until 6–8 weeks of age and therefore delayed compared to MTGH transgenic mice. Growth promotion manifested itself as a 1.3-fold increase in body weight due to selective organ and muscle/connective tissue growth without any apparent increase in skeletal growth [69].

Another factor that is known to influence bone growth is mechanical loading. This was experimentally demonstrated in rodents which underwent a simulated increase in body weight either by means of experimental bipedalism or by chronic centrifugation [70, 71]. In order to judge the effects of mechanical loading due to increased body weight on bone growth of MThGH transgenic mice, we compared their skeletal dimensions with those of NMRI mice reaching similar body weights as a result of continuous selection for high 8-week body weight [65]. Significant differences in the skeletal shape between adults of the two groups were observed. Skeletal proportions of the transgenic mice exceeded those of the selected mice with most obvious differences pertaining to the limb bones. The results of this study clearly suggest that the altered hormonal environment of the transgenic mice is the primary cause of skeletal gigantism, and that bony overgrowth in these animals can only in part be a result of increased mechanical loading due to higher body weight.

Splanchnomegaly is a common finding in transgenic mice expressing various MTGH fusion genes. However, the degree of growth enhancement varies markedly from organ to organ. Furthermore, certain differences with respect to organ enlargement become obvious when published data concerning various strains of MTGH transgenic mice are compared [for review see 48]. In MThGH transgenic mice exhibiting high serum levels of hGH the mean absolute weights of various internal organs were consistently greater than those seen in controls. The percent increase for the various inner organs varied considerably and was greatest for the kidney and the liver. As for whole body weight, no sex-related differences in organ weights were found in the transgenic individuals. Visceral enlargement was, therefore, more pronounced in female than in male transgenic mice when compared to sex-matched controls (fig. 4). Organ-to-body weight ratios in transgenic mice also differed significantly from those seen in controls with greatest differences pertaining to kidney- or liver-to-body weight ratios (fig. 4). Interestingly, a special size increase in the spleen was reported in MTrGH transgenic mice exhibiting a 2.5-fold increase in spleen weight compared to controls [63], whereas the MThGH transgenic mice demonstrated a markedly less pronounced splenic enlargement. The variety of interfering factors that need to be considered as a possible explanation for the variation seen in results concerning body and organ proportions in various strains of GH transgenic mice has been discussed elsewhere in detail [47].

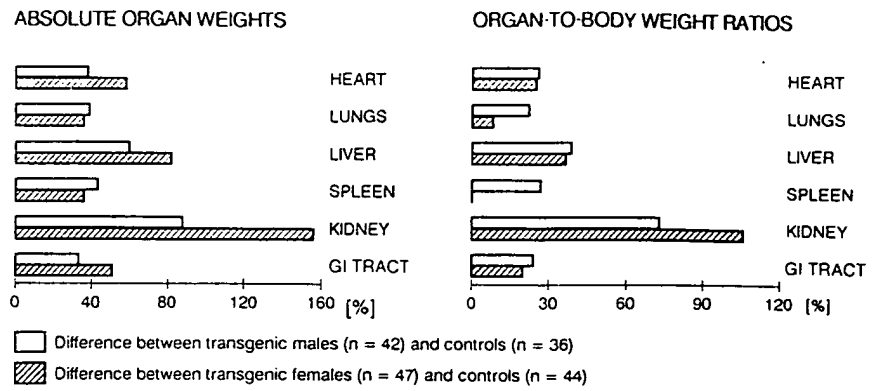

Fig. 4. Absolute organ weights and organ-to-body weight ratios in MThGH transgenic mice as compared to controls.

Serum Chemistry

Blood serum samples taken from MThGH transgenic mice exhibiting chronically high circulating concentrations of hGH were analyzed for a number of chemical parameters. IGF I is thought to play an important role in the GH cascade, so serum concentrations of this peptide growth factor were measured by radioimmunoassay. Serum IGF I levels in the transgenic mice were about 3-fold higher than those in the control animals (fig. 5) and did not correlate with the amount of circulating hGH [data not shown]. Similarly elevated serum IGF I concentrations of about 2- or 3-fold normal values have been noted in transgenic mice expressing either MTrGH or MTbGH fusion genes [72, 73]. Stimulation of IGF I synthesis in mice seems, therefore, to be rather independent of the species of GH.

To study the effects of hGH excess on carbohydrate metabolism we quantified insulin and glucose in the sera of MThGH transgenic mice. Fasting insulin levels were significantly increased in the transgenic mice, whereas glucose levels did not differ significantly from those in control mice (fig. 5) [74]. This type of alteration has also been reported for MTbGH transgenic mice [73,75]. Interestingly, expression of the bGH transgene under the control of a phosphoenolpyruvate carboxykinase (PEPCK) regulatory sequence did not result in hyperinsulinaemia or hyperglycaemia in transgenic mice despite substantial amounts of bGH detected in their serum. Differences in glucose homeostasis between MTbGH and PEPCKbGH transgenic mice may be the result of either the tissue distribution pattern of expression, the developmental time of onset of expression or the hormonal regulation of transcription of the bGH transgene [75]. The lipid status of MThGH transgenic mice was characterized by a significant increase in serum cholesterol levels, while no significant changes were observed for serum levels of triglycerides. Conversely, MTIGF I transgenic mice, which have very low serum concentrations of endogenous GH but IGF I levels that are 1.5-fold greater than those in control mice, exhibited hypertriglyceridaemia but no hypercholesterolaemia [73]. Total protein concentrations were significantly increased in the sera of MThGH transgenic mice, presumably as a result of stimulated hepatic protein synthesis (fig. 5) [47]. In contrast, MTbGH transgenic mice were found to be normoproteinaemic [73]. Analysis of further parameters in the sera of MThGH transgenic mice studied at a mean age of 119 days indicated both markedly reduced kidney function and hepatic disorders, without a distinct reduction in liver function, however [47].

Life Expectancy

Consistently high serum GH levels, as a result of overexpression of MTGH transgenes, have deleterious effects on mice. The mean life expectancy of MThGH transgenic mice expressing the transgene at high levels was drastically reduced in comparison to non-transgenic control mice. Less than 30% of these transgenic animals survived until 6 months of age [47]. A shortened life-span has also been noted in MTbGH transgenic mice exhibiting serum bGH levels up to 1,400 ng/ml. The reduction was less pronounced, however. At 6 months of age 90% of the MTbGH transgenic mice were still alive, and almost 60% of these transgenic animals survived longer than 12 months [unpubl. observation]. Shortening of life expectancy in MTbGH transgenic mice has also been noted by other investigators [73].

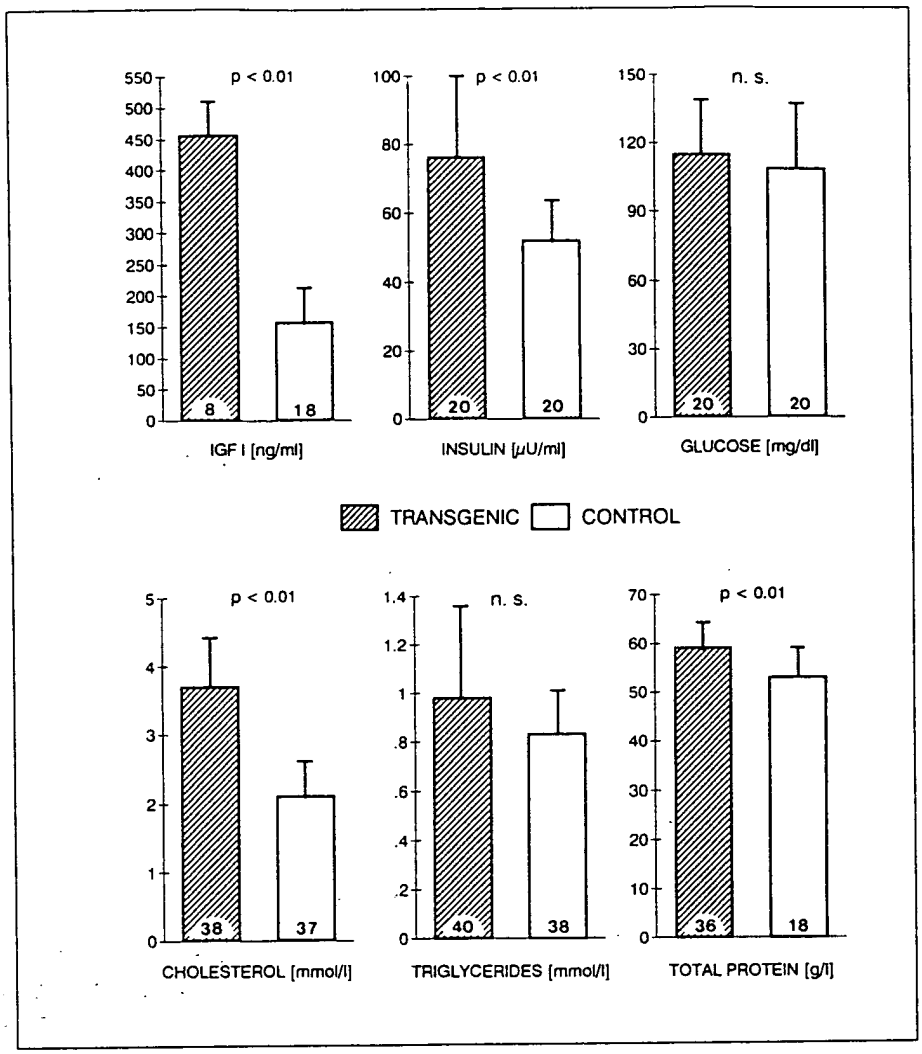

Fig. 5. Chemical parameters in the serum of MThGH transgenic mice and controls. Means and standard deviations are shown for each group. The number of animals is also indicated (bottom of bars).

Pathomorphological Findings

Apart from visceromegaly, a variety of pathological alterations including renal, hepatic, and cardiovascular lesions have been observed in mice expressing MTGH transgenes. In this context it seems especially noteworthy that the expression of an IGF I transgene has been found to result in a different pattern of abnormalities in mice. An overview on pathological findings in mice expressing various transgenes of the growth hormone family has been given elsewhere [48]. Transgenic mice with excess GH production regularly develop kidney alterations. The results of both morphological and clinicochemical investigations indicate renal failure to be the primary cause of the shortened life-span of these animals [47, 73, 76]. The pattern of nephropathological changes is the same for both MThGH and MTbGH transgenic mice. However, we found the degree of renal alterations to be more severe at an earlier age in our MThGH transgenic mice than in their bGH transgenic counterparts. Studies carried out by ourselves and other groups to evaluate the development of renal alterations in MTGH transgenic mice revealed initial glomerular changes including both significant glomerular enlargement and progressive glomerulosclerosis. The glomeruli of transgenic mice with bGH overproduction were found to be disproportionately enlarged, as a function of either kidney or body weight, compared with non-transgenic control mice, and the increase in glomerular size paralleled the degree of mesangial sclerosis [77]. End-stage renal lesions were characterized by a marked atrophy of nephrons and pronounced tubulocystic alterations (fig. 6). Remnant glomeruli demonstrated segmental or total sclerosis and/or hyalinosis. The changes in glomerular morphology were associated with significant glomerular dysfunction, as evidenced by the presence of

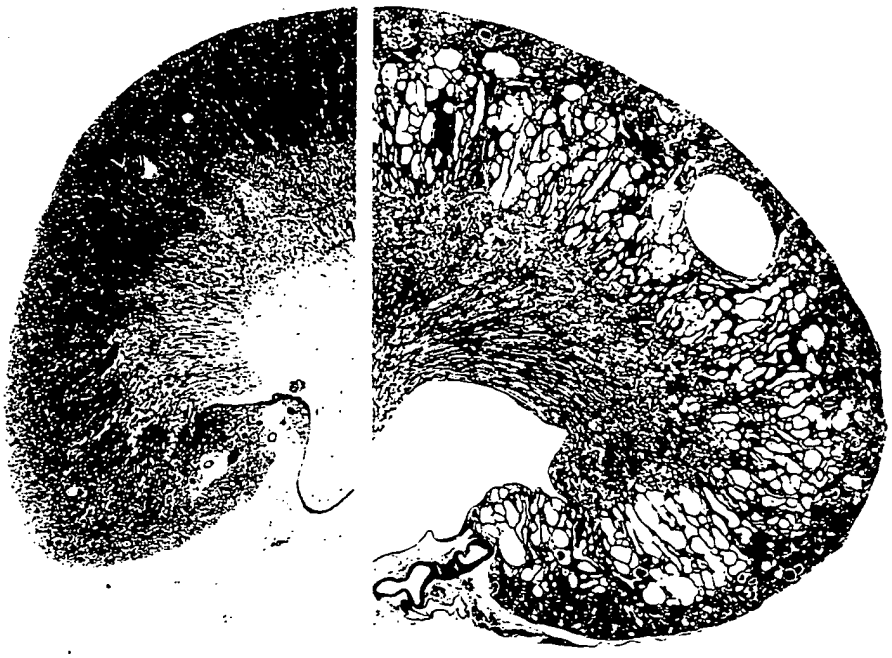

Fig. 6. Histopathology of the kidney of a 7-month-old MTbGH transgenic mouse: nephron atrophy, tubulocystic change, proteinaceous casts (right). A control organ is shown on the left. Note also the difference in kidney size. Original magnification is the same for both (× 3.2).

numerous intratubular proteinaceous casts [47, 48]. In contrast, MTIGF I transgenic mice with serum IGF I levels higher than those in bGH transgenic mice did not develop glomerulosclerosis even though they had significant glomerular hypertrophy [77]. However, the degree of glomerular enlargement did not reach that in bGH transgenic mice which exhibited a significantly higher mean glomerular volume/either kidney or body weight ratio than the IGF I transgenic mice. The fact that neither glomerulosclerotic nor tubulointerstitial changes were found in IGF I transgenic mice [73, 78] suggests that the elevated circulating level of IGF I does not mediate the glomerulosclerosis in MTGH transgenic mice.

Apart from nephropathological changes, hepatic alterations have consistently been observed in mice expressing MTGH transgenes. This is also true of MTGRF transgenic mice in which hypophysial expression of the endogenous GH gene is stimulated by the foreign GRF. Based on the observation that renal as well as hepatic alterations were similar in mice expressing either GH or GRF transgenes it was concluded that the anomalies are not caused by the ectopic production of GH, but result instead from chronic elevation of circulating GH [73, 78]. Both hepatomegaly and a variety of pathological liver alterations have been noted in transgenic mice exhibiting differences with respect to both the species and the level of expression of the particular GH transgene [47, 73]. Histologically, liver changes became apparent in GH transgenic mice at about 3–4 weeks of age [73] and hepatic lesions were found to be progressive with age. Initial alterations were characterized by a centrilobular, hepatocellular and hepatonuclear hypertrophy [47, 48]. The prominent distribution of the enlarged liver cells around central veins suggests that the hypertrophic change is not due to a direct effect of GH on liver cells, but is secondary to the synthesis of a factor resulting from GH stimulation. The absence of these kinds of alterations in the livers from MTIGF I transgenic mice [73] may be taken as an evidence that the hypertrophic liver cell change does not reflect an IGF I mediated effect of GH. The next stage of alteration seen in the livers from our MThGH transgenic mice was a massive diffuse enlargement associated with extreme pleomorphism of the hepatocytes and their nuclei. The latter frequently contained pseudoinclusions resulting from the invagination of portions of cytoplasm by complex infolding of the nuclear membrane. These pseudoinclusions occurred much more often and were much larger than those occasionally found in the livers from control mice. Discrepant answers have been given to the question as to whether liver enlargement in MTGH transgenic mice results predominantly from hyperplasia [39] or hypertrophy [55, 76].

Histomorphometric studies carried out on liver sections of MThGH and MToGH transgenic mice suggest

that the increase in liver weight noted in these transgenic animals is mainly due to liver cell hypertrophy.

Apart from non-neoplastic hepatic alterations, hepatocellular tumours including both adenoma and carcinoma were found very frequently in bGH transgenic mice. The occurrence of liver cell tumours was age-dependent, and their incidence increased to 96% (25/26) of the transgenic mice studied after 8 months of age, which expressed either an MTbGH or a PEPCKbGH fusion gene. Hepatocellular carcinoma was not found in transgenic mice less than 1 year of age, but it occurred in 5 of 14 transgenic mice older than 12 months. The requirement of bGH transgene expression for the development of hepatocellular neoplasms in the transgenic mice was clearly demonstrated by the absence of such tumours in the non-transgenic littermate controls [79]. Similar to our findings pertaining to bGH transgenic mice, MToGH transgenic mice have been reported to develop age-related hepatocellular tumours at a very high frequency. 70% of the MToGH transgenic mice studied after 43 weeks of age demonstrated liver tumours. Hepatocellular carcinoma was not found in transgenic mice less than 4 weeks of age. However, liver cell carcinoma was detected in 60% of the MToGH transgenic mice older than 53 weeks [80].

Conclusions

MTGH transgenic mice provide an excellent experimental system for studying the physiology and pathology of mammalian growth at the level of organ substructures, organs and the whole organism as well. A special advantage is the opportunity provided by transgenic mice to investigate the effects and the mode of action of heterologous growth hormones without having to take interfering immunological reactions into account. The differences in the basal level of expression between various lines of MTGH transgenic mice may be used to study the consequences of long-term exposure to either high or low circulating concentrations of GH. The pathological alterations observed in MTGH transgenic mice are of particular interest. Thus, these animals provide a new approach to investigate the pathogenesis of glomerulosclerosis and the mechanisms involved in the progression of chronic renal disease. GH transgenic mice developing age-related liver cell neoplasms at a high frequency represent a new model for hepatocellular carcinogenesis and illustrate the oncogenic potential of a chronic growth stimulus within an organ. MTGH transgenic mice are therefore considered as valuable models for studies in various fields of medical research, including auxology, endocrinology, nephrology and oncology.

Acknowledgements

Parts of this study were presented at the International Symposium on Endocrinology and Development: Basic and Clinical Aspects, Athens, Greece, October 12–14, 1990. Our work was supported by a grant from the Deutsche Forschungsgemeinschaft (He 1731/1-1; R.W.; W.H.; S.F.) and the Studienstiftung des deutschen Volkes (E.W.). We thank Professor D. Schams for determining serum levels of bGH and IGF I. We also thank Mr A. Ciolovan for excellent technical assistance.

References

1 Palmiter RD, Brinster RL, Hammer RE, et al: Dramatic growth of mice that develop from eggs microinjected with metallothionein-growth hormone fusion genes. Nature 1982: 300:611–615.
2 Jaenisch R, Mintz B: Simian virus 40 DNA sequences in DNA of healthy adult mice derived from preimplantation blastocysts injected with viral DNA. Proc Natl Acad Sci USA 1974:71:1250–1254.
3 Gordon JW, Ruddle FH: Integration and stable germ line transmission of genes injected into mouse pronuclei. Science 1981:214:1244–1246.
4 Palmiter RD, Brinster RL: Transgenic mice. Cell 1985:41:343–345.
5 Cuthbertson RA, Klintworth GK: Transgenic mice – a gold mine for furthering knowledge in pathobiology. Lab Invest 1988:58:484–502.
6 Brem G, Brenig B, Goodman HM, et al: Production of transgenic mice, rabbits and pigs by microinjection into pronuclei. Zuchthyg 1985: 20:251–252.
7 Hammer RE, Pursel VG, Rexroad CE Jr, et al: Production of transgenic rabbits, sheep and pigs by microinjection. Nature 1985:315:680–683.
8 Mullins JJ, Peters J, Ganten D: Fulminant hypertension in transgenic rats harbouring the mouse *Ren*-2 gene. Nature 1990:344:541–544.
9 Brem G: Transgene Nutztiere. Züchtungskunde 1988:60:248–262.
10 Pursel VG, Pinkert CA, Miller KF, et al: Genetic engineering of livestock. Science 1989: 244:1281–1288.
11 Brem G: Zum Stand des Gentransfers beim Nutztier. Züchtungskunde 1991:63:191–200.
12 Camper SA: Research applications of transgenic mice. BioTechniques 1987;5:638–650.
13 Jaenisch R: Transgenic animals. Science 1988; 240:1468–1474.
14 Hanahan D: Dissecting multistep tumorigenesis in transgenic mice. Annu Rev Genet 1988: 22:479–519.
15 Conelly CS, Fahl WE, Iannaccone PM: The role of transgenic animals in the analysis of various biological aspects of normal and pathologic states. Exp Cell Res 1989:183:257–276.

16 Brem G: Transgene Mäuse als Krankheitsmodelle: Drug Res 1990;40:335–343.
17 Van Brunt J: Molecular farming: transgenic animals as bioreactors. Biotechnology 1988;6: 1149–1154.
18 Hennighausen L: The mammary gland as a bioreactor: Production of foreign proteins in the milk. Protein Express Pur 1990;1:3–8.
19 Brinster RL, Chen HY, Trumbauer ME, et al: Factors affecting the efficiency of introducing foreign DNA into mice by microinjecting eggs. Proc Natl Acad Sci USA 1985;82:4438–4442.
20 Hogan B, Costantini F, Lacy E: Manipulating the Mouse Embryo. A Laboratory Manual. Cold Spring Harbor, Cold Spring Harbor Laboratory, 1986.
21 DePamphilis ML, Herman SA, Martinez-Salas E, et al: Microinjecting DNA into mouse ova to study DNA replication and gene expression and to produce transgenic animals. BioTechniques 1988;6:662–679.
22 Costantini F, Lacy E: Introduction of a rabbit β-globulin gene into the mouse germ line. Nature 1981;294:92–94.
23 Palmiter RD, Brinster RL: Germ-line transformation of mice. Annu Rev Genet 1986;20: 465–499.
24 Robertson EJ: Pluripotential stem cell lines as a route into the mouse germ line. Trends Genet 1986;2:9–13.
25 Capecchi MR: Altering the genome by homologous recombination. Science 1989;244:1288–1292.
26 DeChiara TM, Efstratiadis A, Robertson EJ: A growth-deficiency phenotype in heterozygous mice carrying an insulin-like growth factor II gene disrupted by targeting. Nature 1990;345: 78–80.
27 DeChiara TM, Robertson EJ, Efstratiadis A: Parental imprinting of the mouse insulin-like growth factor II gene. Cell 1991;64:849–859.
28 Lavitrano M, Camaioni A, Fazio VM, et al: Sperm cells as vectors for introducing foreign DNA into eggs: Genetic transformation of mice. Cell 1989;57:717–723.
29 Brinster RL, Sandgren EP, Behringer RR, et al: No simple solution for making transgenic mice. Cell 1989;59:239–241.
30 Barinaga M: Making transgenic mice: Is it really that easy? Science 1989;245:590–591.
31 Brenig B, Brem G: Integration of hGH gene in transgenic mice and transmission to next generation; in Beynen AC, Solleveld HA (eds). New Developments in Biosciences: Their Implications for Laboratory Animal Science. Dordrecht, Nijhoff, 1988, pp 331–336.
32 Wilkie TM, Brinster RL, Palmiter RD: Germline and somatic mosaicism in transgenic mice. Dev Biol 1986;118:9–18.
33 Wagner EF, Covarrubias L, Stewart TA, et al: Prenatal lethalities in mice homozygous for human growth hormone gene sequences integrated in the germ line. Cell 1983;35:647–655.
34 Covarrubias L, Nishida Y, Terao M, et al: Cellular DNA rearrangements and early developmental arrest caused by DNA insertion in transgenic mouse embryos. Mol Cell Biol 1987; 7:2243–2247.
35 Hammer RE, Palmiter RD, Brinster RL: Partial correction of murine hereditary growth disorder by germ-line incorporation of a new gene. Nature 1984;311:65–67.
36 Palmiter RD, Norstedt G, Gelinas RE, et al: Metallothionein-human GH fusion genes stimulate growth of mice. Science 1983;222:809–814.
37 Hamer DH: Metallothioneins. Annu Rev Biochem 1986;55:913–951.
38 Nartey NO, Banerjee D, Cherian MG: Immunohistochemical localization of metallothionein in cell nucleus and cytoplasm of fetal human liver and kidney and its changes during development. Pathology 1987;19:233–238.
39 Hammer RE, Brinster RL, Palmiter RD: Use of gene transfer to increase animal growth. Cold Spring Harbor Symp Quant Biol 1985;50: 379–387.
40 Adams TE: Tolerance to self-antigens in transgenic mice. Mol Biol Med 1990;7:341–357.
41 Brem G, Meyer J: Fertility data in mice with regard to embryo transfer programmes. Z Versuchstierkd 1985;27:78.
42 Brenig B, Müller M, Brem G: A fast detection protocol for screening large numbers of transgenic animals. Nucleic Acids Res 1989;17: 6422.
43 Wolf E, Brem G: 'High-dose hook effect' as a pitfall in quantifying transgene expression in metallothionein-human growth hormone (MT-hGH) transgenic mice. Clin Chem 1991;37: 763–765.
44 Hammer RE, Brinster RL, Rosenfeld MG, et al: Expression of human growth hormone-releasing factor in transgenic mice results in increased somatic growth. Nature 1985;315: 413–416.
45 Stefaneanu L, Kovacs K, Horvath E, et al: Adenohypophyseal changes in mice transgenic for human growth hormone-releasing factor: A histological, immunocytochemical, and electron microscopic investigation. Endocrinology 1989;125:2710–2718.
46 Kirchgessner M, Roth FX, Schams D, et al: Influence of exogenous growth hormone (GH) on performance and plasma GH concentrations of female veal calves. J Anim Physiol Anim Nutr 1987;58:50–59.
47 Brem G, Wanke R, Wolf E, et al: Multiple consequences of human growth hormone expression in transgenic mice. Mol Biol Med 1989;6: 531–547.
48 Wanke R, Hermanns W, Folger S, et al: Accelerated growth and visceral lesions in transgenic mice expressing foreign genes of the growth hormone family. An overview. Pediatr Nephrol 1991;5:513–521.
49 Norstedt G, Palmiter R: Secretory rhythm of growth hormone regulates sexual differentiation of mouse liver. Cell 1984;36:805–812.
50 MacLeod JN, Pampori NA, Shapiro BH: Sex differences in the ultradian pattern of plasma growth hormone concentrations in mice. J Endocrinol 1991;131:395–399.
51 Wolf E, Wanke R, Hermanns W, et al: Growth characteristics of metallothionein-human growth hormone transgenic mice as compared to mice selected for high eight-week body weight and unselected controls. I. Body weight gain and external body dimensions. Growth Dev Aging 1991;55:225–235.
52 Bartke A, Steger RW, Hodges SL, et al: Infertility in transgenic female mice with human growth hormone expression: Evidence for luteal failure. J Exp Zool 1988;248:121–124.
53 Brem G, Baunack E, Müller M, et al: Transgenic offspring by transcaryotic implantation of transgenic ovaries into normal mice. Mol Reprod Dev 1990;25:42–44.
54 Naar EM, Bartke A, Majumdar SS, et al: Fertility of transgenic female mice expressing bovine growth hormone or human growth hormone variant genes. Biol Reprod 1991;45:178–187.
55 Orian JM, Lee CS, Weiss LM, et al: The expression of a metallothionein-ovine growth hormone fusion gene in transgenic mice does not impair fertility but results in pathological lesions in the liver. Endocrinology 1989;124: 455–463.
56 DeNoto FM, Moore DD, Goodman HM: Human growth hormone DNA sequence and mRNA structure: Possible alternative splicing. Nucleic Acids Res 1981;9:3719–3730.
57 Miller WL, Martial JA, Baxter JD: Molecular cloning of DNA complementary to bovine growth hormone mRNA. J Biol Chem 1980; 255:7521–7524.
58 Orian JM, O'Mahoney JV, Brandon MR: Cloning and sequencing of the ovine growth hormone gene. Nucleic Acids Res 1988;16: 9046.
59 Vize PD, Wells JRE: Isolation and characterization of the porcine growth hormone gene. Gene 1987;55:339–344.
60 Page GS, Smith S, Goodman HM: DNA sequence of the rat growth hormone gene: Location of the 5′ terminus of the growth hormone mRNA and identification of an internal transposon-like element. Nucleic Acids Res 1981;9: 2087–2104.
61 Linzer DIH, Talamantes F: Nucleotide sequence of mouse prolactin and growth hormone mRNAs and expression of these mRNAs during pregnancy. J Biol Chem 1985;260: 9574–9579.
62 Gluckman PD: Fetal growth: An endocrine perspective. Acta Paediatr Scand 1989;349 (Suppl):21–25.
63 Shea BT, Hammer RE, Brinster RL: Growth allometry of the organs in giant transgenic mice. Endocrinology 1987;121:1924–1930.
64 Wolf E, Rapp K, Brem G: Expression of metallothionein-human growth hormone fusion genes in transgenic mice results in disproportionate skeletal gigantism. Growth Dev Aging 1991;55:117–127.
65 Wolf E, Rapp K, Wanke R, et al: Growth characteristics of metallothionein-human growth hormone transgenic mice as compared to mice selected for high eight-week body weight and unselected controls. II. Skeleton. Growth Dev Aging 1991;55:237–248.

66 Shea BT, Hammer RE, Brinster RL, et al: Relative growth of the skull and postcranium in giant transgenic mice. Genet Res (Camb) 1990; 56:21–34.
67 Isaksson OGP, Lindahl A, Nilsson A, et al: Mechanism of the stimulatory effect of growth hormone on longitudinal bone growth. Endocr Rev 1987;8:426–438.
68 Rutanen EM, Pekonen F: Insulin-like growth factors and their binding proteins. Acta Endocrinol (Copenh) 1990;123:7–13.
69 Mathews LS, Hammer RE, Behringer RR, et al: Growth enhancement of transgenic mice expressing human insulin-like growth factor I. Endocrinology 1988;123:2827–2833.
70 Simon MR, Papiersky P: Effects of experimental bipedalism on the growth of the femur and tibia in normal and hypophysectomized rats. Acta Anat 1982;114:321–329.
71 Simon MR, Holmes KR, Olsen AM: The effects of quantified amounts of increased intermittent compressive forces for 30 and 60 days on the growth of limb bones in the rat. Acta Anat 1984;120:173–179.
72 Mathews LS, Hammer RE, Brinster RL, et al: Expression of insulin-like growth factor I in transgenic mice with elevated levels of growth hormone is correlated with growth. Endocrinology 1988;123:433–437.
73 Quaife CJ, Mathews LS, Pinkert CA, et al: Histopathology associated with elevated levels of growth hormone and insulin-like growth factor I in transgenic mice. Endocrinology 1989;124: 40–48.
74 Buchmüller T, Wanke R, Hermanns W, et al: Hyperinsulinaemia in normoglycaemic mice developing glomerulosclerosis. Diabetologia 1990; 33(suppl):A148.
75 McGrane MM, Yun JS, Moorman AFM, et al: Metabolic effects of developmental, tissue-, and cell-specific expression of a chimeric phosphoenolpyruvate carboxykinase (GTP)/bovine growth hormone gene in transgenic mice. J Biol Chem 1990;265:22371–22379.
76 Brem G, Wanke R: Phenotypic and pathomorphological characteristics in a half-sib-family of transgenic mice carrying foreign MT-hGH genes: in Beynen AC, Solleveld HA (eds): New Developments in Biosciences: Their Implications for Laboratory Animal Science. Dordrecht, Nijhoff, 1988, pp 93–98.
77 Doi T, Striker LJ, Gibson CC, et al: Glomerular lesions in mice transgenic for growth hormone and insulin like growth factor-I. I. Relationship between increased glomerular size and mesangial sclerosis. Am J Pathol 1990;137: 541–552.
78 Doi T, Striker LJ, Quaife C, et al: Progressive glomerulosclerosis develops in transgenic mice chronically expressing growth hormone and growth hormone releasing factor but not in those expressing insulin like growth factor-1. Am J Pathol 1988;131:398–403.
79 Wanke R, Folger S, Hermanns W, et al: Induktion neoplastischer und nicht-neoplastischer Leberveränderungen durch Wachstumshormon-Überproduktion bei bGH-transgenen Mäusen. Verh Dtsch Ges Pathol 1991;75:312.
80 Orian JM, Tamakoshi K, Mackey IR, et al: New murine model for hepatocellular carcinoma: transgenic mice expressing metallothionein-ovine growth hormone fusion gene. JNCI 1990;82:393–398.

This Page is Inserted by IFW Indexing and Scanning Operations and is not part of the Official Record

BEST AVAILABLE IMAGES

Defective images within this document are accurate representations of the original documents submitted by the applicant.

Defects in the images include but are not limited to the items checked:

- ☐ BLACK BORDERS
- ☐ IMAGE CUT OFF AT TOP, BOTTOM OR SIDES
- ☐ FADED TEXT OR DRAWING
- ☑ BLURRED OR ILLEGIBLE TEXT OR DRAWING
- ☐ SKEWED/SLANTED IMAGES
- ☐ COLOR OR BLACK AND WHITE PHOTOGRAPHS
- ☐ GRAY SCALE DOCUMENTS
- ☐ LINES OR MARKS ON ORIGINAL DOCUMENT
- ☐ REFERENCE(S) OR EXHIBIT(S) SUBMITTED ARE POOR QUALITY
- ☐ OTHER: _____

IMAGES ARE BEST AVAILABLE COPY.
As rescanning these documents will not correct the image problems checked, please do not report these problems to the IFW Image Problem Mailbox.